Slick Spectra: A Spectral Fluorescence Study of the Water-Accommodated Fraction of Crude Oil

By

Leslie Slasor

A THESIS

Presented to the Division of Environmental and Biomolecular Systems
and the Oregon Health and Science University
Institute of Environmental Health
in partial fulfillment of the requirements for the degree of

Master of Science

in

Environmental Science and Engineering

August 2012

Division of Environmental and Biomolecular Systems

Institute of Environmental Health

Oregon Health and Science University

Certificate of Approval

_____

This is to certify that the Master's thesis of

Leslie A. Slasor

has been approved

_____

Dr. Joseph Needoba, Assistant Professor

Thesis Research Advisor

_____

Dr. Paul Tratnyek, Professor and Associate Division Head

_____

Dr. Andrew Barnard, Senior Research Scientist, WET Labs, Inc.

External Examiner

DEDICATION

For my Dad

ACKNOWLEDGEMENTS

I am extremely grateful to my academic advisor Dr. Joseph Needoba, and the rest of the community that makes up the Division of Environmental and Biomolecular Systems, for their guidance, support and encouragement. I would like to thank Dr. Andrew Barnard (WET Labs, Inc.) and Dr. Paul Tratnyek for serving on my committee and reviewing my work. Both Dr. Tratnyek and Dr. Needoba have been wonderful mentors and invaluable sources of scientific and professional advice. A special thanks to Dr. Corey Koch at WET Labs, Inc. for his collaboration, mentoring, and for keeping me positive and motivated along this journey.

For their valuable feedback, professional support and general camaraderie I must thank the Needoba-Peterson lab. For his hard work and genuine enthusiasm, I thank Nathan Hinkle, my dedicated summer intern. From the Pankow Group Mass Spectrometry Facility at PSU, I am extremely grateful for Dr. Wentai Luo and Dr. Lorne Isabelle. Their help and guidance on everything GC was invaluable.

I would also like to thank my special team of scientific, professional and personal consultants including family and friends, but most especially Dr. Wesley Asher, Brianna Paisley, and Megan Kaufman for hanging with me through phone calls and emails, reviewing and editing first drafts, showering me with encouragement, and keeping me grounded. I thank my parents for instilling in me the belief that I can succeed at anything I put my mind to. Last but never least; for his unending support, patience and love, I thank Paul Mullen.

Partial funding was provided by the National Science Foundation research grant "RAPID Deepwater Horizon Oil Spill: In-situ tracking of oil in seawater and the aging process using spectral fluorescence" (OCE-1048455).

TABLE OF CONTENTS

LIST OF FIGURES

LIST OF TABLES

ABSTRACT

All crude oil, including that released in the Gulf of Mexico, contains toxic and/or carcinogenic polycyclic aromatic hydrocarbons (PAHs). Many PAHs freely dissolve and can persist in the environment, increasing their potential to bioaccumulate in exposed organisms. Ever-increasing exploitation of oil resources and subsequent accidents (such as the Deepwater Horizon spill, the largest marine oil spill in United States history) demand a greater understanding of their environmental impacts to improve response and recovery.

Due to the presence of PAHs (the fluorescent component of crude oil), spectral fluorescence techniques are used to help characterize crude oil. During the 2010 Gulf of Mexico spill, highly sensitive fluorometers were used for in situ tracking of the underwater hydrocarbon plumes that resulted from crude oil released on the sea floor. However, existing fluorometers are not designed to specifically target PAHs. While fluorometric data provide valuable information, it is unclear how changing fluorescence signals relate to the dynamic environmental fate of crude oil. Concerns over sensitivity, relative performance of different sensor products, interferences, and simply how fluorescence signals should be interpreted highlight the need to better understand fluorescence behavior of oil during spills.

An investigation of the fluorescence properties of the water-accommodated fraction (WAF) of a variety of crude oils in seawater was undertaken to further refine in

situ instrument sensitivity for targeting PAHs. A subset of these samples was subjected to photodegradation to determine changes associated with this weathering process. In addition, we used two-dimensional gas chromatography analysis with time of flight mass spectrometry detection was employed to verify WAF composition and PAH concentration.

Key excitation and emission wavelength ranges (240-270 nm and 305-360 nm, respectively) were ubiquitous throughout the crude oils tested. After exposure to a full-spectrum solar simulator (2500 $\mu E/m^2/sec$) over seven hours, degradation rate constants of key excitation/emission (ex/em) peak pairs showed persistent fluorescence signals at 270/310 and 270/325 nm ex/em for Merey crude oil WAF, 270/305 nm for Hoops crude oil WAF, and 270/305 nm for South Louisiana crude oil WAF. GCxGC-TOFMS analysis of the WAF of two distinctive crude oils revealed compositional similarities of PAH constituents. The known PAH compounds found in WAF solution of the crude oils tested make a compelling case for refined in situ tracking of dispersed toxic crude oil components. In situ fluorometers could be adapted for improved tracking of a variety of crude oils, targeting the persistent peaks found in the range of 240-270 nm ex and 305-360 nm em.

CHAPTER 1

Introduction to Crude Oil and Spectral Fluorescence

1.1 Crude Oil in Seawater

Crude oil in seawater can be from natural or anthropogenic sources. Total worldwide input of hydrocarbon pollution into the ocean is estimated to be 1.3 million to 2.4 million tons per year (Laws 2000; National Research Council 2003). Of those, an estimated 600,000 tons per year are from natural sources. Natural sources of crude oil include seeps that have formed over time by the migration of crude oil deposits to the earth's surface (Laws 2000). They can be found in many coastal areas, however, they are particularly abundant on the Pacific continental shelf, including the eastern Pacific Ocean, off California and Alaska (Reed et al., 1977; Hornafius et al., 1999).

Anthropogenic sources make up the majority of petroleum pollution at an estimated minimum of 700,000 tons per year (National Research Council 2003). The continuing demand for crude oil has created lasting environmental effects from pollution introduced through the extraction, transportation and consumption of petroleum products (National Research Council 2003; IEO 2011; Kirby 2012).

Tanker collisions, groundings, hull failures, fires and explosions are the main causes of large spills (Laws 2000). These can be explained by aging vessels, higher maritime traffic, and increased probability of human error, due to rising demand of crude oil from growing populations and continued industrialization. The *Exxon Valdez* ran aground in Prince William Sound, Alaska, in 1989, spilling 36,000 tons of crude oil. In

2002 the *Prestige* sustained a hull breach off the coast of Galicia, Spain, spilling over 60,000 tons (Peterson et al., 2003; Gonzalez et al., 2006). Both vessels were single hulled tankers, an inferior construction compared to new double-hulled tankers (National Research Council 2003).

Natural reserves of crude oil vary geographically due to local geochemical makeup, allowing for regionally distinct physical and chemical composition. This creates an opportunity for unique source identification (Laws 2000; Wang et al., 2006; Sharma et al., 2009). The behavior of spilled oil in the environment depends on the release conditions, including temperature, currents, rate and amount of oil spilled, surface or underwater release, and presence of gas (Zhu et al., 1992; Johansen et al., 2003). It also depends on the oil's physical and chemical properties including density, viscosity, and chemical stability. The composition of oil is altered by environmental factors after exposure, a process called weathering. Understanding the weathering process of crude oil will help determine its environmental impact and improve oil spill response and recovery.

1.1.1 2010 Gulf of Mexico Oil Spill

Though there have been other spills involving the extraction of petroleum in coastal waters, such as the 1969 Santa Barbara oil spill off the coast of California (NOAA 1992), the 2010 Gulf of Mexico spill, also known as the Macondo blowout and the Deepwater Horizon spill (DWH), is one of the largest in history (Mendelssohn et al., 2012). An estimated 4.1 million barrels of oil was released off the Louisiana coast after a lethal drilling rig explosion (Allan et al., 2012). It has presented new challenges to oil

spill response and recovery as well as an opportunity for greater understanding of the impacts of crude oil spills, specifically deep sea drilling. The importance of studying the long term effects of DWH stems from the continued push toward deep sea drilling operations following rising energy demands of our growing global population.

Crude oil pollution has been in the forefront of coastal research due to the tragic outcome of the DWH spill. DWH presented new challenges to the scientific community due to the combination of crude oil and dispersants released at an approximate depth of 1500 m, and the dynamic physical conditions encountered off the coast of Louisiana (DeHaan et al., 2005; Reddy et al., 2011). This resulted in the distribution of toxic hydrocarbons throughout the water column to an extent never before recorded (Camilli et al., 2010; Diercks et al., 2010; Kirby 2012). Techniques including gas chromatography-mass spectroscopy (GCMS), high-performance liquid chromatography (HPLC), and fluorescence spectroscopy have been applied toward detection and tracking of hydrocarbon contamination (Johansen et al., 2003; Ryder 2005; Rodgers et al., 2011). Because ecological impacts may not be immediately evident, continued evaluations are needed to assess the consequences of a spill like DWH. Faced with new conditions and challenges, there is a need for new in situ detection instrumentation designed to specifically target components of crude oil dispersed throughout the water column.

1.1.2 Composition

Crude oil is composed of a complex mixture of compounds (Figure 1.1), consisting of three main groups of hydrocarbons (paraffins, naphthelenes and aromatics) and two non-hydrocarbon groups (resins and asphaltenes). The chemical composition of

different crude oil varies regionally, allowing spilled oils to be distinguished from one another (Wang et al., 2006; Sharma et al., 2009). This creates the opportunity for source identification. Characterization of crude oil can be based on the relative abundance of the dominant groups of components, density of oil, and/or sulfur content (Lyons et al., 2005).

Crude oils are described using the hydrocarbon and/or non-hydrocarbon compound groups that make up their composition (Figure 1.1). Paraffins, or alkanes, are the simplest hydrocarbon compounds found in crude oil. Most paraffinic oil is light or medium in density and can be waxy. Naphthenic oils consist of naphthenes, or cycloalkanes, which are similar to paraffins in that they are saturated, but are also cyclic (the carbon chain forms a ring). Most naphthenic oils are medium to heavy density, and have a greater molecular weight than paraffins. Aromatic crude oils are medium to heavy density, consisting of unsaturated cyclic hydrocarbon compounds that have a greater molecular weight than naphthenes. Aromatics can be multi-cyclic (more than one carbon ring) as seen in fluorene, one of the simplest polycyclic aromatic hydrocarbons (PAH) found in crude oils (Figure 1.2).

Asphaltenes are the heaviest compounds in crude oil and are categorized as a non-hydrocarbon component, composed mainly of aromatics that contain nitrogen, sulfur and oxygen (Buenrostro-Gonzalez et al., 2004; Strausz et al., 2009). Asphaltenic oils tend to be very dense, higher in viscosity, have high sulfur content, and produce tarry residues that are used in road construction (bitumen). Resins, like asphaltenes, are highly polar and consist of sulfur- and nitrogen-containing compounds such as thiophenes and quinolones (Rudzinski et al., 2000; Buenrostro-Gonzalez et al., 2004).

The American Petroleum Institute (API) uses the unitless API gravity in place of density to compare relative densities of different crude oils. The range in density is due to the concentrations of the various components of crude oil. For example if a particular oil has a higher concentration of aromatics than paraffins it will most likely be more dense due to the greater number of heavier aromatic molecules, by volume. Crude oil is classified by API using a formula comparing the density of water to oil density (Hyne 2001; National Research Council 2003).

[Formula 1] The formula for API gravity can be expressed as:

$$API = (141.5 / SG) - 131.5 \qquad (1)$$

API = Degrees API Gravity

SG = Specific Gravity (at 15.6˚C)

[Formula 2] Specific gravity calculated from density:

$$SG_{oil} = \rho_{oil}/\rho_{H2O} \qquad (2)$$

ρ_{oil} *= Density of the oil sample*

ρ_{H2O} *= Density of water*

An API of more than ten is lighter than water (less dense) and an API less than ten is heaver (more dense). This is simplified by classification of 'light', 'medium' and/or 'heavy' as a reflection of the API gravity of the oil. For example, 'light' would mean low density, high API due to their inverse relationship.

Sulfur content is another factor used to differentiate crude oils. Sulfur is found in all crude oils in some form, and is considered an undesirable impurity by refineries (Carrales et al., 1975; Hyne 2001; Lyons et al., 2005). The removal of sulfur during the

refining process is necessary to prevent corrosion and other harmful chemical reactions (Carrales et al., 1975; Hyne 2001). Removal also prevents the release of pollutants like sulfur dioxide from the burning of high sulfur crude oil, which can react in the atmosphere to form acid rain. High sulfur crude oils are designated 'sour,' having more than 1% sulfur by weight. Low sulfur crude oils are 'sweet,' containing less than 1% sulfur by weight (Hyne 2001; Lyons et al., 2005).

1.1.3 Weathering

Crude oil undergoes immediate and complicated weathering processes that alter its chemical and physical properties when introduced to the natural environment (Figure 1.3) (Gorden et al., 1976; Nicodem et al., 1997; Boehm et al., 2007). On the ocean surface, volatile compounds evaporate. The rate and loss of volatilization depends on surface to volume ratio. Volatilization is inversely proportionally to the thickness of surface oil layer (Cormack 1999).

Photooxidation and microbial oxidation occur when oil is exposed to ultraviolet light and microbial degradation, respectively (Reed et al., 1977; Leahy et al., 1990). Photooxidation degrades less soluble, higher molecular weight molecules, whereas microbial oxidation initially affects smaller, more soluble molecules (Leahy et al., 1990; Nicodem et al., 1998; Dutta et al., 2000; Prince et al., 2003).

Oil droplets disperse into the water column, often creating stable water/oil emulsions, such as tar balls, that slow the evaporation and spreading of spilled crude (Fingas 2008). Dissolution of water-soluble components of crude oil spilled into seawater is augmented when oil droplets are formed, due to the increased surface area,

thereby increasing the introduction of toxic compounds (Boehm et al., 2007). The use of dispersants can amplify this process (Yamada et al., 2003; Couillard et al., 2005). Dissolved and dispersed crude oil components will diffuse throughout the water column as a result of currents. Some compounds will adsorb to particulates in solution, causing sedimentation (Backhus et al., 1990; Prince et al., 2003).

Water-accommodated fraction (WAF) is defined as the components of an oil slick which dissolve and disperse into solution (seawater), and do not form emulsions. For this study, WAF also describes the solution itself.

1.1.4 Toxicity

One form of environmental damage occurs via toxicity associated with ingestion or absorption of dissolved and dispersed crude oil. Many aromatic compounds like benzene and fluorene (Figure 1.2) are on the EPA's priority pollutant list (EPA 2012). Toxic unresolved complex mixtures of aromatic hydrocarbon contaminants from crude oil have been shown to bioaccumulate in mussels, reducing their feeding rate through nonspecific narcosis (Booth et al., 2007). Application of dispersants increases the toxic hazard of crude oil in seawater by improving the bioavailability of less soluble PAHs for marine larval fish (Couillard et al., 2005; Allan et al., 2012). WAFs of chemically dispersed South Louisiana crude oil have been determined to be toxic to larval shrimp and estuarine fish (Hemmer et al., 2010).

The toxicity of oil is predominantly determined by its chemical composition (Mendelssohn et al., 2012), form (crude or refined, surface slick or dispersed), and

molecular weight (Laws 2000). High molecular weight PAHs are the most toxic hydrocarbons found in oil, but many high molecular weight PAHs have an extremely low solubility compared to lower molecular weight PAHs, and the latter are considered more dangerous.

Weathering alters the chemical composition of crude oil, changing its bioavailability, therefore affecting toxicity. Most microbial degradation targets long chain alkanes and smaller molecular weight molecules first. As a result, higher molecular weight PAHs stay in solution longer. Weathering via photooxidation targets larger molecules such as PAHs, first (Prince et al., 2003, Mendelssohn et al., 2012). Crude oil released below the photic zone, or beneath an oil slick blocking UV light, will undergo very limited or no photodegradation, allowing continued transport of PAHs into the environment. In areas where natural seeps occur, ecological impacts are reduced due to the combination of slow rate of release and acclimated biota (National Research Council 2003; Hazen et al., 2010). However, anthropogenic sources, such as the DWH spill, can saturate the environment, overwhelming natural remediation processes beyond their threshold (Camilli et al., 2010).

Dispersants are intended to dissolve and separate surface oil slicks, helping to prevent the formation of emulsions and expedite the degradation process. However, addition of dispersants causes an increase of the less soluble, highly toxic, higher molecular weight PAHs (Yamada et al., 2003; Couillard et al., 2005). Furthermore, the dispersant Corexit®, which was applied during the DWH spill, is toxic to oil-degrading bacteria, increasing the persistence of toxic PAHs that would otherwise naturally biodegrade (Hamdan et al., 2011). The transport of hydrophobic PAHs can also be

enhanced by mobile organic and inorganic colloids found in natural waters (Backhus et al., 1990).

1.2 Oil Identification and Spectral Fluorescence

The complex composition of petroleum is challenging for analysts, creating the need for sophisticated instrumentation, and generally time-consuming sample preparation, which can make the process costly. Crude oil can be characterized using several analytical techniques, including GCMS, inductively coupled plasma mass spectroscopy (ICPMS), high performance liquid chromatography (HPLC), and fluorescence spectroscopy (Rodgers et al., 2011). The use of these techniques independently, or in concert, provides detailed, comprehensive compositional data. Industry and academia have utilized these analytical techniques to detect, identify and understand crude oil (Ryder 2005; Rodgers et al., 2011). However, not all of these techniques are equally useful. Limitations of analytical techniques like GC, HPLC and ICP include temperature sensitivity, and time- and resource-consuming sample preparation (Booksh et al., 1996). Chromatographic column specificity is not necessarily ideal for the initial compositional analysis of highly complex, unknown petroleum samples, in part because of the added expense when multiple columns are needed.

Because PAHs are fluorophores (molecules that fluoresce) they can be tracked using fluorescence spectroscopy. Some techniques used to study crude oil are not as robust or user-friendly, and most are not as portable as fluorescence spectroscopy (Stedmon et al., 2008; Rodgers et al., 2011). Spectral fluorescence is a nondestructive, relatively inexpensive, quantitative and qualitative optical technique used in research,

refineries, and spill response (Ryder 2005; Steffens et al., 2010; Rodgers et al., 2011). All this combined with high sensitivity, portability and user-friendly instrumentation makes fluorescence spectroscopy the foremost optical method available. The study of crude oil fluorescence would help improve in situ fluorometers to target toxic PAHs and track them in aquatic environments.

1.2.1 Introduction to Spectral Fluorescence

In the most simplified terms, fluorescence is the re-emission of energy at a longer wavelength (lower energy) by a molecule after it absorbs light energy at a shorter wavelength (higher energy). The absorbed and re-emitted energy is light energy in the form of photons. Absorbance at shorter wavelengths and emission at longer wavelengths is called a Stokes Shift, and the decrease in energy is caused by vibrational relaxation of the excited electrons. Fluorescence can be represented in a simplified Jablonski Diagram (Figure 1.4).

Some molecules can absorb energy at certain wavelengths but cannot re-emit this energy at higher wavelengths. As a result, they do not fluoresce. Other molecules have an absorption spectrum that overlaps with a fluorophore's emission spectrum and can effectively quench, or extinguish, fluorescence (Figure 1.4). Energy that has been absorbed by a molecule can also be subject to non-radiative emission in the form of heat energy or vibrational relaxation. In samples with high turbidity, or optical density, other molecules, including other fluorophores, will absorb incoming excitation and re-emitted light energy from nearby fluorophores. These are the main sources of inner filter effects

(IFE). IFEs lead to an apparent decrease in fluorescence intensity, but the resulting data can be corrected.

Fluorophores are quite common. They can be found in antifreeze, tonic water, asphalt, in the atmosphere from internal combustion engine exhaust, and in rivers and oceans as a component of colored dissolved organic matter (CDOM). Fluorophores are also used as DNA stains and probes (Marr et al., 1999; Lakowicz 2006; Coble 2007; Montgomery et al., 2011). Fluorophores have been used to characterize petroleum products for many years (Steffens et al., 2010). The wavelengths of light energy that a fluorophore absorb and re-emit are unique to that compound, allowing for distinct identification through spectral fluorescence techniques.

1.2.2 Fluorophores and Oil: What Fluoresces?

There are many molecules that absorb light energy, but not all fluoresce. Fluorophores have a specific structure that determines fluorescence properties and allows the re-emittance of absorbed energy at a lower energy/longer wavelength (Lakowicz 2006; Steffens et al., 2010). Part, if not all, of their structure is made of conjugated double bonds in cyclic form (aromatics). The simplest, and perhaps most recognized aromatic structure is that of benzene (Figure 1.2). Benzene rings are stable and allow for low energy electron transition. Aromatic molecules are less susceptible to dissociation and intersystem crossing than less complex alkyl compounds, and more likely to fluoresce (Turro 1991; Watson et al., 2001; Van Hold et al., 2006).

Aromatic compounds make up one of the compositional groups found in crude oil (Figure 1.1). PAHs make up the majority of the aromatic compounds found in crude oil

and are responsible for the majority of crude oil fluorescence (Reed et al., 1977; Dabestani et al., 1999). PAHs are molecules made up of multiple fused benzene rings. The simplest PAH found in crude oil is fluorene (Figure 1.2). Other aromatic compounds found in crude oil include heterocyclic molecules (molecules that have at least one other element besides carbon in the ring structure). Heterocyclic molecules that are fused to homocyclic compounds (such as asphaltene to benzene) are more likely to fluoresce than a simple, un-fused heterocyclic molecule because of the increased stability and lowered energy transitions (Ralston et al., 1996; Groenzin et al., 1999).

All fluorophores have a unique fluorescence signature, or fingerprint. Many high molecular weight molecules, including aromatic asphaltenes and large PAHs, are insoluble or have an extremely low solubility, and so will not contribute to the fluorescence signature of the dissolved portion of crude oil.

1.2.3 Spectroscopic Instrumentation

In any given sample there will be a variety of dissolved molecules, some which fluoresce. All molecules that fluoresce will absorb light energy, but not all molecules that absorb light energy are fluorophores. Spectrophotometers determine light absorbance by measuring the amount of light that is transmitted through a sample (Figure 1.5). Molecules that are dissolved in a sample, and are capable of absorption, will absorb light at specific wavelengths and intensities. Absorbance measurements are taken to help determine fluorescence intensity and correct for IFE.

Fluorescence, or the re-emission of light at lower energy (longer wavelengths), is measured using a spectrofluorometer (Figure 1.6). Light energy is sent through a

monochromator to selectively isolate specific wavelengths and is sent through a sample. Molecules in a sample will absorb the light, and any fluorophores in the sample will re-emit at a longer wavelength. Re-emitted light is sent through a second monochromator, which isolates a selected range of wavelengths as the signal is sent to the photomultiplier tube (PMT). Incident light is designated by excitation wavelengths, and re-emitted light by emission wavelengths (Figure 1.6). Both excitation and emission spectra can be displayed in a three-dimensional representation of sample fluorescence called an excitation emission matrix (EEM) (Figure 1.7) (Booksh et al., 1996).

The practical application of fluorescence spectroscopy has been a part of petroleum detection for over six decades (Steffens et al., 2010; Rodgers et al., 2011). The versatility and usefulness of this technique is demonstrated by its availability from relatively portable bench top spectrofluorometers to in situ instrumentation (Ryder 2005). In many cases minimal preparation is needed for the nondestructive and noncontact sample analysis (Ostgaard et al., 1983; Maher 1986; Ziolli et al., 2002; Boehm et al., 2007). While the study of neat (unweathered) crude oil in seawater using fluorometers are relatively new, evaluating crude oil WAF is particularly novel (Ryder 2005). This study explores the WAF of crude oils, adding to our understanding of the dissolved and dispersed portion of crude oil and its fluorescence behavior in seawater.

1.2.4 Fingerprinting Crude Oil – Characterization and Identification

Spectral fluorescence studies have shown that EEMs (Figure 1.7) of compounds and combinations of compounds have specific fluorescence signatures, or fingerprints (Lakowicz 2006; Christensen et al., 2007; Coble 2007). Crude oil can be differentiated

by its specific EEM signatures due to variability of chemical composition (Stasiuk et al., 1997; Ryder 2005; Hegazi et al., 2001; Steffens et al., 2010). Many oils share similar chemical qualities, varying in relative composition and concentration of these components (Figure 1.1) (Ryder 2005). Molecules that do not fluoresce can play a principal role in affecting fluorescence due to IFEs, quenching and energy transfer between fluorophores and other molecules. Neat crude oil will have a higher concentration of fluorophores than WAFs due to low solubility of many fluorescent components. Fluorescence signatures of neat crude oil can be differentiated from WAFs due to the decreased quenching rate of the diluted components and higher quantum yields (Patra et al., 2001; Ryder 2005). Heavier oils have an increased concentration of high molecular weight molecules (i.e., more fluorophores). This can lead to complications in fluorescence, including higher rates of quenching. However, these complications can ultimately translate into a unique fluorescence signature.

Oil emulsions (sometimes called mousse or "chocolate mousse") are viscous, stable mixtures of crude oil and seawater that form during oil spills. Asphaltenes are found in heavy crude oils and are central to the formation of emulsions (Bridie et al., 1980; Fingas 2008). The fluorescent properties of asphaltenes are dependent on their molecular weight (Strausz et al., 2009). Like neat fuels and crude oil WAFs, emulsions are subject to energy transfer and quenching processes.

Fingerprinting crude oil is not limited to spectral fluorescence EEM analysis. Other analytical techniques like GCMS are used in conjunction with fluorescence to further characterize crude oil components (Christensen et al., 2004; Wang et al., 2006). Fluorescence spectroscopy is a relevant tool in oil spill recovery and response as seen in

the continued research at Prince William Sound and Galicia, Spain from the *Exxon Valdez* and *Prestige* spills, respectively (OSRI 2000; Huggett et al., 2003; Gonzalez 2006). Its application during DWH was vital in helping track the subsurface oil plume in the Gulf of Mexico (Camilli et al., 2010; Diercks et al., 2010; MBARI 2010). Used on its own or in a suite of methods, fluorescence spectroscopy provides valuable quantitative and qualitative information (Stedmon et al., 2008; Steffens et al., 2010).

1.2.5 Complications and Considerations

Several factors affect fluorescence, including instrument artifacts, the optical properties of the samples, and sample conditions. It is important to understand these factors and to control them as much as possible. Complications in fluorescence can be intrinsic, generated by the instrument, solvents or contamination.

Stray light can distort and invalidate excitation and emission spectra. Diffraction gratings and filters are used in the design of spectrofluorometers to eliminate stray light, from both internal and external sources.

The scattering of light must also be taken into account. Rayleigh and Raman scattering are inherent to spectroscopy. Raman scatter will occur from all solvents, even water (Lakowicz 2006). Rayleigh scatter has a strong dependence on emission wavelengths, and can interfere when fluorescence emission wavelengths are close to the excitation wavelengths. Raman scatter is independent of excitation wavelengths, but in fluorescence spectra it is seen at a consistent difference relative to excitation wavelengths. Scatter can be eliminated, or corrected for, by the subtraction of blank or control sample spectra.

As previously mentioned, samples with high turbidity or optical density can cause the absorbance of light from non-fluorescent components, or reabsorption of fluorescence, affecting analysis. IFEs cause an apparent decrease in fluorescence intensity. These effects are reduced by the right angle observation found in spectrofluorometers (Figure 1.6).

Energy transfer and other forms of quenching also arise due to chemical and physical complexities of samples. High concentrations of fluorophores can result in a higher rate of quenching and lower quantum yield, or intensity. Sample dilution can resolve some of these issues by decreasing the quenching rate and raising the quantum yield of some components (Ryder 2005; Lakowicz 2006). However, a diluted sample could still have a lower overall fluorescence compared to neat crude oil. Some of these influences can create key signatures, unique to a sample or set of samples. It is important to be aware of factors that may complicate fluorescence signatures when dealing with complex samples such as crude oil.

Other factors arise outside the laboratory that will affect fluorescence including temperature and naturally occurring fluorescent compounds like CDOM. Temperature and concentration of aromatic compounds are inversely proportional (Maher 1982). Fluorescence intensity is influenced by fluorophore concentration; thus, at low temperatures there is an increase in fluorescence signals (Maher 1982; Zhu et al., 1992). Increased temperatures can cause an increase in non-radiative relaxation of molecules in solution, also called thermal quenching (Zhu et al., 1992). Although fluorescence of CDOM can interfere with crude oil fluorescence, there are ways to distinguish their various signals (Patsayeva 1995; JAG 2010). Having an understanding of the known

biological or physical processes in a sampling area, and collecting fluorescence data over a range of ex/em wavelengths can help determine the contributing source of fluorescence signals.

Weathering of crude oil changes its chemical and physical properties and thus its fluorescence properties. Volatile substances are lost via evaporation. Photodegradation has a particularly destructive effect on PAHs and other high molecular weight molecules in petroleum (Nicodem et al., 1998; Dutta et al., 2000; Prince et al., 2003). Microbial degradation at low rates occurs first on lower molecular weight, less polar compounds, and then begins to affect aromatics and other higher molecular weight, polar molecules (Leahy et al., 1990; Dutta et al., 2000; Prince et al., 2003).

Crude oil released in the water column is not exposed to the same conditions as on the water's surface, and thus weathers differently. Volatile and UV sensitive compounds are not immediately exposed to atmosphere and light, and will stay in solution (Boehm et al., 2007). Partitioning, or density stratification, of hydrocarbons has been observed during the DWH spill caused by thermal stratification, salinity differences, and higher pressures encountered in deep water. Specific chemical components were found in the underwater plume, while others diffused to the surface waters (Johansen et al., 2003; Gonzalez et al., 2006; Camilli et al., 2010; Diercks et al., 2010).

Introduction of dispersants to crude oil samples enhances fluorescence emission (Kepkay et al., 2008; Bugden et al., 2008). The dispersant Corexit® causes an increase in the aqueous concentration of less soluble, higher molecular weight PAHs (Yamada et al., 2003; Couillard et al., 2005). The increase in PAHs in solution corresponds to the increase in fluorescence (Kepkay et al., 2008). The effectiveness of dispersants decreases

as crude oil weathers (Chandrasekar et al., 2006); however, some dispersants are toxic to oil degrading bacteria (Hamdan et al., 2011) which would interfere with natural microbial degradation.

Though forms of quenching and weathering as well as the addition of chemical dispersants could be described as interferences rather than simple complicating factors of spectral analysis, they can also be key fluorescence signatures, unique to the specific micro-environment and situation. Studying crude oil in the laboratory and in the natural environment using in situ fluorescence to monitor its changes over time will help gain a better understanding of these processes.

1.2.6 In Situ Fluorescence

Major differences between surface, shallow-water and deep-water spills are due to changes in physical conditions and weathering. Aerial views of surface slicks cannot determine what fraction and how much of spilled oil has dissolved and dispersed. In situ fluorometers are used as cost-effective tools to detect fluorophores in different aquatic environments, identifying portions of spills that cannot be seen or easily tracked. Application of in situ fluorescence sensors to detect and monitor spilled crude oil occurred after the DWH spill as a first response measure (Camilli et al., 2010; Diercks et al., 2010; JAG 2010; MBARI 2010).

The partitioned underwater plume detected during the DWH spill showed a greater abundance of toxic aromatic hydrocarbons in deeper waters than at the surface (Camilli et al., 2010). Only one of the sensors used during the DWH spill is designed to target aromatic hydrocarbons. However, knowledge regarding the complex degradation

of crude oil in the environment and its effect on fluorescence is limited. Fluorescence spectroscopy has the potential for improved targeting of the fluorescent components of crude oil, specifically PAHs.

1.3 Rationale and Objectives

The increase in demand for crude oil, and subsequent rise in extraction, transportation and use, creates lasting environmental effects resulting from the reintroduction of petroleum products into the environment as contaminants. This requires diligent and effective observation to fully assess damages of persistent pollution, and to design and implement optimal remediation methods.

In situ application of fluorescence spectroscopy is cost-effective and has the potential for improved specificity of hydrocarbon detection. An investigation of the degradation and changing fluorescence signatures of crude oil determined optimized fluorescence peaks that can be applied to responder fluorometers. These data could be used to develop more economical and efficient in situ instrumentation as well as facilitate an improved understanding of current and future oil spill response fluorescence data.

The purpose of this study was to investigate the spectral fluorescence properties of the WAF of crude oil in seawater and how fluorescence signatures change when it is exposed to weathering conditions, specifically photooxidation. Our goals included determining whether there is any pervasive fluorescence signatures found throughout a variety of crude oil WAF, how these signatures differed, how photooxidation affected fluorescence over time, if any pervasive signatures were resistant to degradation, and if

any they could be used to differentiate oil spill properties and discriminate from background signals.

1.4 Chapter 1 Figures and Tables

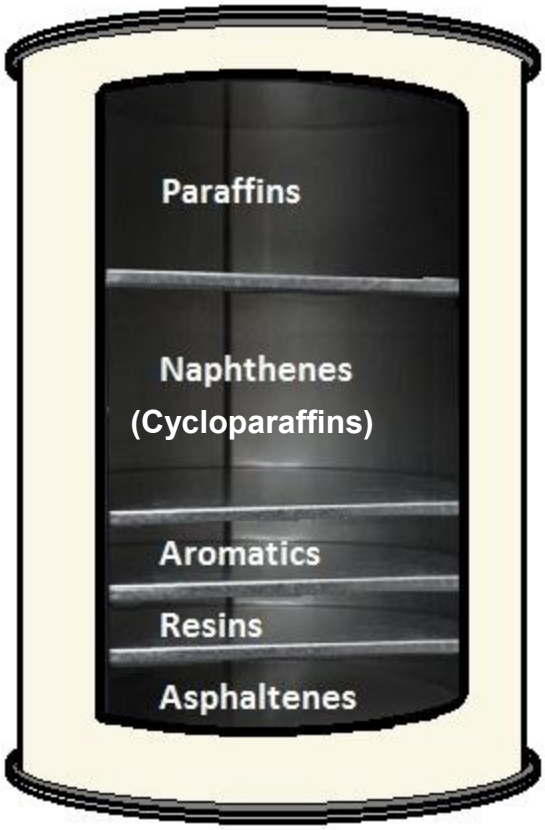

Figure 1.1. Crude Oil Barrel. This figure illustrates the major identifying components of crude oil: hydrocarbons (Paraffins, Naphthenes, also called Cycloparafins, and Aromatics) and non-hydrocarbons (Resins and Asphaltenes). The concentration and relative amounts of major components (represented by space in the barrel) will change based on crude oil source.

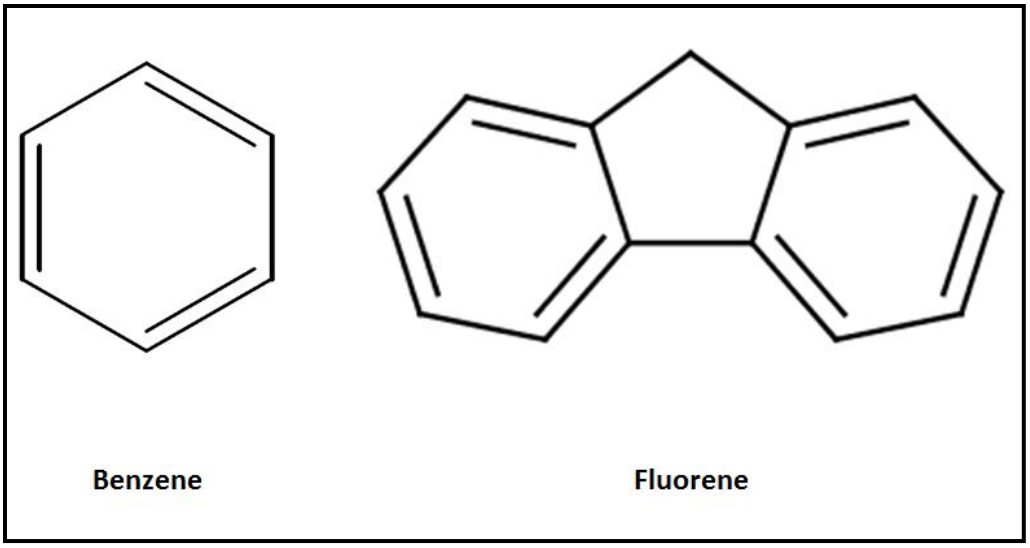

Figure 1.2. Aromatic Hydrocarbons. Benzene is the simplest aromatic structure, and fluorene is one of the simplest polycyclic aromatic hydrocarbon compounds.

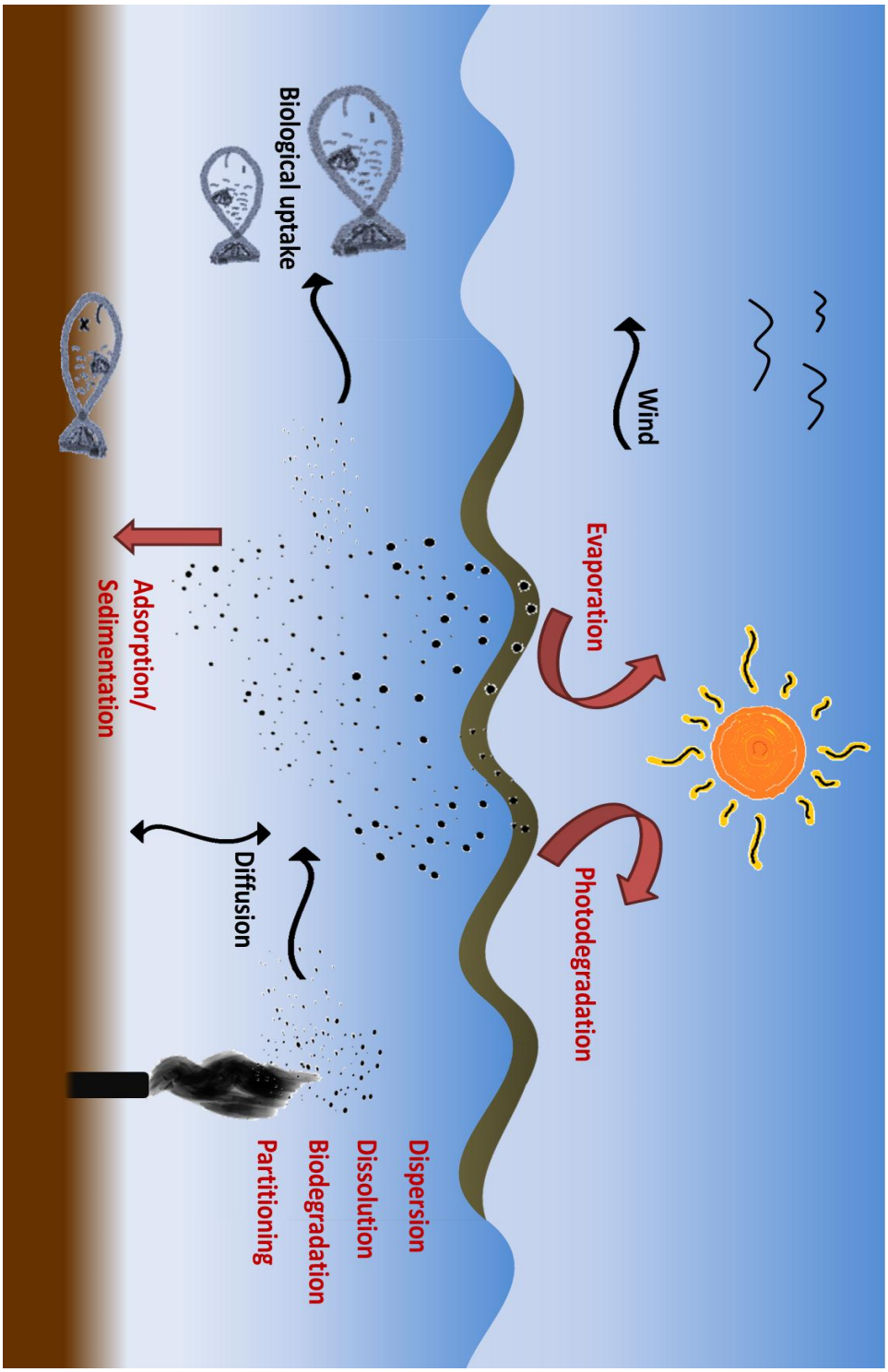

Figure 1.3. Weathering of Crude Oil. Chemical and physical changes are represented in red. Black arrows represent physical influence and transport. Vertical and horizontal diffusion is caused by water currents and mixing.

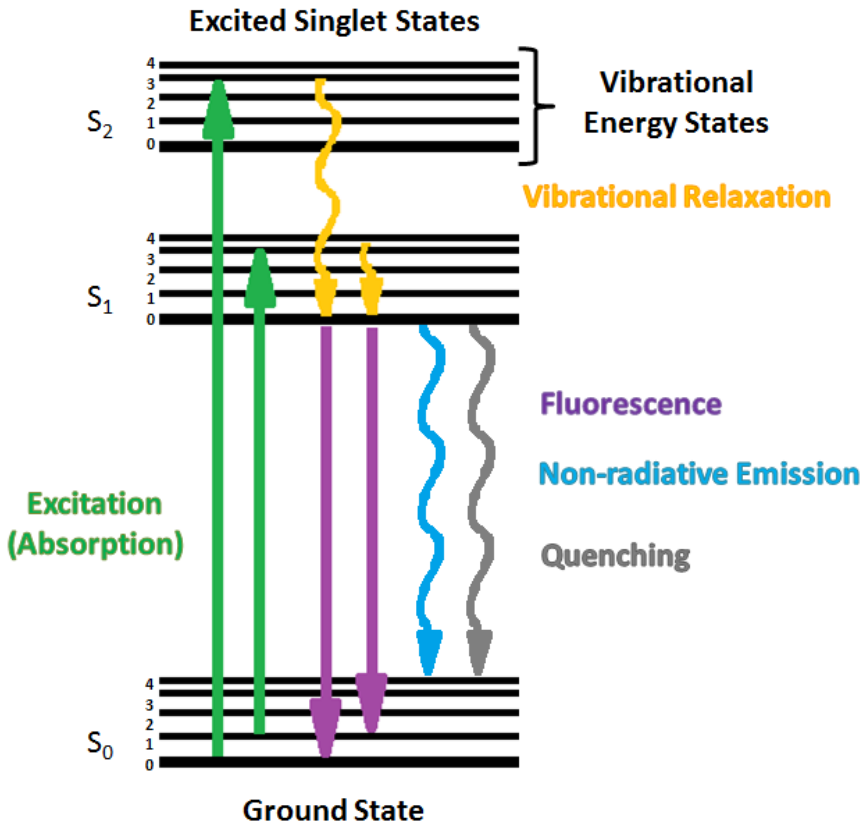

Figure 1.4. Simplified Jablonski Diagram. This figure shows a simplified example of fluorescence: A molecule is excited by light energy from its ground state to an excited singlet state, then experiences vibrational relaxation, then will re-emit at a lower energy level. Green arrows: Excitation (absorption). Purple arrows: Fluorescence. Yellow arrows: Vibrational relaxation. Blue arrows: Non-radiative emission such as intersystem crossing and energy transfer.

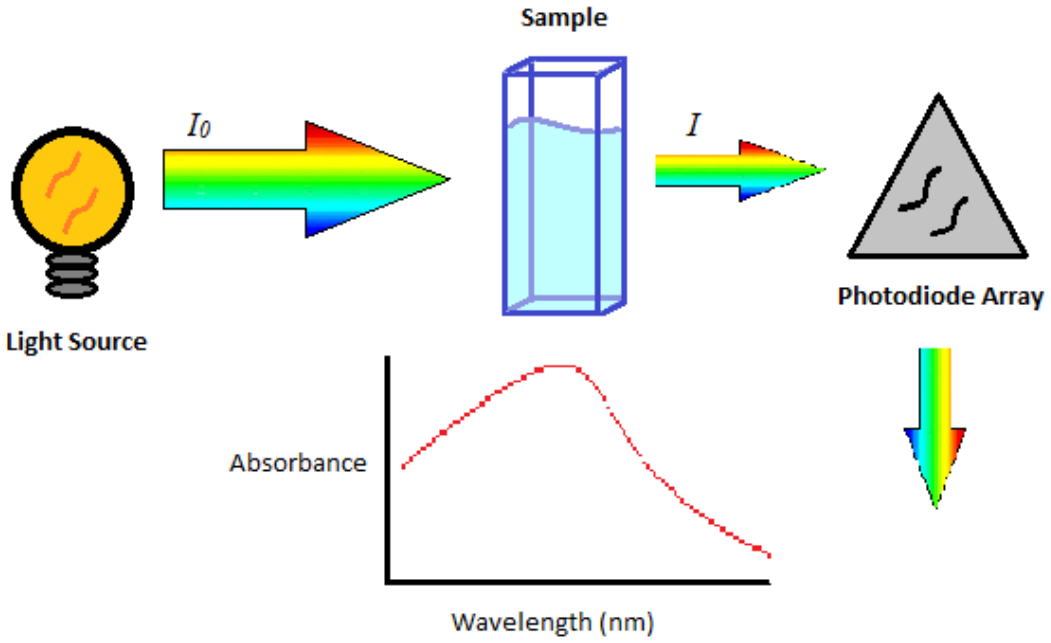

Figure 1.5. Spectrophotometer. A light source is directed at a sample at a particular intensity (I_0) while a photodiode array is used to detect the intensity of light that passes through the sample (I).

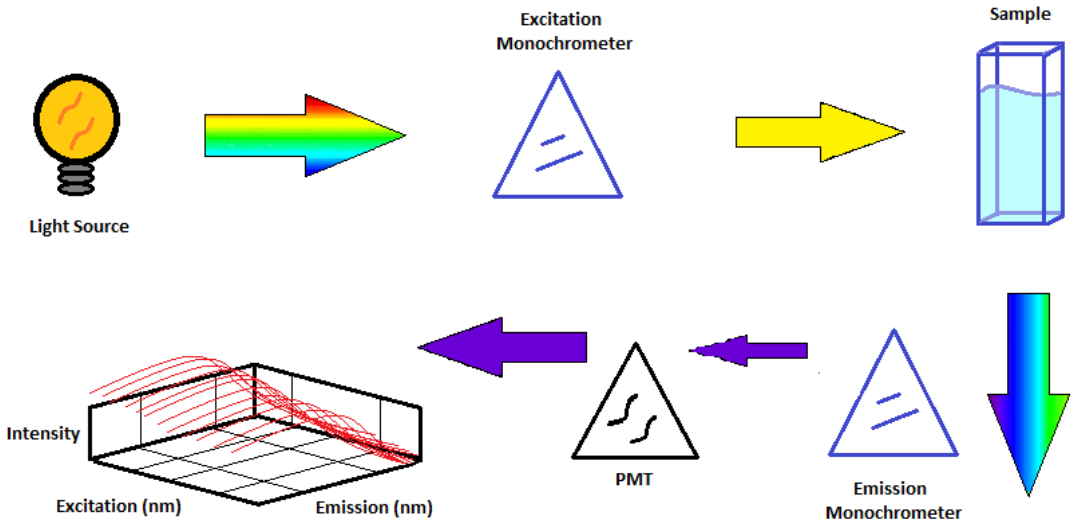

Figure 1.6. Spectrofluorometer. A light source is directed at a sample at a particular intensity. An excitation monochromator isolates a desired wavelength. Fluorophores in the sample absorb the excitation light then re-emit at a lower energy. An emission monochromator incrementally isolates re-emitted light over desired range of wavelengths. This process is repeated sequentially over a selected range of excitation wavelengths. A photomultiplier tube (PMT) is used as a detector.

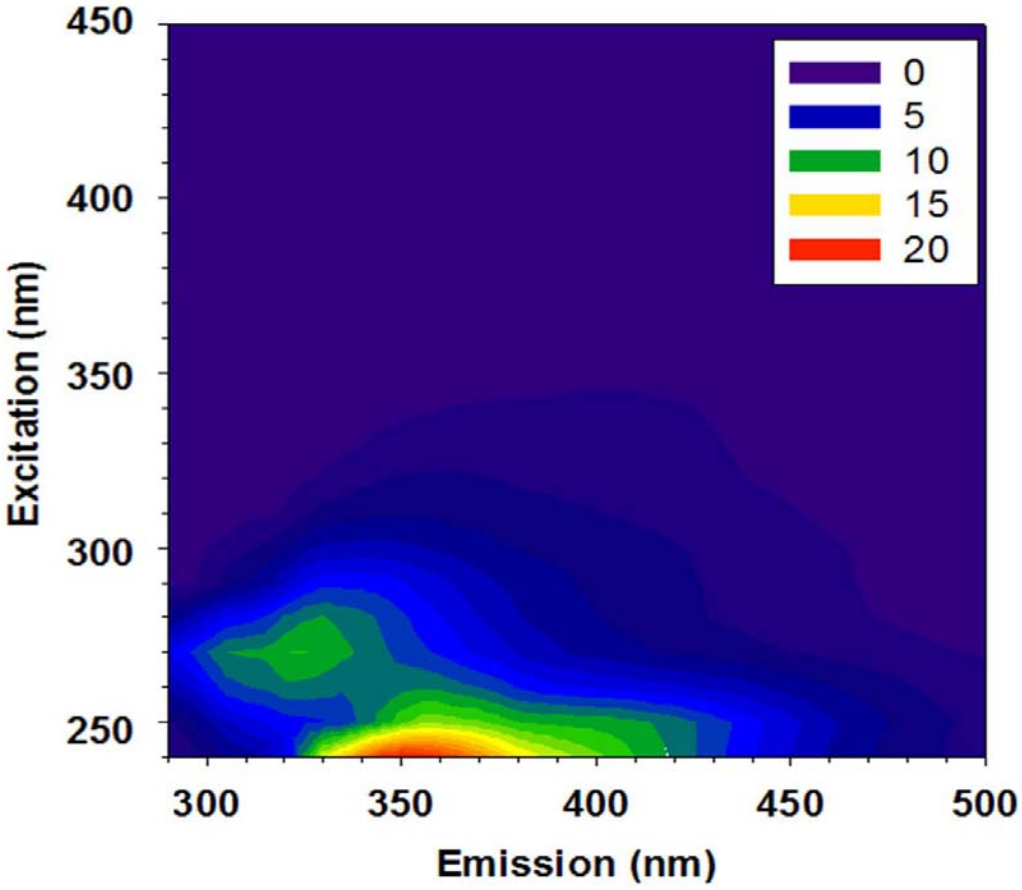

Figure 1.7. Excitation Emission Matrix. Scanning fluorometers combine fluorescence emission spectra measured from a series of different excitation wavelengths to create excitation emission matrices (EEMs).

CHAPTER 2

A Spectral Fluorescence Study of Crude Oil WAF with GCxGC-TOFMS Analysis

2.1 Abstract

As exploitation of oil resources increases, the need to respond to accidents and better understand the impact of oil in the environment is growing commensurately. During the 2010 Gulf of Mexico oil spill, highly sensitive fluorometers were employed as cost effective tools for in situ tracking of the underwater hydrocarbon plumes that resulted from crude oil released on the sea floor. However, concerns over sensitivity, relative performance of different sensor products, interferences, and simply how fluorescence signals should be interpreted, highlight the need to better understand fluorescence behavior of oil during spills.

Polycyclic aromatic hydrocarbons (PAHs) are an important and potentially toxic component of the crude oil spills, and many individual PAHs are fluorescent. However, existing fluorometers are not designed to specifically target PAHs. An investigation of the fluorescence properties of the water-accommodated fraction (WAF) of a variety of crude oils in seawater was undertaken to further refine in situ instrument sensitivity for targeting PAHs. A subset of these samples was subjected to photodegradation to determine changes associated with this weathering process. In addition, we used two-dimensional gas chromatography analysis with time-of flight-mass spectrometry detection to verify WAF composition and PAH concentration.

Key excitation and emission wavelength ranges (240-270 nm and 305-360 nm, respectively) were ubiquitous throughout the crude oils tested. After exposure to a full-spectrum solar simulator (2476.82 $\mu E/m^2/sec$) over seven hours, degradation rate constants of key excitation/emission (ex/em) peak pairs showed persistent fluorescence signals at 270/310 and 270/325 nm ex/em for Merey crude oil WAF, 270/305 nm for Hoops crude oil WAF, and 270/305 nm for South Louisiana crude oil WAF. GCxGC-TOFMS analysis of the WAF of two distinctive crude oils revealed compositional similarities of PAH constituents. Of the similarities, fluorene is a contributing factor to the source of the persistent fluorescence signals at 270 nm ex. The known PAH compounds found in WAF solution of the crude oils tested make a compelling case for refined in situ tracking of dispersed toxic crude oil components. In situ fluorometers could be adapted for improved tracking of a variety of crude oils, targeting the persistent peaks found in the range of 240-270 nm ex and 305-360 nm em.

2.2 Introduction

The effects of the Deepwater Horizon spill (DWH) are far reaching and likely to have an enduring impact on ecosystems of the Gulf of Mexico. Crude oil spilled and dispersants released at approximately 1500 m depth resulted in the distribution of hydrocarbons throughout the water column to an extent never before recorded (Camilli et al., 2010; Diercks et al., 2010; JAG 2010; Mendelssohn et al., 2010). In addition, the dynamic water currents and deep circulation of the Gulf of Mexico are encumbrances that can make finding and tracking subsurface plumes difficult (Welsh et al., 2000; DeHaan et al., 2005; Maltrud et al., 2010). One consequence of the spill occurring at the bottom of

the water column was the partitioning of PAHs between surface and deep waters (Camilli et al., 2010; Diercks et al., 2010).

The use of fluorescence in the detection and long-term monitoring of crude oil is well established (OSRI 2000; Gonzalez et al., 2006). Several in situ fluorometers were deployed to track the subsurface plume in the Gulf of Mexico caused by the DWH (Table 2.1) (Camilli et al., 2010; Diercks et al., 2010; MBARI 2010). From the table you can see that all of these fluorometers detect signals at one excitation/emission pair, but only one of the four sensors is designed to target aromatic hydrocarbons. It is not known which fluorescence signals of the dissolved portion of crude oil are the most robust when faced with weathering. While fluorometric data provide valuable information, it is unclear how changing fluorescence signals relate to the dynamic environmental fate of crude oil.

The multifaceted weathering process undergone by crude oil in the environment includes evaporation, dissolution, dispersion, photodegradation, and biodegradation (Laws 2000; National Research Council 2003). Weathering facilitates introduction of carcinogens into the food web when different trophic levels found throughout the water column are exposed to crude oil constituents like PAHs (Neff et al., 2000; Peterson et al., 2003). Investigating how PAH fluorescence signals change with weathering will help us better understand how to design optimized sensors to track crude oil and its toxic components, and how environmental processes affect fluorescence signatures.

These experiments focus on the WAF of crude oil in seawater and the effects of photooxidation on its fluorescent components. In this study WAF refers to both the components of an oil slick which dissolve and disperse into solution and do not form

emulsions, and the artificial saltwater (ASW) solution containing these components (Figure 2.1). We explore changes in spectral fluorescence due to weathering by evaluating the Excitation Emission Matrices (EEMs) of several different crude oil WAFs. Ubiquitous and persistent ex/em signals were identified and can be used to improve the selectivity of discrete fluorometers to target PAHs. These data will improve our understanding of fluorescent signature changes due to weathering processes and facilitate interpretation of EEMs from field samples, placing the volumes of discrete fluorometer data collected in response to oil spills in a broader context.

2.3 Experimental

2.3.1 Crude Oil

Three crude oils, including South Louisiana, Hoops and Merey (Table 2.2), were selected to exemplify the range of existing properties, including density (light, medium and heavy), and proximity to the Gulf of Mexico. South Louisiana crude was chosen to represent the oil released during the Deepwater Horizon spill (Reddy et al., 2011). The oil was purchased in 4 mL vials and 100 mL amber jars from the fossil fuel distributor ONTA Inc. (Toronto, Canada). These were kept at room temperature and in the dark, except during experiment preparation.

2.3.2 Medium

Artificial saltwater (ASW) with an ionic strength comparable to seawater was prepared using 32.16g/L sodium chloride (NaCl), 7.12g/L magnesium sulfate ($MgSO_4 \cdot 7H_2O$), and 0.17g/L sodium bicarbonate ($NaHCO_3$) in Milli-Q water (18 MΩ.cm @ 25˚C), and was filtered (0.2 μm) and stored in a sterile 10 L glass carboy at room temperature. ASW was used to prepare the crude oil WAF for method verification and equilibration study, and the photooxidation study.

2.3.3 Method Verification and Crude Oil WAF Equilibration Study

A simulated oil slick was prepared (at a 1:40 ratio of oil to ASW) to extract the WAF of the chosen crude oils, corresponding to previous methods (Maher 1982; Ostgaard et al., 1983; Maher 1986; Ziolli et al., 2000; JAG 2010). Oil addition was performed using the weighing-by-difference method, carefully layering 6 mL by weight on top of 240 mL of ASW in glass biological oxygen demand (BOD) bottles. Oil volume was calculated from supplier-provided densities; temperatures during preparation ranged from 20-25 ˚C. Stainless steel (316 SS) tubes were used for extracting the WAF via nitrogen gas displacement, and high-purity platinum-cured silicone stoppers were used to seal the BOD bottles (Figure 2.1). During the addition of the oil layer, stoppers with SS tubes installed were pulled up and to the side of the neck of each BOD bottle, leaving a portion of the longer sampling tube submerged in ASW. We did this to prevent oil from getting inside the sampling tube during sampling (and thus contaminating the WAF). BOD bottles were chosen to maintain uniform oil-water contact surface area as WAF was displaced due to sampling.

Each oil sample was prepared in triplicate. A control was prepared in triplicate consisting of ASW with no crude layer added. The headspace of all oil samples and control BODs was purged with nitrogen gas to prevent oxidation of the surface slick. Sampling tubes were sealed with high-purity silicone tubing with clamps on the end of each tube to decrease the potential for oxidative degradation of the oil surface. All samples were placed on a shaker table (90 rpm) (JAG 2010), in the dark, at room temperature (25 ˚C). WAF was sampled using pressure displacement by supplying low-pressure nitrogen gas into the top of the BOD bottles through the short SS tube, collecting ASW from below the oil slick through the long SS tube into combusted amber vials (Figure 2.1).

2.3.4 Photooxidation

Photooxidation experiments were performed on the WAF of all three chosen crude oils. The oils were first prepared as described in the WAF equilibration study. After the equilibration period, the aqueous extract was separated into open amber glass vials, placed into a rack, and kept between 15-20 ˚C via partial submersion in an ice water bath. The rack was positioned under a full spectrum Newport ORIEL solar simulator with a 1 kW xenon arc lamp emitting between 300-722 nm (2500 $\mu E/m^2/sec$), and agitated continually throughout the experiment to ensure mixing within the vials. Five time points were tested, from zero (no UV exposure) to seven hours of UV exposure (T0 = 0 hrs, T1 = 1 hr, T2 = 2 hrs, T3 = 5 hrs, and T4 = 7 hrs), and dark controls were tested after seven hours (two amber vials were covered in combusted foil for seven hours). Duplicate samples were tested to show that positioning under the solar simulator

lamp did not change the effect of UV exposure on fluorescence. At the respective time points, sample vials were covered with combusted foil to block any continued exposure to light and kept at room temperature for the remainder of sample analysis.

2.3.5 Fluorescence Analysis

All fluorometric analysis was performed using a Horiba Jobin Yvon Fluoromax-4 spectrofluorometer (Fluoromax 4) with a 150-W xenon lamp, 5 nm bandpass. Excitation emission matrices (EEMs) were obtained by exciting the samples between 240-450 nm in increments of 10 nm, and collecting emission spectra between 290-500 nm in increments of 5 nm. Instrument correction factors were used to correct for artifacts inherent to imperfections in the optical components. These data were also blank subtracted. Absorbance measurements were conducted using a J&M TIDAS spectrophotometer (Tidas I) from 186-722 nm. Fluorometric sample data was corrected for the inner filter effect (IFE) (Lakowicz 2006) and Raman normalized according to Murphy et al., 2010. These corrections formed a standard procedure that was followed to process all raw fluorescence data, allowing for reliable data comparability.

2.3.6 GCxGC-TOFMS Analysis

Two-dimensional gas chromatography with time-of-flight mass spectroscopy detection (GCxGC-TOFMS) was used to analyze WAF samples from South Louisiana and Merey crude oil. GCxGC is a powerful multidimensional technique that is able to

characterize complex samples, like crude oil, reduce interference and provide highly resolved data in a way that one-dimensional GC cannot.

The WAF from both South Louisiana and Merey crude oil were spiked with chrysene-D12 and fluorene-D10 surrogate standards and PAHs were extracted by solid phase extraction (SPE) using Supelclean ENVI-18 tubes (Sigma-Aldrich part # 57064). The PAH WAF extract was eluted using 2mL toluene:MeOH (10:1). Eluate was dried using sodium sulfate, concentrated to dryness, brought up to 150 uL with CH_2Cl_2, then spiked with 10uL phenanthrene-D10 and naphthalene-D8 internal standard. An aliquot of the South Louisiana and Merey CH_2Cl_2 solution was injected and analyzed using a Leco Pegasus 4D comprehensive GCxGC-TOFMS. The primary column was a non-polar Agilent DB-5ms, phenyl arylene polymer, 30 m length, 0.25 mm id, and a 0.25 μm film thickness. The secondary column was a polar SGE BPX-50, 50% phenyl polysilphenylene-siloxane, 1.5 m length, 0.10 mm id, and a 0.10 μm film thickness. The primary oven program was set to 50 °C for 2 min, 8 °C/min until 310 °C, 10 °C/min to 330 °C, then held at 330 °C for 5min. The secondary oven was programed to 55 °C for 2 min, 8 °C/min until 315 °C, 20 °C/min to 355 °C, then held at 355 °C for 5 min. The carrier gas was helium with a column flow rate of 1.35 mL/min. GC inlet temperature was 300 ˚C and was operated in split mode. The transfer line was set at 259 ˚C. Thermal modulator temperature was offset 25 ˚C relative to the primary oven. The modulation period was 4 s with an 0.8 s hot pulse time and a 1.20 s cool time. TOFMS detector was set to scan between 34-500 amu with an acquisition rate of 150 spectra/s, Electron ionization ion source at 200 ˚C, 1550 V detector voltage, -70 ev electron energy.

2.4 Results and Discussion

The fluorescence spectra (EEMs) of WAFs from the selected crude oils identified peak formations over three key excitation wavelengths: 240, 250 and 270 nm. The apparent decrease in fluorescence signal after seven days for South Louisiana, and 21 days for Merey, could be attributed to adsorption onto the surface of the BOD bottles, which has been mentioned in the literature (Maher 1982). There is a slight rise in intensity at 240/350 and 250/360 nm ex/em for Merey crude oil that is likely due to continued slow dissolution of less soluble components.

Commonalities of key spectral emission peaks are seen between the range of light, medium and heavy oil at 250 and 270 nm excitation (Table 2.3). The WAF equilibration study showed that these peak pairs stabilize quickly (approximately two days) and remain so over approximately 30 days (Figure 2.2). WAF equilibration also showed the lightest oil having the lowest fluorescence intensity, and the heaviest oil having the highest at 240 and 250 nm excitation. South Louisiana and Hoops shared similar fluorescence intensities at 240 and 250 nm excitation. All three crude oil WAF signals had similar peak pairs and intensities at 270 nm excitation. This could denote the same signal source and concentration.

Some peak shifting was observed in the emission spectra of all three oils during the WAF equilibration, and the Hoops and Merey oil photooxidation experiments (Table 2.3). Shifts seen are likely due to the varying solubility of different crude oil components. For continuity, only the prevailing emission maximum is listed in the table.

Percent loss was calculated for each crude oil WAF that underwent photooxidation, in an attempt to discriminate between photooxidation and volatilization,

and determine which may be the dominant process degrading the fluorescence signal (Table 2.4). First, calculated P-values indicated a significant difference between seven hours of exposure (T4) and corresponding DCs. Apparent loss due to photodegradation was calculated using T0 and T4 (%Light loss). Potential loss due to volatilization was calculated using T0 and DC (%Dark loss). Loss due to photodegradation was calculated as the difference between % Dark and % Light loss. Table 2.4 shows the highest calculated loss due to photodegradation was the fluorescence signal 250/405 nm ex/em for Merey oil (58 %). This resembles the ex/em of anthracene (Berlman 1971; Beltran et al., 1998), a higher molecular weight PAH expected to be susceptible to photooxidation. The fluorescence signals for South Louisiana at 250/350 nm, Hoops at 250/350 nm, and Merey oil at 250/360nm are also relatively susceptible to photodegradation and resemble phenanthrene and highly alkylated anthracene signals (Berlman 1971).

Fluorescence signals that had comparatively low susceptibility to either photodegradation or volatilization were 270/305 nm for South Louisiana, 270/305 nm for Hoops, and 270/310 and 270/325 nm for Merey crude oil, with Merey at 270/310 being the least vulnerable to degradation (8%). These ex/em pairs resemble fluorene and naphthalene (Berlman 1971; Ostgaard et al., 1983; Beltran et al., 1998), lower molecular weight PAHs that would be less susceptible to photooxidation than the previously mentioned anthracene, phenanthrene and their derivatives.

Photooxidation experiments indicate a persistence of fluorescence signals of crude oil WAF after several hours of significant UV exposure (Figure 2.3). A first-order kinetic model was used to fit photodegradation data (Figure 2.4) and calculate rate constants of key peak pairs (Figure 2.5). This is consistent with methods used in the past

to evaluate crude oil photolysis (Miller et al., 2001; Fasnacht et al., 2002). It is clear that the Merey signal at 250/405 nm ex/em does not share the same linearity as the other key ex/em peaks in a first-order kinetic model (Figure 2.4). This signal is unique to the heavy crude WAF. The cause of non-linearity is unclear based on our data, and further inquiry was outside the scope of this study.

Degradation rate constants for chosen peak pairs were relatively low (Figure 2.5). Merey crude showed a strong fluorescence signal at 250/405 nm ex/em (Figure 2.2) that seemed to degrade much faster than any other signal from any of the oils (Figure 2.3), but was excluded from rate calculations because it did not fit the first-order kinetic model used. It is clear, however, that all crude oil WAF signals at 270 nm excitation and 305-310 nm emission have the lowest calculated rate constant, suggesting this signal is less susceptible to photooxidation.

Fluorescence intensity of these peaks represents a consortium of fluorophores and their concentration in solution, which can be influenced by other components in solution. It is important to remember that simple kinetic models cannot be expected to fully account for the complex degradation of crude oils (Ryder 2005).

GCxGC-TOFMS analysis was performed to verify the presence of polycyclic aromatic hydrocarbons (PAH) in the WAF South Louisiana and Merey crude oils (Figure 2.6). The most abundant PAHs found in either oil were naphthalene and its derivatives. Based on literature comparisons of fluorescence ex/em pairs of PAHs (Berlman 1971; Freed et al., 1972; Schwarz et al., 1976; Beltran et al., 1998; Christensen et al., 2005; Orain et al., 2011), the fluorescence signals identified over the range of crude oils tested do correspond with the PAHs identified by GCxGC-TOFMS. Fluorene, though not very

soluble in water, was found in both crude oil WAFs (slightly higher in Merey than South Louisiana). Naphthalene and fluorene signals resemble the most robust fluorescence peaks found in all three oils (270/305 nm for South Louisiana, 270/305 nm for Hoops, and 270/310 and 270/325 nm for Merey) (Berlman 1971; Beltran et al., 1998; Christensen et al., 2005).

Heavier crude oils like Merey are expected to have weaker fluorescence emissions compared to lighter crude oils due to high energy transfer and quenching caused by a higher concentration of fluorophores (especially larger PAHs). However, crude oil WAF is highly diluted and the larger PAHs in heavy oils are less soluble, lessening the effects of self-quenching and energy transfer in Merey WAF fluorescence signal. The relative fluorescence intensity of Merey WAF was higher than the medium Hoops and lighter South Louisiana oils, shown in Figure 2.2.

An evaluation of GCxGC-TOFMS data revealed a higher concentration of naphthalene and its derivatives in South Louisiana crude compared to Merey. High concentrations of fluorescent and non-fluorescent components in solution can decrease fluorescence signals due to high rates of energy transfer and quenching (Ryder 2005). There is potential that the non-fluorescent components of South Louisiana crude oil in tandem with the relatively high concentration of naphthalene and its derivatives in the WAF could effectively quench the fluorescence signal, potentially explaining the low fluorescence intensity of key peaks in South Louisiana compared to Merey crude, although these samples are very dilute. The diverse chemical composition of neat crude could also be affecting the partitioning of similar components within these oils. GCxGC-TOFMS data was not evaluated for all polar or non-fluorescent compounds.

It is likely that the relative fluorescence quantum efficiency of components in South Louisiana and Merey is causing the difference in fluorescence signal intensity. Fluorene has higher fluorescence quantum efficiency than naphthalene in cyclohexane (Berlman 1971). It was found in both South Louisiana and Merey crude at similar concentrations, and corresponds to the signals found at similar intensities in all three oils at 270 nm excitation. Though GCxGC-TOFMS data showed that South Louisiana has a higher concentration of naphthalene than Merey, the quantum efficiency of fluorene, and other low concentration/high quantum efficiency compounds like anthracene, phenanthrene and their derivatives, is likely a greater influence on fluorescence intensity in crude oil WAF.

The relatively low % photodegradation loss of Merey at 270/310 and 270/325 nm, Hoops at 270/305 nm, and South Louisiana at 270/305 nm combined with a relatively low degradation rate (Table 2.4 and Figure 2.5) would suggest persistence of WAF components that fluoresce in that range. GCxGC-TOFMS data identified specific PAHs in the WAF solution of South Louisiana and Merey crude oils, including fluorene and naphthalene. Excitation and emission of fluorene has been reported at approximately 265 nm excitation and 302-310 nm emission (Berlman 1971; Beltran et al., 1998; Christensen et al., 2005), and is likely the strongest contributing factor causing the persistent fluorescence signals at 270 nm excitation throughout the crude oils tested.

Weathering dynamics, potential background interferences, crude oil's inherently complex spectral fluorescence, and the presence or absence of dispersants can limit the effectiveness of current in situ fluorometers (Ryder 2005; Kepkay et al., 2008). Fluorescent dissolved organic matter (FDOM), like tyrosine and tryptophan-like signals

at 270/305 and 270/340 ex/em (Coble 2007) are similar to what is found in our samples (Table 2.3). However, monitoring fluorescence over a range of excitation and emission wavelengths will enable the differentiation between crude oil fluorescence and FDOM (Patsayeva 1995). Continued studies regarding the effects of microbial degradation and dispersants on the fluorescence of crude oil WAF are needed for a fully developed understanding of PAH dynamics in the environment.

The results of this study indicate that weathering by photooxidation is more significant than volatilization in this experiment, and that there are key ex/em wavelengths found in a variety of crude oils that persist in solution over time. Our studies show dissolved components of crude oil fluoresce between 240-270 nm excitation and 305-360 nm emission. Only one of the fluorometers used during the DWH spill would be able to detect a signal over this range (Table 2.1). However, it would not be able to detect the key WAF signals that this study has determined to be the most robust when exposed to photooxidation. An in situ fluorometer designed to target fluorescence excitation at 270 nm and emission at both 305-310 nm and 320-325 nm would be a valuable tool for first response or long-term studies of PAHs due to its versatility tracking such a wide range of crude oils.

2.5 Chapter 2 Figures and Tables

Table 2.1. List of fluorometers used during the Deepwater Horizon spill.

Sensor	Manufacturer	Model	Signal (nm)	Detector	Source
CDOM Fluorometer	WET Labs	ECO-FL	370ex/460em	Photodiode	MBARI 2010; Diercks et al., 2010
Chrolorphyll Fluorescence	HOBI Labs	HydroScat-2	420ex/700em	N/A	MBARI 2010
Aromatic Hydrocarbon Fluorometer	Chelsea Instruments	UV AQUAtracka	239ex/360em	Photomultiplier tube	Camilli et al., 2010
CDOM Fluorometer	Seapoint Sensors	SUVF	370ex/440em	Photodiode	Camilli et al., 2010

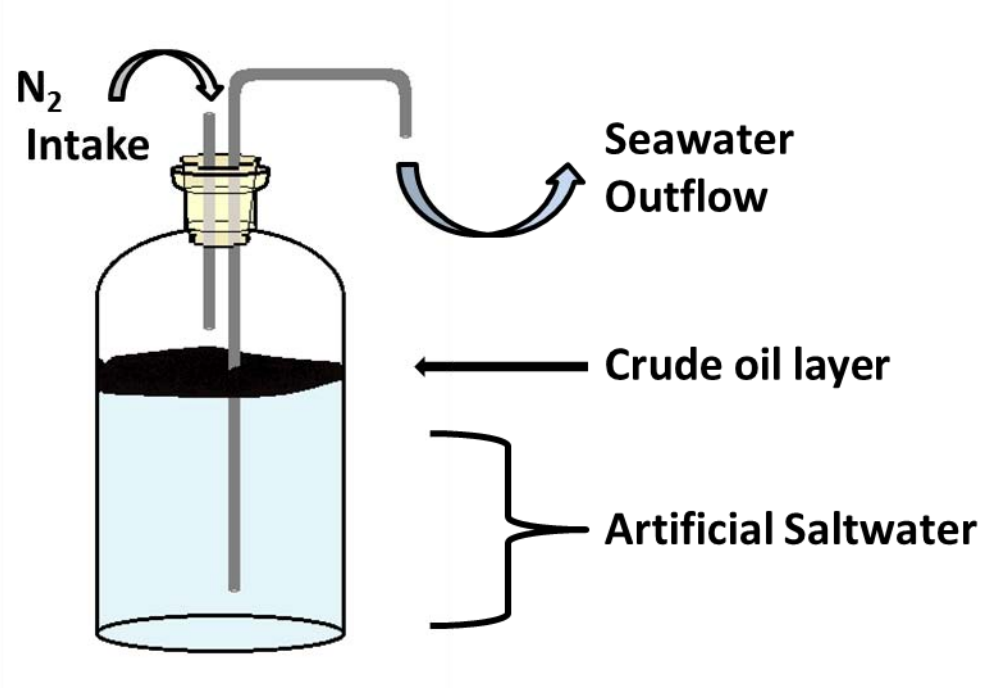

Figure 2.1. Diagram of BOD Bottle. The ASW forms the resulting crude oil WAF in the biological oxygen demand bottle. Stoppers were placed on the ends of the stainless steel tubes while not in use in order to prevent oxidation

Table 2.2. ONTA Inc. Crude Oil Properties for South Louisiana, Hoops and Merey Crude Oil.

Crude oil (ID)	South Louisiana (SL)	HOOPS (H)	Merey (M)
Location	Louisiana, USA	Texas, USA	Venezuela, South America
Description	Paraffinic	Naphthenic	Aromatic-asphaltic
Heavy/Light	Light	Medium-heavy	Extra-heavy
Density (g/ml)	0.839	0.869	0.968
API	37	31.4	14.7
Sweet/Sour	Sweet	Sour	Sour
% Sulfur	0.21	1	2.74

Table 2.3. Key Excitation and Emission Wavelengths. Key ex/em wavelengths from crude oil WAF EEMs. Fluorescence emissions shifted slightly for some peaks (¤ blue shift, § red shift). The predominant emission maximum is listed in the table.

WAF Equilibration			
Crude oil (ID)	South Louisiana (SL)	HOOPS (H)	Merey (M)
Excitation (nm)	Emission (nm)		
240	345¤	345	350§
240	-	-	405
250	320	330§	360
250	350	350	405
270	300	305	310
270	320	325	325§
Photodegradation			
Crude oil (ID)	South Louisiana (SL)	HOOPS (H)	Merey (M)
Excitation (nm)	Emission (nm)		
240	350	345	350
240	-	-	-
250	320	330	360¤
250	350	350	405
270	305	305§	310
270	320	325	325¤

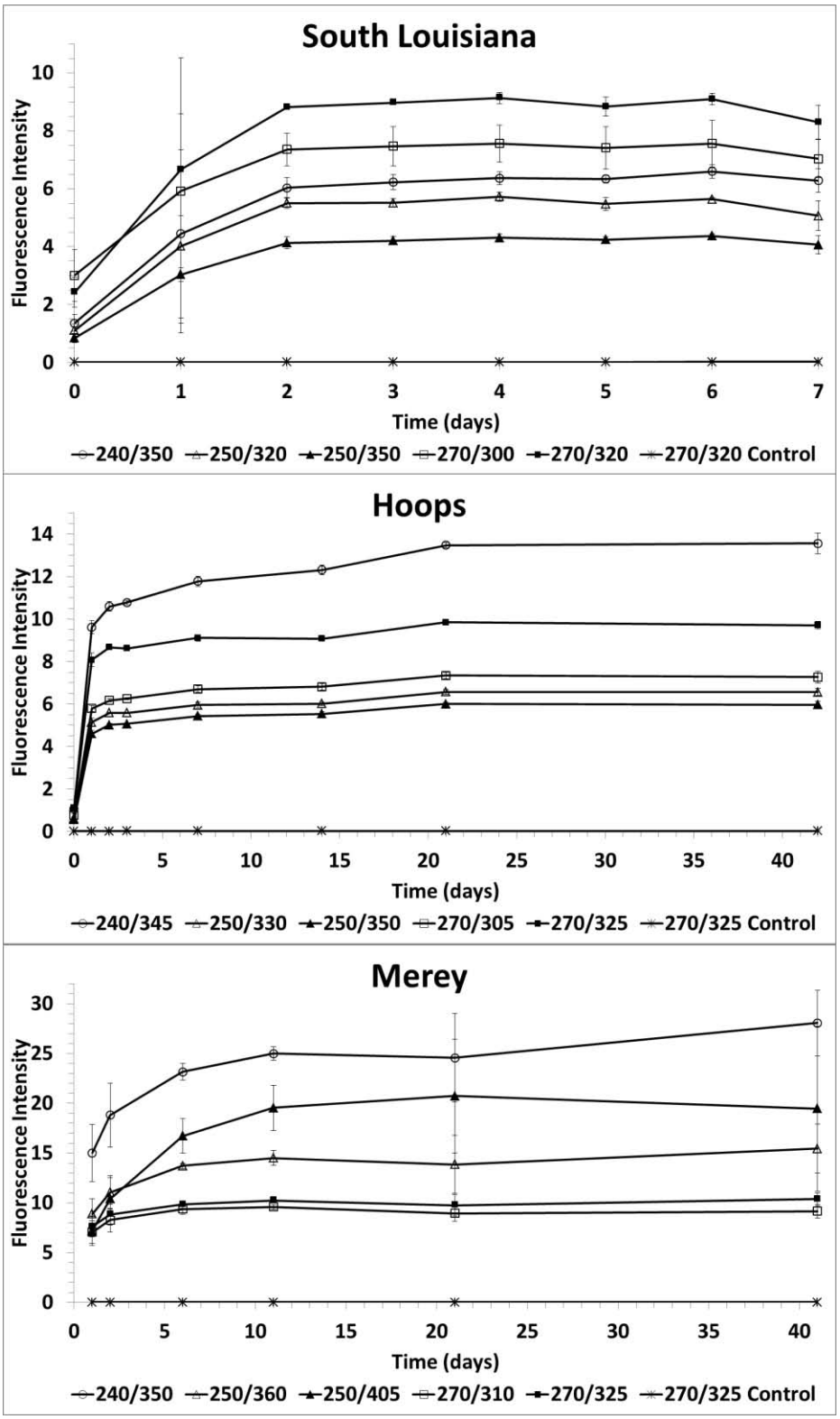

Figure 2.2. WAF Equilibration for South Louisiana, Hoops and Merey Crude Oil. Fluorescence intensity over Time (days) for key ex/em peaks of each of the oils shows fluorescence stability of the WAF solution over time.

Table 2.4. Percent Loss. % Light Loss represents apparent loss due to photodegradation of fluorescence intensity after 7 hrs of full spectrum UV exposure of crude oil WAF. % Dark Loss represents the decrease in fluorescence intensity after 7hrs of the dark control.

South Louisiana			
Ex/Em	**% Light Loss**	**% Dark Loss**	**% Photodegradation Loss**
240/350	29	5	24
250/320	44	14	30
250/350	40	8	32
270/305	25	9	16
270/320	42	14	28
Hoops			
Ex/Em	**% Light Loss**	**% Dark Loss**	**% Photodegradation Loss**
240/345	30	2	28
250/330	32	6	26
250/350	34	3	31
270/305	16	3	13
270/325	30	6	24
Merey			
Ex/Em	**% Light Loss**	**% Dark Loss**	**% Photodegradation Loss**
240/350	38	10	28
250/360	46	10	36
250/405	68	10	58
270/310	18	10	8
270/325	27	11	16

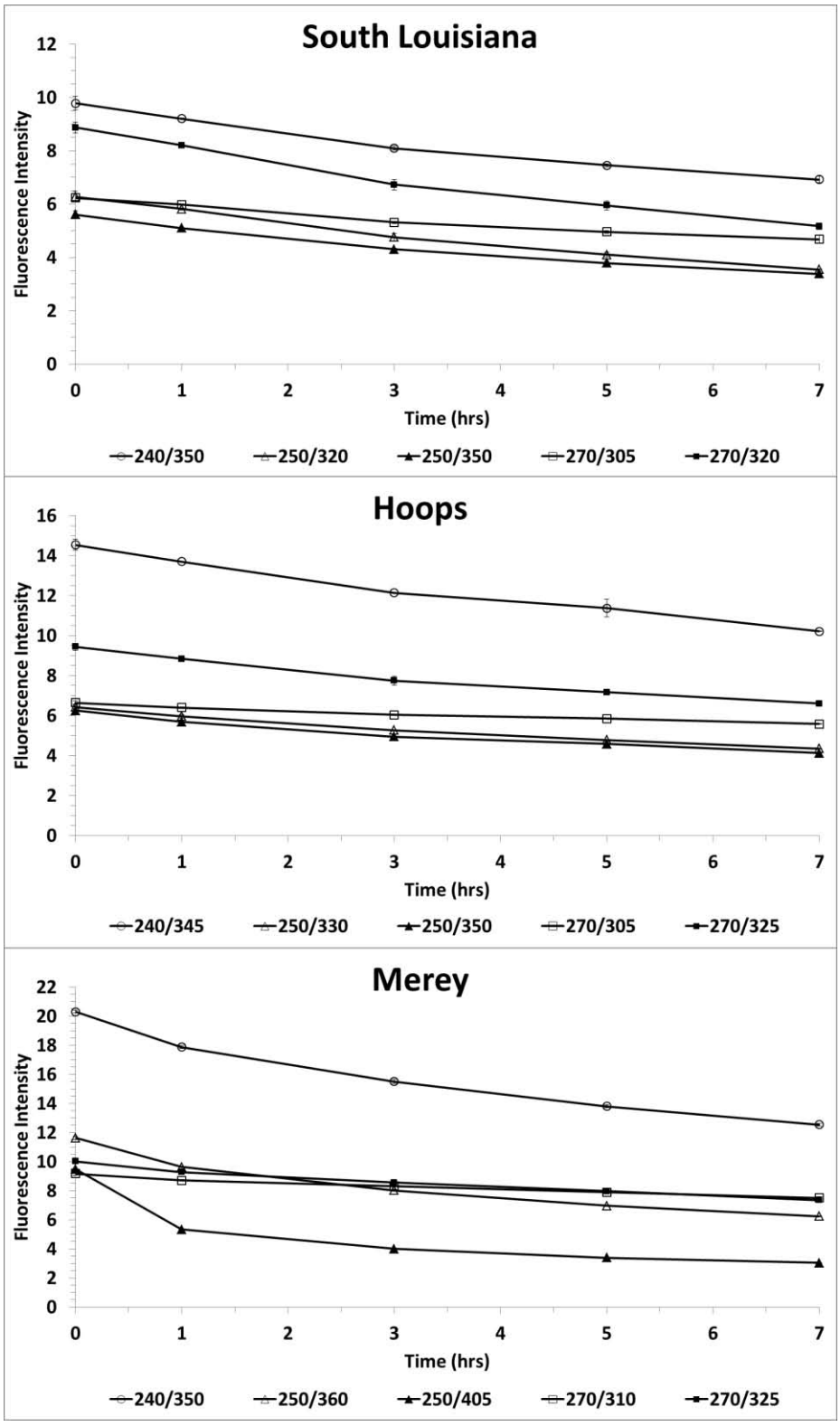

Figure 2.3. Photooxidation. Fluorescence Intensity vs Time for South Louisiana, Hoops and Merey Crude Oil.

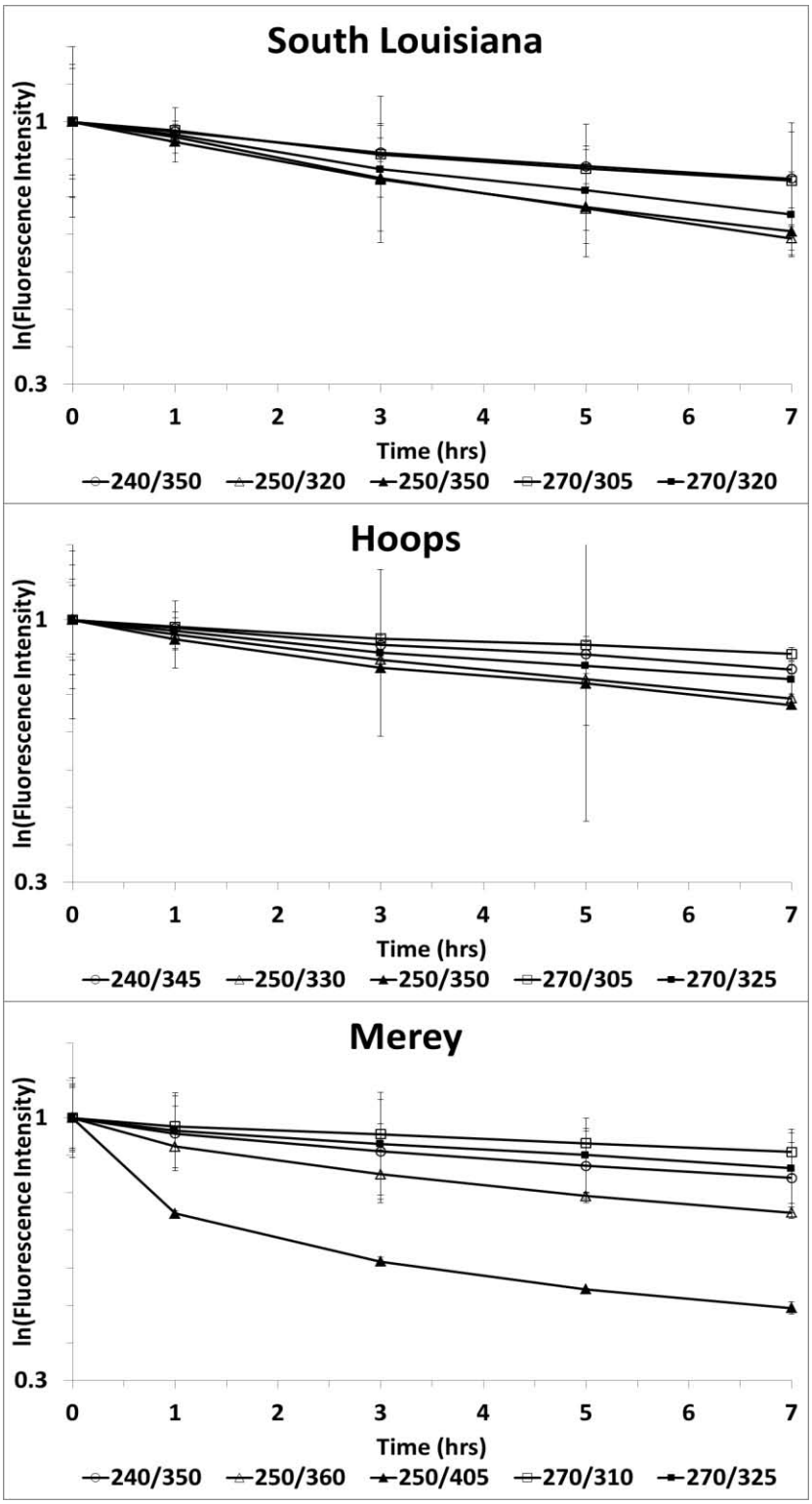

Figure 2.4. First-order Kinetic Model of Photooxidation. ln(Fluorescence Intensity) normalized to T0 vs Time (hrs) of photooxidation for key ex/em pairs of South Louisiana, Hoops and Merey Crude Oil.

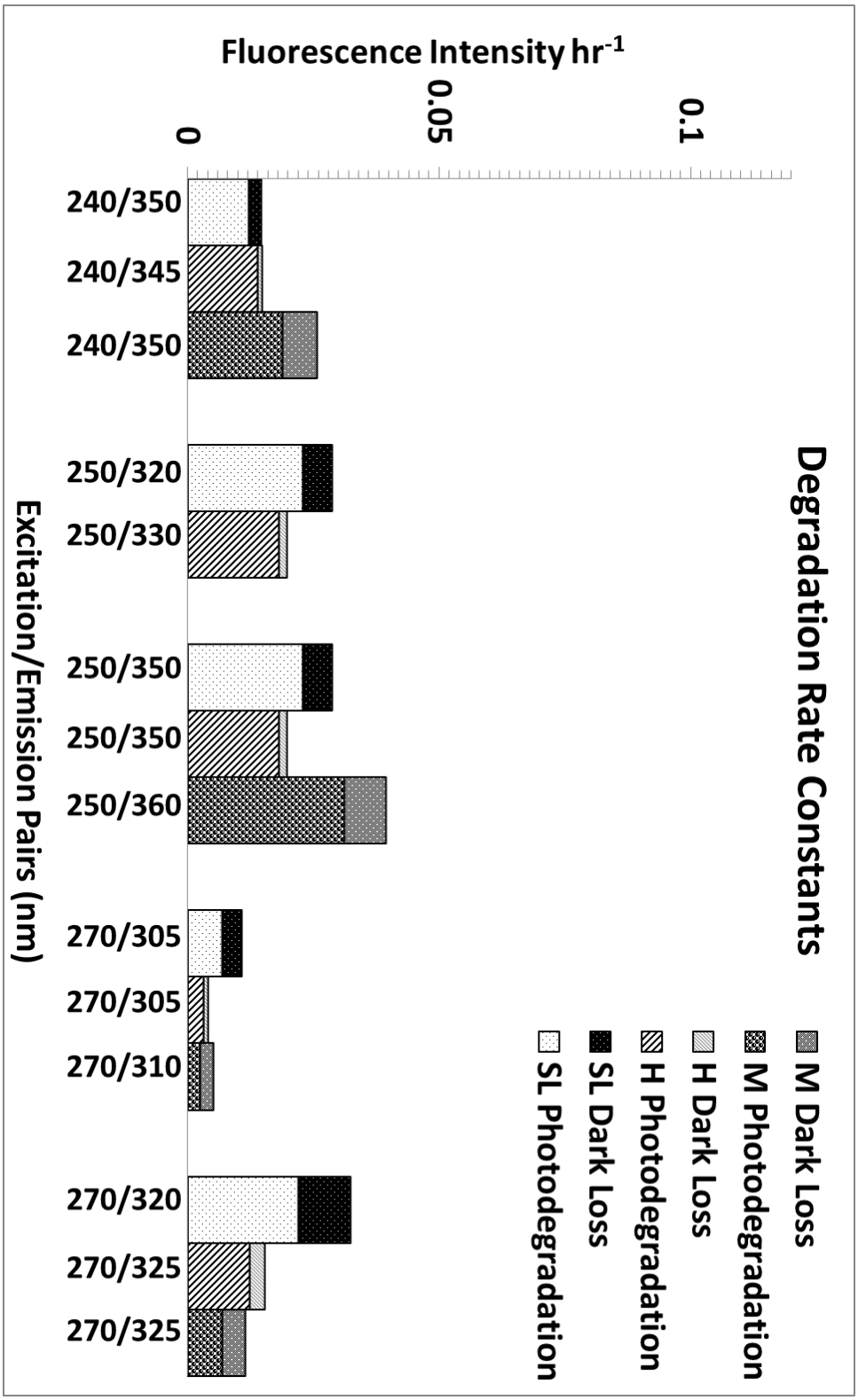

Figure 2.5. Photooxidation Rate Constants. South Louisiana, Hoops and Merey crude oil rate constants. The k values (Fluorescence Intensity hr^{-1}) were calculated using first-order kinetic model.

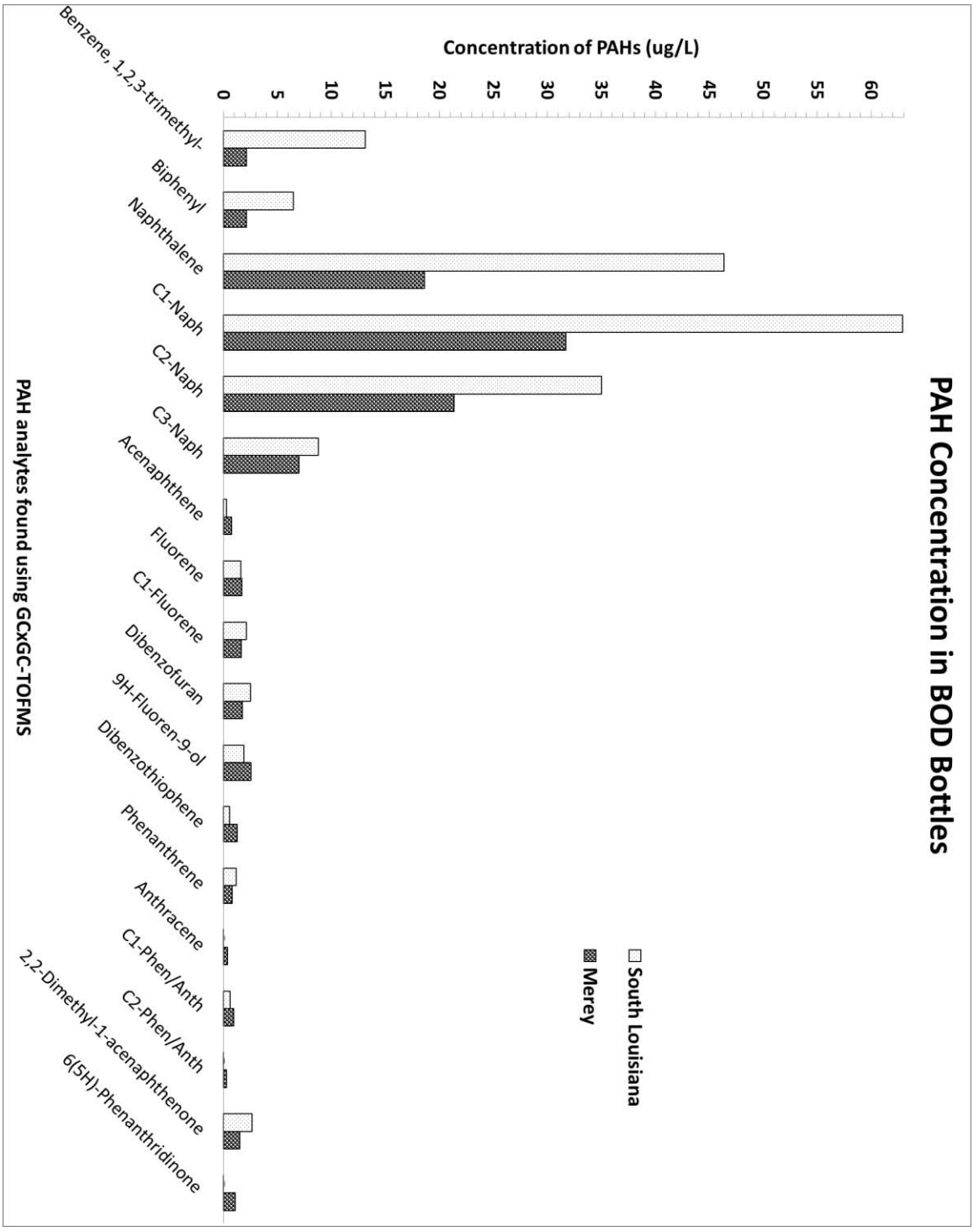

Figure 2.6. GCxGC-TOFMS PAH Concentrations. Concentrations (ug/L) of PAHs found in equilibrated South Louisiana and Merey crude oil WAFs via GCxGC-TOFMS analysis.

CHAPTER 3

Materials, Experimental Methods, and Results Excluded From Publication

3.1 Introduction

A spectral fluorescence study was designed to observe the effects of weathering on the water-accommodated fraction (WAF) of crude oil in seawater. However, due to the multitude of approaches taken in previous studies (Reisfeld 1972; Maher 1982; Ostgaard et al., 1983; Maher 1986; Ehrhardt et al., 1992; Ziolli et al., 2000; JAG 2010), a unique method was created that best fit the scope of our experimental goals. Proper materials selection was important in order to remove or significantly reduce fluorescence contamination. Appropriate boundary conditions had to be determined, including temperature, mixing speed and light exposure.

Two experiments were devised. The first was a verification of our methods while elucidating WAF stability for five different crude oils. The next experiment represented weathering of crude oil WAF by photooxidation. Ranging from light to heavy crude, South Louisiana, Qua Iboe, Hoops, Vasconia, and Merey oils (Table 3.1) were used in the first experiment (WAF equilibration). Only four of these oils underwent photooxidation experiment. South Louisiana and Merey crude oils were chosen for the GCxGC-TOFMS analysis, representing the two extremes of available crudes. These results were discussed in chapter 2. Qua Iboe and Vasconia were excluded from chapter 2 and their results will be discussed latter on in this chapter.

3.2 Materials

3.2.1 Crude oil

Crude oil was purchased from the Canadian fossil-fuel distributor ONTA Inc. Sets of 4mL vials and 100mL jars were selected due to the range of physical and chemical differences available. Table 3.1 lists the five oils that were originally chosen to best represent these differences and to verify our initial methodology. Oils were kept at room temperature (25 ˚C) and in the dark unless being used during experiment preparation.

3.2.2 Water

Artificial saltwater (ASW) with an ionic strength comparable to seawater was used during the concentration of the WAF of crude oil and photooxidation experiments, and was prepared in the lab following the Astoria-Pacific International seawater method preparation guidelines using 32.16 g/L sodium chloride (NaCl), 7.12 g/L magnesium sulfate ($MgSO_4 \cdot 7H_2O$), and 0.17 g/L sodium bicarbonate ($NaHCO_3$) in Milli-Q water (18 MΩ·cm @ 25 ˚C). ASW was filtered (0.2 μm) and stored in in sterile glass carboys at room temperature.

3.2.3 Chemicals and Other Apparatus

A detailed list of supplies, including chemicals, can be found in Table 3.2.

3.3 Methods

3.3.1 Cleaning Procedure

All glassware was acid-washed in 10% hydrochloric acid, and rinsed thoroughly with Milli-Q water prior to use. All vials, foil, and pipette tubes were combusted in a furnace at 500 ˚C for a minimum of five hours. All tubing (stainless steel and teflon), stoppers and clamps were washed with Contrex EZ (an enzymatic detergent used to prevent protein contamination) and rinsed thoroughly with Milli-Q water. All biochemical oxygen demand (BOD) bottles, flasks, pipette tubes and stainless steel tubes were hexane rinsed and air dried prior to use.

3.3.2 WAF Equilibration Methods

The WAF of crude oil in seawater was prepared in the same fashion for each experiment and GCxGC-TOFMS analysis. 240 mL of ASW was measured for each BOD bottle. A calibrated mass balance was used to weigh out 6mL of each crude oil, using the weighing by difference method. This was pipetted into labeled BOD bottles, onto ASW, creating an oil slick (Figure 3.1A). Previous studies show that boundary conditions like temperature and mixing speed are important factors in emulsion formation (Ehrhardt et al., 1992; JAG 2010). The prepared BOD bottles were placed in a shaker table set at 90 rpm, at room temperature in the dark (Figure 3.1B), preventing emulsion formation and photooxidation during the equilibration period. Teflon tubing on the end

of stainless steel tubes was clamped shut to help prevent evaporation. WAF samples were taken from beneath the oil slick through stainless steel tubes via Nitrogen displacement into combusted amber vials, then covered with combusted foil and kept at room temperature. Fluorescence and absorbance measurements were taken as soon as possible, the day the samples were collected.

3.3.3 Photooxidation Methods

Samples for the photooxidation experiments were prepared following the WAF equilibration sample preparation methods. WAF equilibration data demonstrated that most samples equilibrated within thirty days or less, so the length of time allowed for equilibration of photooxidation samples varies based the initial crude oil equilibration time. After an equilibration period ranging from 27 to 48 days, depending on the oil, the aqueous extract was separated into six or eight open amber glass vials and two amber vials covered in combusted foil as dark controls (DCs). Each time point was tested in duplicate: T0 = 0 hrs, T1 = 1 hr, T2 = 2 hrs, T3 = 5 hrs, and T4 = 7 hrs for South Louisiana, Hoops and Merey crude oil WAF and T0, T1, T3, and T3 for Vasconia WAF. Duplicate dark controls (DC = 5 hrs for Vasconia, and DC = 7 hrs for all other oils) were used to determine a difference between volatilization and photodegradation. Vasconia crude oil WAF was only exposed to five rather than seven hours because it was chosen to test our methods and had a more limited sample volume. Vials were randomly placed into a sample rack that was partially submerged in an ice-water bath kept between 15-20 ˚C to prevent loss of the sample due to heat from the lamp. Duplicate samples were taken to show that random positioning under the solar simulator lamp did not change the effect of

UV exposure on fluorescence. The ice-water bath with sample rack was positioned under a full spectrum Newport ORIEL solar simulator with a 1 kW xenon arc lamp emitting between 300-722 nm. The sample rack was agitated continuously throughout the experiment to ensure mixing within the vials. At the respective time points, sample vials were covered with combusted foil to block any continued exposure to light, and kept at room temperature for the remainder of sample analysis (between 5 to 25 min).

3.3.4 Fluorometric Methods

All fluorometric measurements were performed using a Horiba Jobin Yvon Fluoromax-4 spectrofluorometer (Fluoromax 4) with a 150-W xenon lamp, 5 nm bandpass. The Fluoromax-4 was used to provide a more comprehensive look at the fluorescence of crude oil WAF compared to in situ signals. Excitation/emission matrices (EEMs) were obtained by exciting the samples from 250-450 nm in increments of 10 nm and collecting emission spectra from 290-500 nm in increments of 5 nm. Absorbance measurements were conducted using a J&M TIDAS spectrophotometer (Tidas I) ranging from 186-722 nm, and used for data corrections.

3.3.5 GCxGC-TOFMS Methods

WAF samples of Merey and South Louisiana oil were prepared as in the crude oil WAF equilibration study. Samples were spiked with surrogate standards (chrysene-D12 and fluorene-D10) then filtered through SPE cartridges following Supelco application 80-207 for polycyclic aromatic hydrocarbons (PAHs) in water (Figure 3.2). Even though the

application was strictly followed, the eluate consisted of a water and toluene layer. The toluene phase was taken off and set aside. To ensure PAH concentration, a second extraction was performed using 2 mL of toluene added to the water phase, shaken vigorously. The first and second toluene phase extracts were combined and run through anhydrous dry sodium sulfate. Extracts were brought to volume using 150 uL dichloromethane (DCM) and then spiked with 10uL phenanthrene-D10 and naphthalene-D8 as internal standards.

A six point curve was prepared using Restek 18 compound PAH standard and surrogate standards (chrysene-D12 and flourene-D10) with the concentrations of 100, 50, 10, 5, 2, and 1 μg/mL for each point, respectively (Table 3.2). Internal standards phenanthrene-D10 and naphthalene-D8 were added to each curve point at 5 μg/mL each (Table 3.2). Each curve point was filled to volume with DCM.

An aliquot of the Merey and South Louisiana DCM solution was injected and analyzed using a Leco Pegasus 4D comprehensive two-dimensional gas chromatography with time-of-flight mass spectrometer (GCxGC-TOFMS). The primary column was a non-polar Agilent DB-5ms, phenyl arylene polymer, 30 m length, 0.25 mm id, and a 0.25 μm film thickness. The secondary column was a polar SGE BPX-50, 50% phenyl polysilphenylene-siloxane, 1.5 m length, 0.10 mm id, and a 0.10 μm film thickness. The primary oven program was set to 50 °C for 2 min, 8 °C/min until 310 °C, 10 °C/min to 330 °C, then held at 330 °C for 5 min. The secondary oven was programed to 55 °C for 2 min, 8 °C/min until 315 °C, 20 °C/min to 355 °C, then held at 355 °C for 5 min. The carrier gas was He with a column flow rate of 1.35 mL/min. GC inlet temperature was 300 ˚C and was operated in split mode. The transfer line was set at 259

˚C. Thermal modulator temperature was offset 25 ˚C relative to the primary oven. The modulation period was 4 s with an 0.8 s hot pulse time and a 1.20 s cool time. TOFMS detector was set to scan between 34-500 amu with an acquisition rate of 150 spectra/s, EI ion source at 200 ˚C, 1550 V detector voltage, -70 ev electron energy.

3.4 Data Analysis

3.4.1 Fluorometric Data

All fluorometric data corrections followed a consistent protocol for quality assurance and data comparability. Figure 3.3 is a flow diagram depicting the standard correction procedures applied to all raw EEM data in this study. Instrument correction factors provided by the manufacturer were used to correct all fluorescence data due to artifacts inherent to imperfections in the optical components. These data were corrected for inner filter effect (IFE) and blank subtracted. Because WAF samples were so dilute, IFE corrections may have been unwarranted. However, comparison between IFE corrected and non-corrected fluorescence data determined that the correction applied did not negatively affect the data, and therefore was included in our data processing. Fluorometric sample data was also Raman normalized (Lackowicz 2006; Stedmon et al., 2008; Murphy et al., 2010).

Key peak emission data at 240, 250, and 270 nm excitation of all crude oil WAF equilibration, and photooxidation, can be seen in Figure 3.4-3.18 and Figure 3.19-3.30, respectively. Key peaks for all five oils can be seen in Table 3.3.

WAF equilibration is illustrated by Figure 3.31 depicting fluorescence intensity over time for Qua Iboe and Vasconia crude oils. Figure 3.32 demonstrates the photodegradation of Vasconia WAF over five hours of intense UV exposure. To distinguish between apparent photooxidation and loss due to volatilization for Vasconia crude oil, percent loss was calculated between T0 and T3 (% Light Loss, or loss due to apparent photodegradation) and T0 and DC (% Dark Loss). The difference between %Dark and %Light loss represents the percent loss after five hours due to photodegradation (Table 3.4).

Photooxidation data for Vasconia was fit to a first-order kinetic model (Figure 3.33). The peak pair at 250/405 nm ex/em stands out in that it does not show linearity as the other key peak pair signals in this first-order model, similar to the 250/400 nm ex/em peak for Merey in chapter 2. The Vasconia signal at 250/405 nm was likewise excluded from rate constant calculations. Degradation rate constants were determined for all other key peak pairs found for Vasconia and can be compared with all crude oil rate constants in Figure 3.34.

3.4.2 GCxGC-TOFMS Data

GCxGC-TOFMS data was processed by evaluating the PAHs and their alkylated constituents found in the WAF solutions of South Louisiana and Merey crude oil. The response factor (RF) for the calibration curve and surrogate standards (chrysene-D12 and fluorene-D10) were calculated using their known concentrations and peak areas and known internal standard (naphthalene-D8 and phenanthrene-D10) concentration and peak areas. RF values of the calibration and surrogate standards were then used to calculate

the concentration of PAHs and verify the concentration of surrogate standards in crude oil WAF. Because the standard curve was limited to eighteen PAHs, values calculated for any PAHs or constituents not included in the calibration curve are estimated concentration. All GCxGC-TOFMS results and discussion can be found in chapter 2 (Figure 2.5).

3.5 Discussion of Omitted Results

Out of five crude oils tested the results from three, South Louisiana, Hoops and Merey crude, are discussed in chapter 2. Qua Iboe and Vasconia crude oils were excluded because the three chosen oils (South Louisiana, Hoops, and Merey) effectively represented the range from light to heavy crude oils based on fluorescence signatures and densities. Their results, as well as comparisons with the crude oil fluorescence results in chapter 2, are discussed here.

Qua Iboe and Vasconia crude have shared qualities with those previously mentioned (Table 3.1) including key fluorescence peaks ranging from 240-270 nm excitation and 305-360 nm emission (Table 3.3). The two designated heavy oils, Vasconia and Merey, share an excitation signal at 250 nm and emission at 400 and 405 nm, respectively, that was not see in any of the other crude oils tested (Figures 3.14, 3.17, 3.26, and 3.29).

WAF equilibration study revealed that the majority of fluorescence signals at key excitation/emission pairs stabilized after two to ten days. For Qua Iboe, Vasconia, and a few signals for Merey however, at 240 nm excitation their respective maximum emission wavelengths continued to increase in fluorescence intensity after approximately thirty

days (Figure 3.31 and Ch 2 Figure 2.2). This is most likely due to the continued dissolution of less soluble fluorophores into ASW solution.

Photooxidation studies were conducted on Vasconia but not Qua Iboe. This had to do with the timing of experiments, existing availability of crude oil WAF, and the narrowing down of which oils to use as representatives of the variety of crudes at hand. Calculations of percent loss due to apparent photodegradation (%Light Loss) and volatilization (%Dark Loss) after five hours of exposure to a full spectrum solar simulator (2500 $\mu E/m^2/sec$) can be seen in Table 3.4. The difference in losses represents loss due to photodegradation (% Photodegradation Loss).

Similar to the oils discussed in chapter 2, the percent loss of fluorescence for Vasconia WAF at 270/305 nm was relatively low compared to the other key peaks. The peak pair at 240/355 nm was the exception, being the least affected by either photodegradation or volatilization having both low %Light and Dark loss. Excitation signals at 270 nm, and emission at 305 and 355 nm for Vasconia WAF correspond to fluorene (Berlman 1971; Ostgaard et al., 1983; Beltran et al., 1998). The 240/355 nm ex/em signals resemble naphthalene (Ostgaard et al., 1983).

The heavy oils, Vasconia and Merey, had similar fluorescence signals and interesting stokes shifting in both the WAF equilibration and photooxidation study. Comparable red shifting was seen in WAF equilibration fluorescence experiment (Table 3.3). This red shift in heavy oils was expected due to the slow increase in fluorophores in WAF solution, which can cause energy transfer and quenching (Ryder 2005). Red shifting seen in the photooxidation series of Vasconia WAF can be explained by the lack of equilibration of some fluorescent components seen in the WAF equilibration

experiment. The peaks at 250/400 nm and 250/405 nm ex/em for Vasconia and Merey, respectively, correspond to high molecular weight PAHs including anthracene and its derivatives (Berlman 1971). These PAHs are expected to be highly susceptible to photooxidation. Though we did not calculate rate constants for these peak pairs, percent loss calculations agree with that expected result (Table 3.4).

3.6 Conclusions

Though most crude oil WAF signals equilibrated after ten days, Vasconia WAF did not fully equilibrate over a thirty day period. This was most likely due to the low solubility of chromophores. However, high fluorescence intensity and other similarities of heavy oils (Merey and Vasconia) reinforce the impression that energy transfer in their crude oil WAF is not a limiting factor for fluorescence detection of PAHs in solution when compared to lighter crude oil WAFs like South Louisiana.

Results for Qua Iboe and Vasconia agree with chapter 2, maintaining the conclusion that in situ instrumentation targeting fluorophores between the ranges of 240-270 nm excitation and 305-360 nm emission would be able to detect low levels of persistent PAHs dissolved and dispersed into aquatic environments from a variety of crude oils.

3.7 Chapter 3 Figures and Tables

Table 3.1. ONTA Inc. Crude Oil Properties and Descriptions.

Crude oil (ID)	South Louisiana (SL)	Qua Iboe (QI)	HOOPS (H)	Vasconia (V)	Merey (M)
Location	Louisiana, USA	Nigeria, West Africa	Texas, USA	Colombia, South America	Venezuela, South America
Description	Paraffinic	Paraffinic	Naphthenic	Aromatic-naphthenic	Aromatic-asphaltic
Heavy/Light	Light	Light-medium	Medium-heavy	Heavy	Extra-heavy
Density (g/ml)	0.839	0.846	0.869	0.909	0.968
API	37	35.8	31.4	21.2	14.7
Sweet/Sour	Sweet	Sweet	Sour	Sour	Sour
% Sulfur	0.21	0.12	1	0.56	2.74
Notes		Waxy with a high pour point of 7*C		Tendency toward heavier, dense, waxy residues (resins)	Tendency toward more dense, tarry residues (asphaltenes)

Table 3.2. Supply List.

Vendor	Vendor Part #	Description
ONTA	Crude Oil set #2	Set of 9 4 mL crude oil samples
ONTA	Light Crude Oil set	Set of 4 4 mL light crude oil samples
ONTA	LA-Light-80mL	80 mL vial of LA light sweet crude
ONTA	Merey-80mL	80 mL vial of Merey crude
Cole Parmer	EW-62994-18	High-purity silicone stopper, size 4 (package of 10)
Cole Parmer	EW-62994-14	High-purity silicone stopper, size 2 (21D) (package of 10)
McMaster Carr	51845K55	High purity silicone tubing 1/8"IDx1/4"OD (10 feet)
McMaster Carr	9797T123	Cleaned and capped 316 SS tubing 1/4" OD, 6' long
McMaster Carr	5031K11	Clamp-Style Pinch Valve for Tubing Acetal, 1/4" Max Tube OD
McMaster Carr	5031K12	Clamp-Style Pinch Valve for Tubing Acetal, 7/16" Max Tube OD
Wheaton	227497-00G	Wheaton 300 mL borosilicate biochemical oxygen deman (BOD) bottles
Fisher	S146-0040	Thermo Scientific amber VOC vials
Sigma-Aldrich/ Supelco	57064	Supelclean ENVI-18 Tube, SPE cartridges
Restek	31269	WA EPH Aromatic Hydrocarbon Standard (18 compounds), calibration for GCxGC-TOFMS
Cambridge Isotope Laboratory	DLM-261-1	Chrysene D12, surrogate standard
Cambridge Isotope Laboratory	DLM-365-1	Naphthalene D8, internal standard
Cambridge Isotope Laboratory	DLM-371-1	Phenanthrene D10, internal standard
KOR isotopes Inc.	DJL-1-180	Fluorene D10, surrogate standard
Fisher	H302-1	Hexanes (HPLC)
Fisher	A144-212	Hydrochloric Acid
Fisher	A998-1	Acetonitrile (HPLC)
Fisher	D143SK-4	Methylene Chloride (HPLC)
Fisher	T290-1	Toluene (HPLC)
Fisher	A4524	Methanol (HPLC)
Airgas	NI UHP200	Nitrogen Ultra High Purity Gas
ACROS Organics	S271-3	Sodium Chloride
Sigma Aldrich	M5921-1	Magnesium Sulfate Heptahydrate
Fisher	S233-500	Sodium Bicarbonate

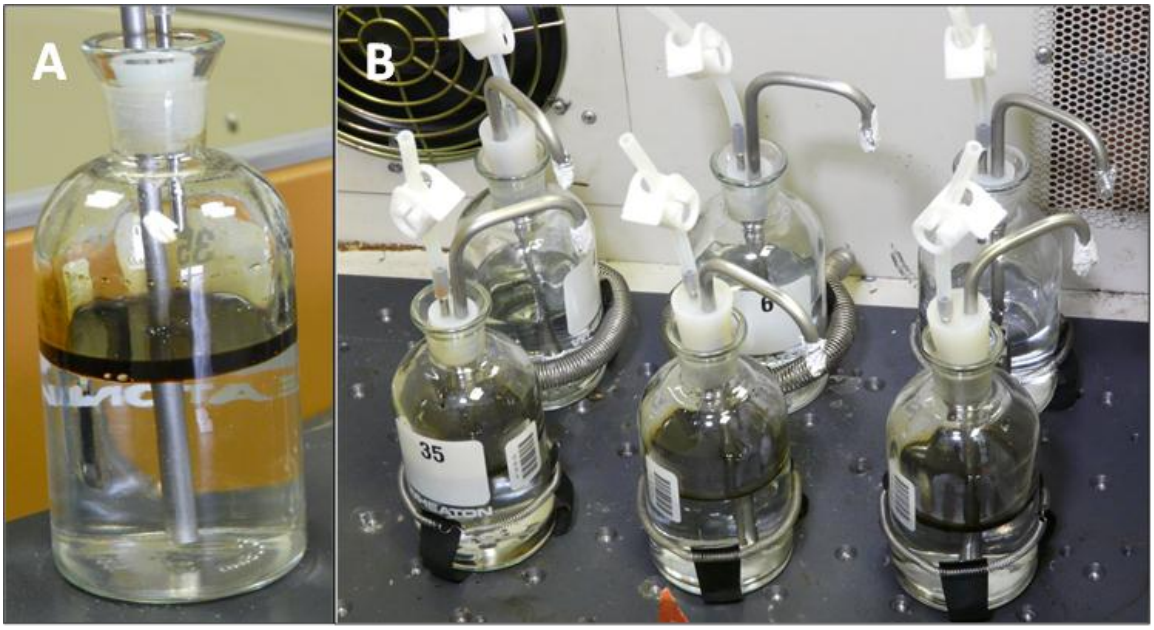

Figure 3.1. BOD Bottle and Setup. A) Close up of the oil slick on top of artificial seawater and B) BOD crude oil duplicates and controls set up in the shaker table.

Figure 3.2. SPE Filtration. Crude oil WAF was SPE filtered inside a fume hood prior to GCxGC-TOFMS analysis.

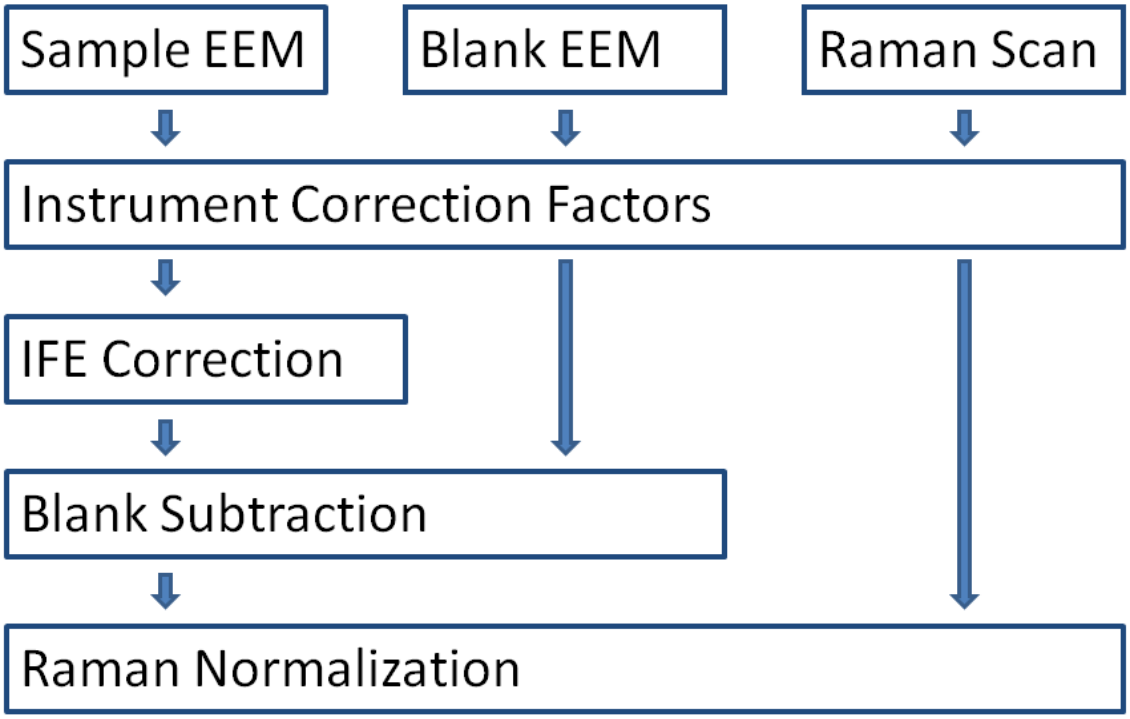

Figure 3.3. Flow Diagram of EEM Correction Procedures.

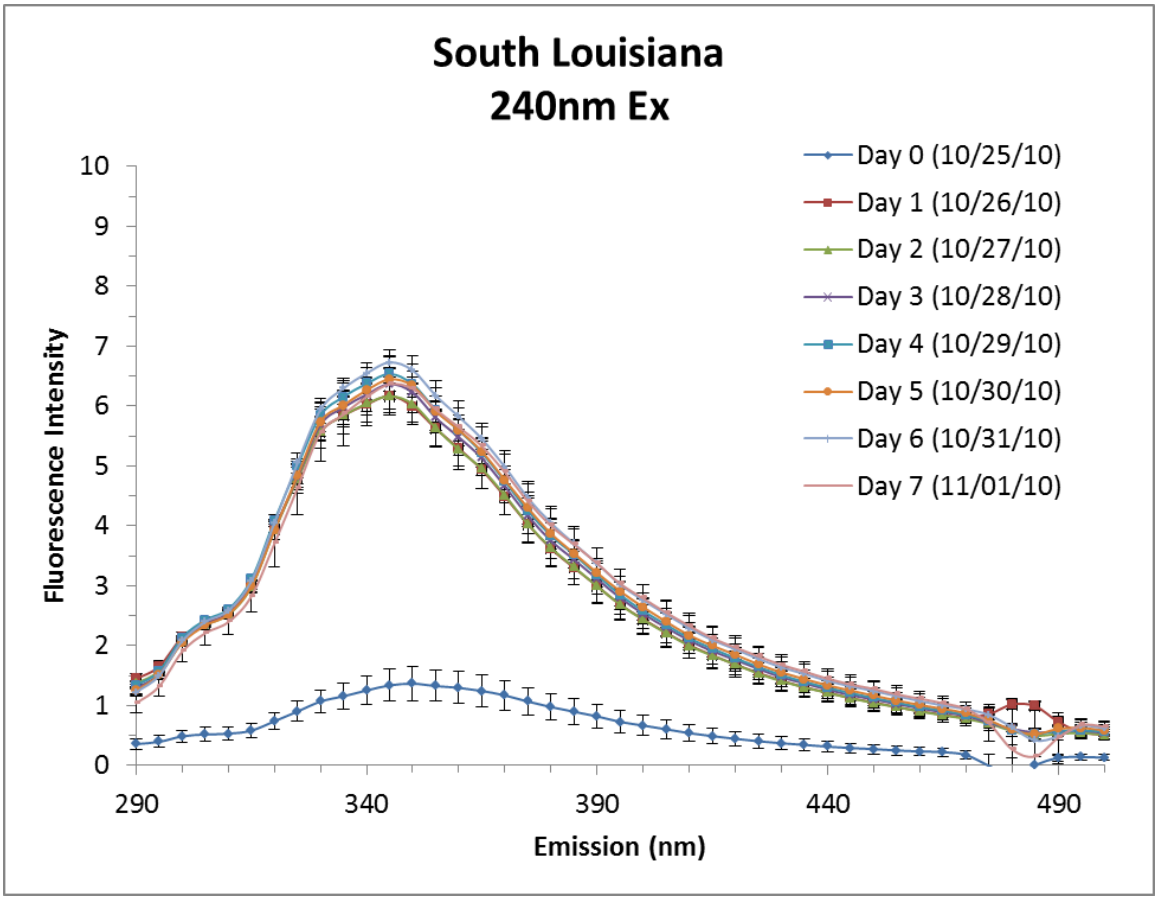

Figure 3.4. South Louisiana EEM Cross-section at 240 nm Excitation. Fluorescence intensity vs Emission of crude oil WAF equilibration.

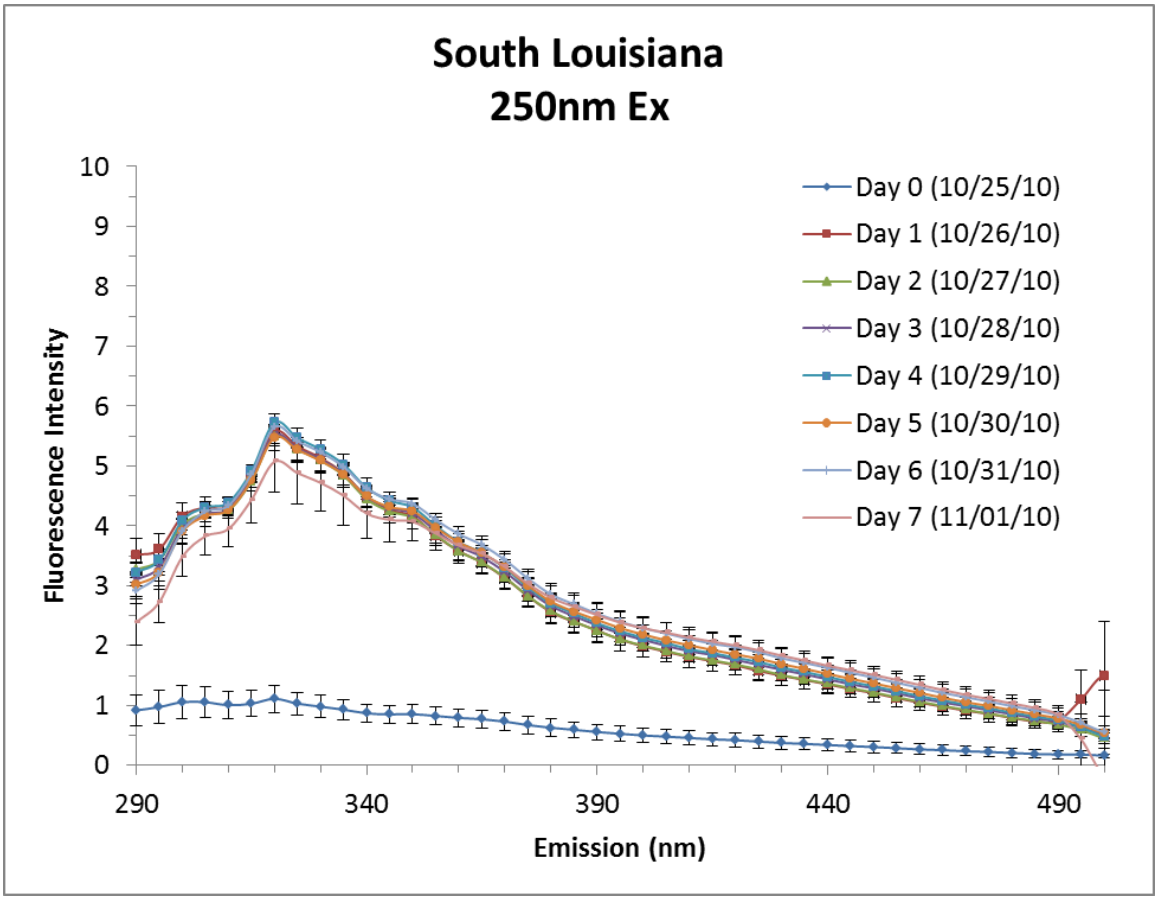

Figure 3.5. South Louisiana EEM Cross-section at 250 nm Excitation. Fluorescence intensity vs Emission of crude oil WAF equilibration.

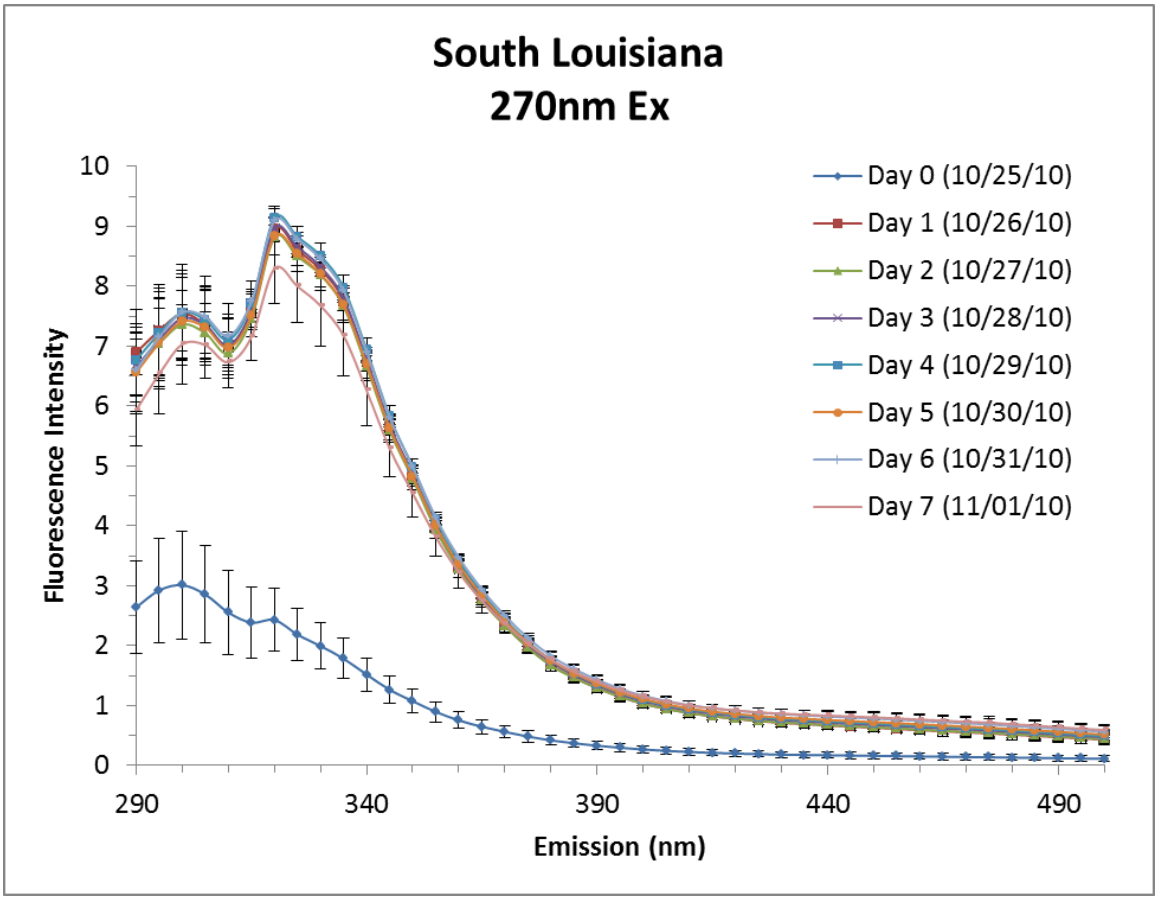

Figure 3.6. South Louisiana EEM Cross-section at 270 nm Excitation. Fluorescence intensity vs Emission of crude oil WAF equilibration.

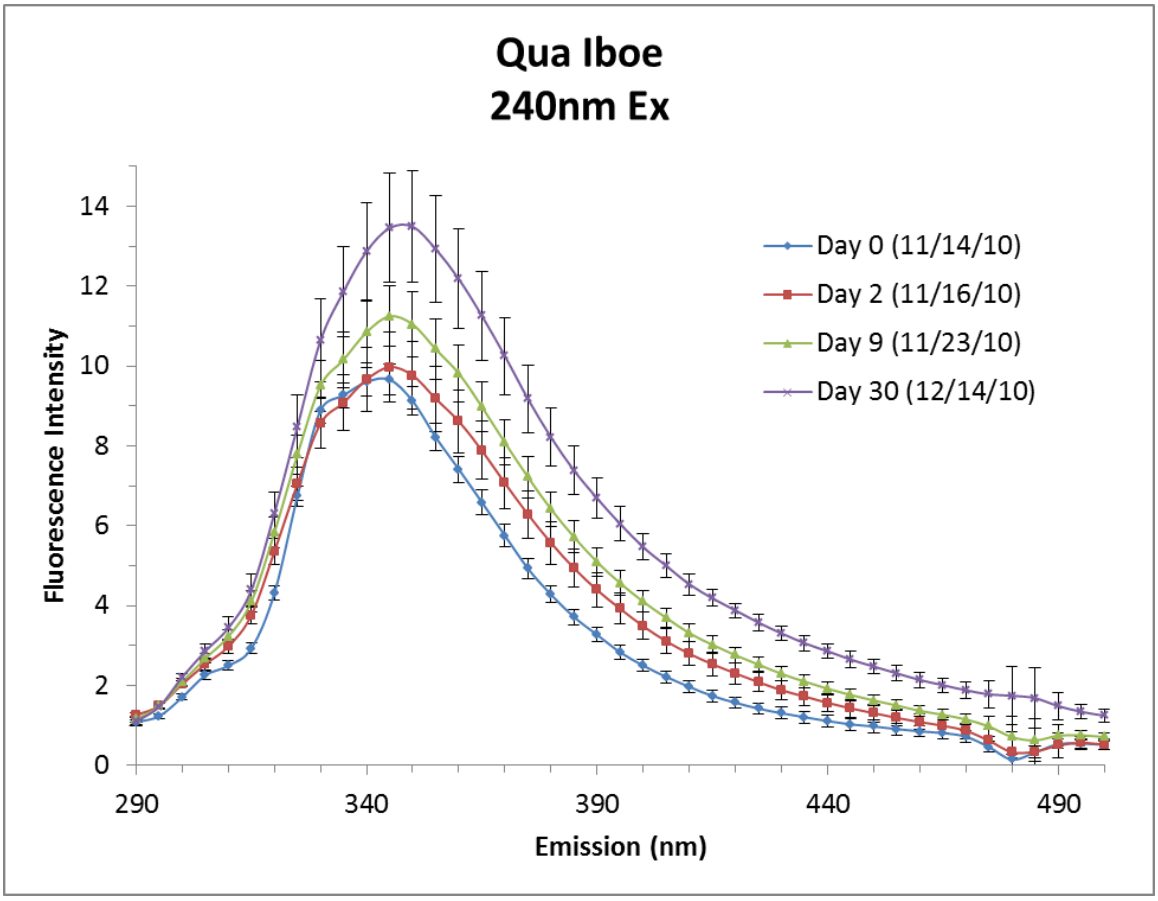

Figure 3.7. Qua Iboe EEM Cross-section at 240 nm Excitation. Fluorescence intensity vs Emission of crude oil WAF equilibration.

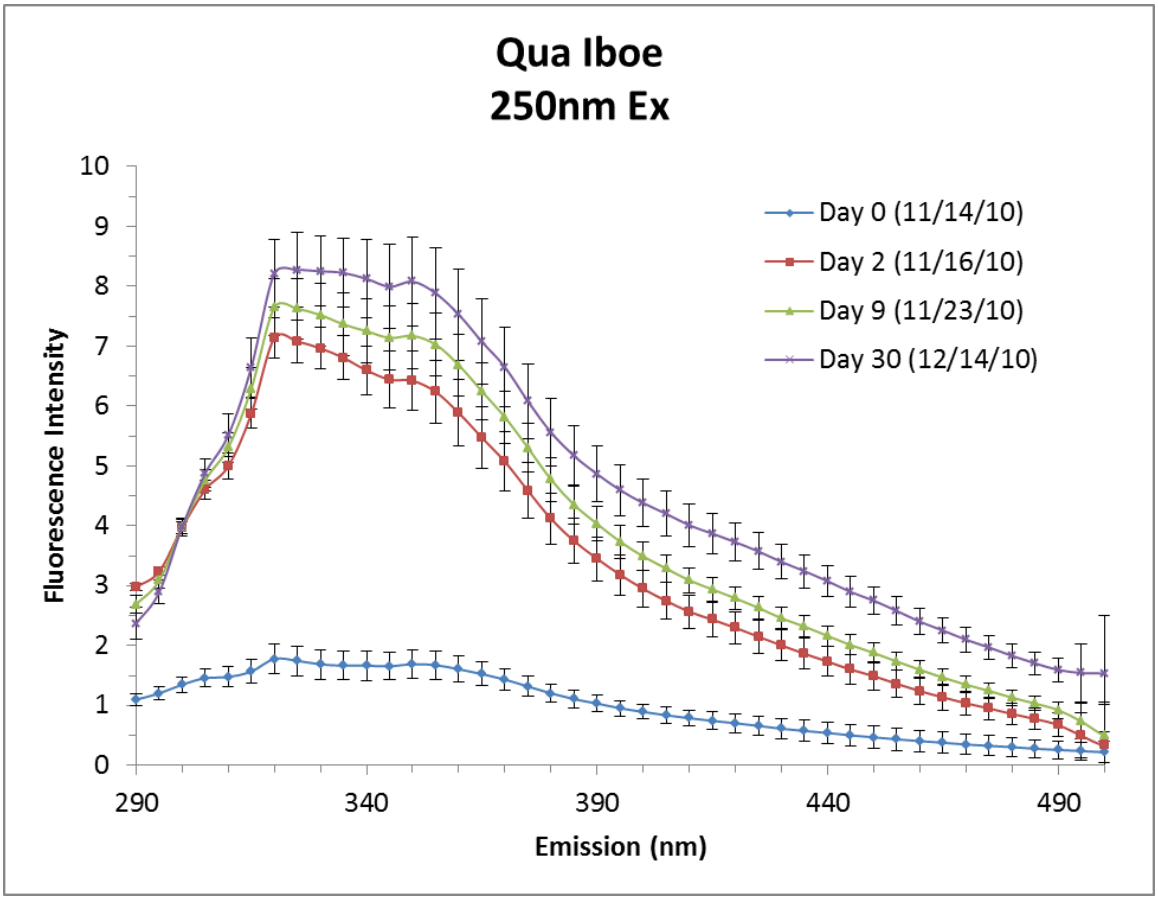

Figure 3.8. Qua Iboe EEM Cross-section at 250 nm Excitation. Fluorescence intensity vs Emission of crude oil WAF equilibration.

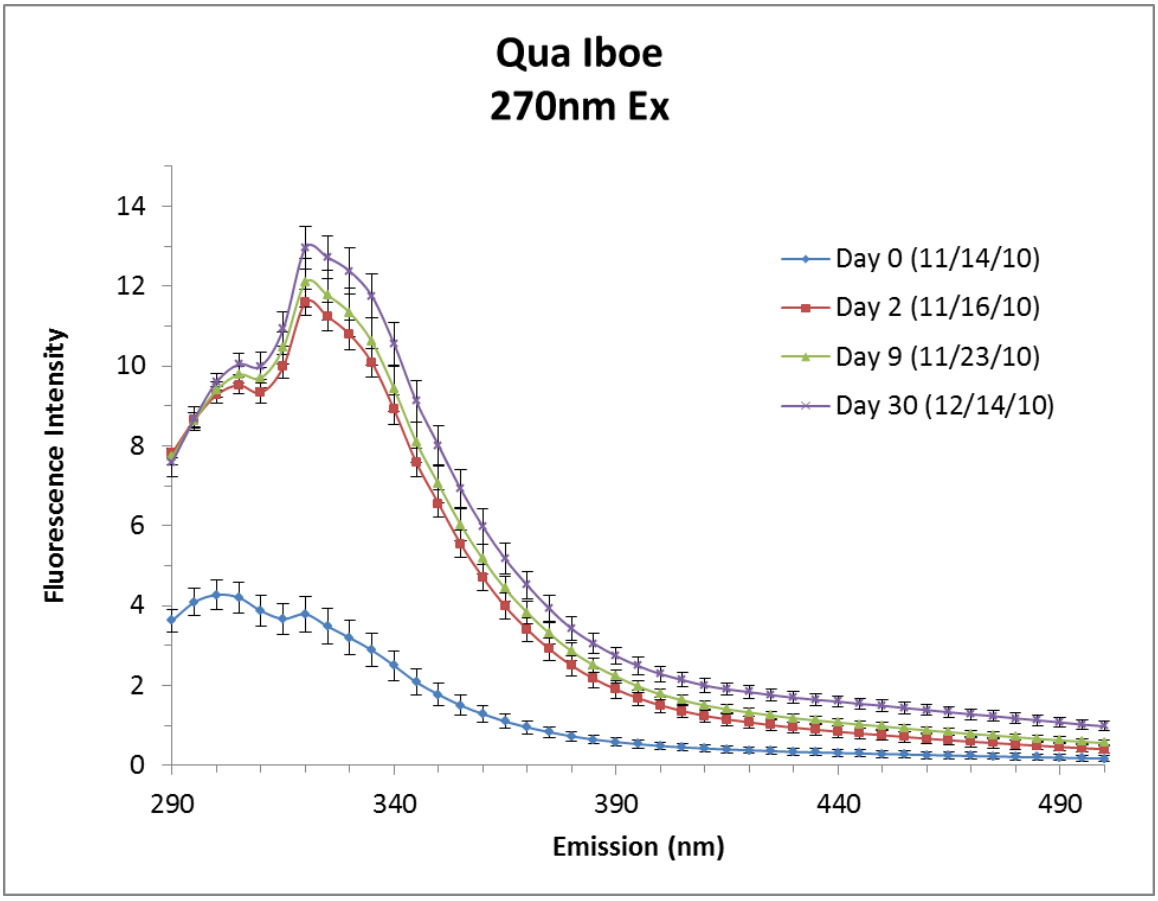

Figure 3.9. Qua Iboe EEM Cross-section at 270 nm Excitation. Fluorescence intensity vs Emission of crude oil WAF equilibration.

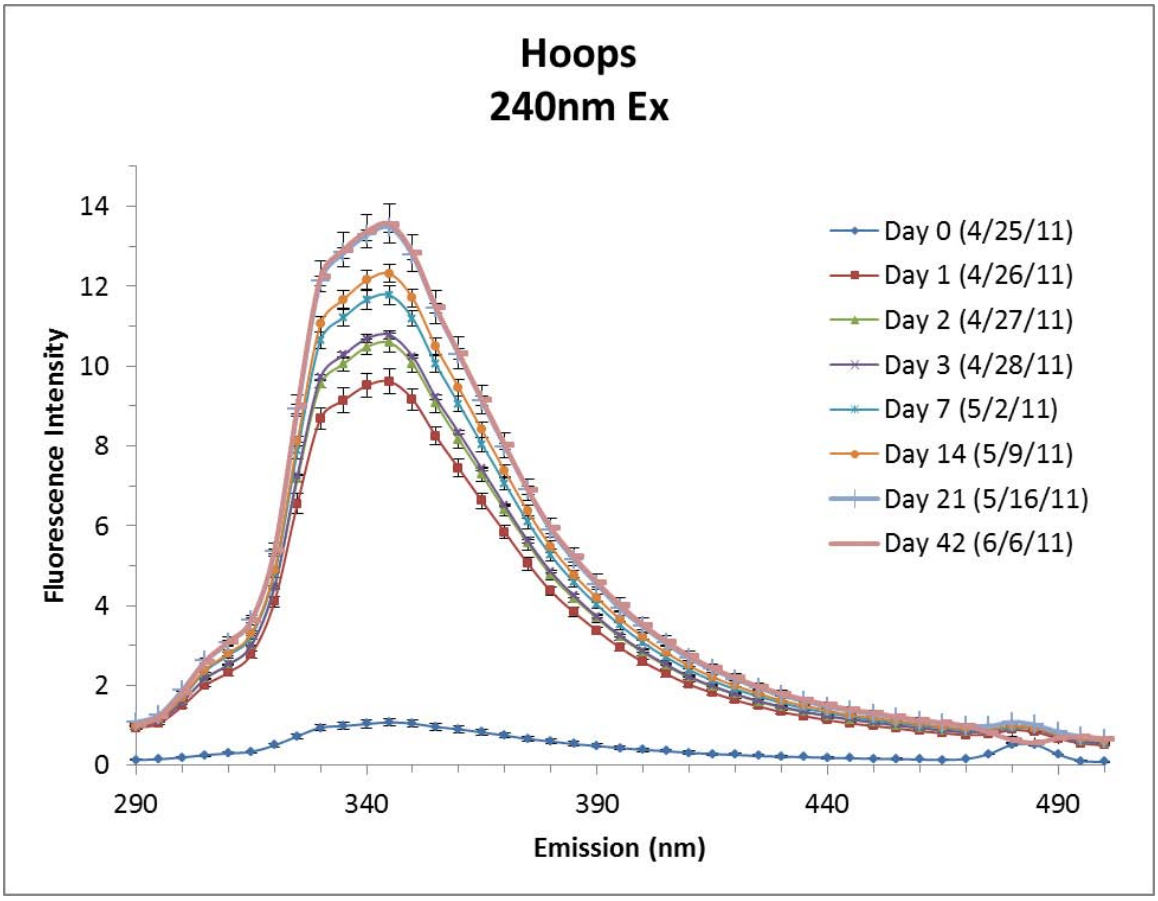

Figure 3.10. Hoops EEM Cross-section at 240 nm Excitation. Fluorescence intensity vs Emission of crude oil WAF equilibration.

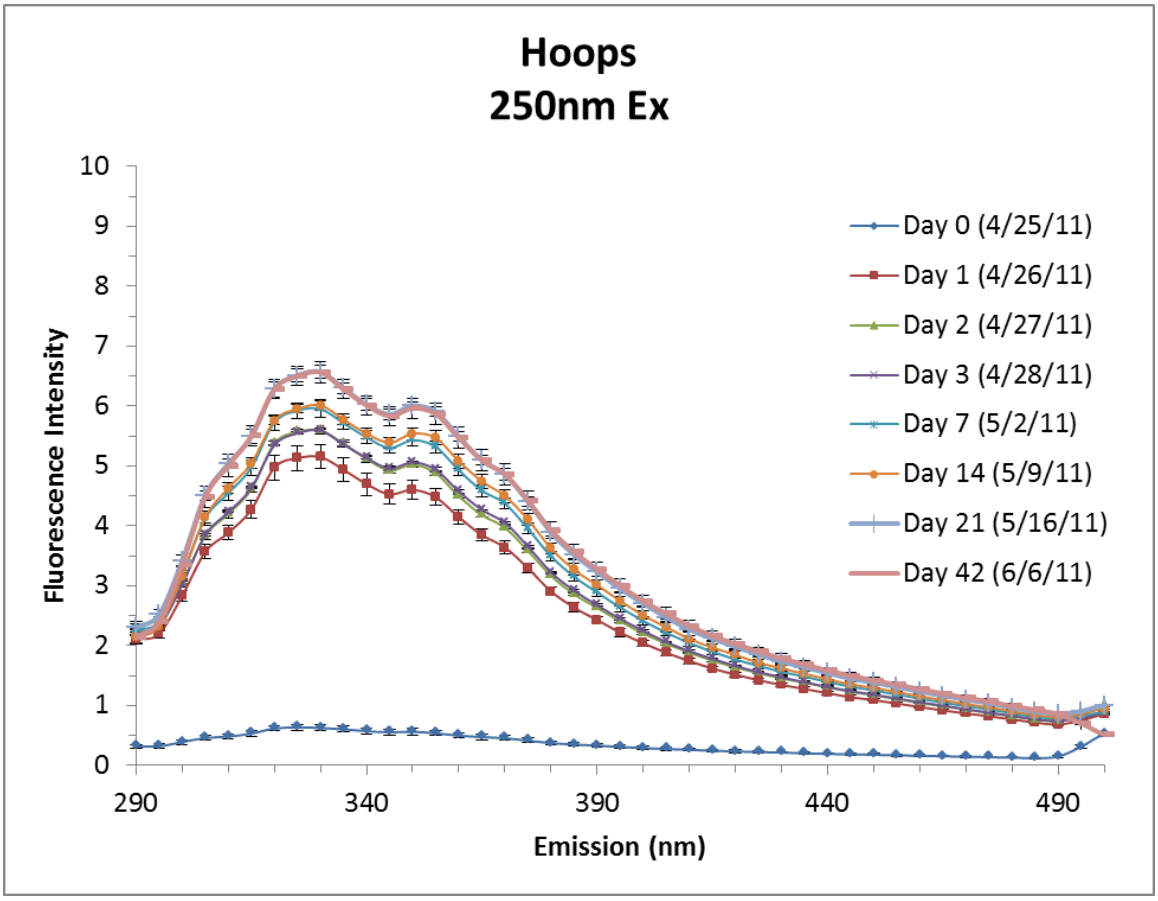

Figure 3.11. Hoops EEM Cross-section at 250 nm Excitation. Fluorescence intensity vs Emission of crude oil WAF equilibration.

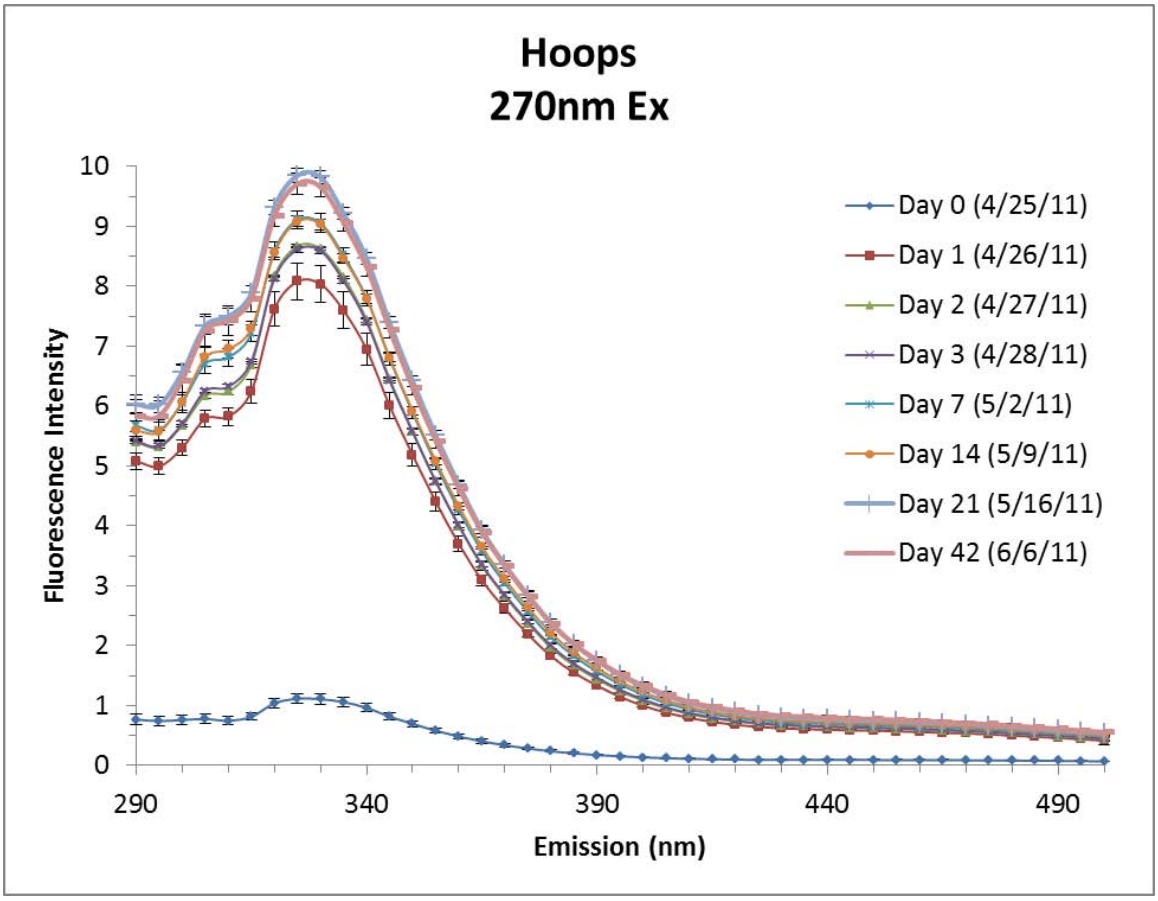

Figure 3.12. Hoops EEM Cross-section at 270 nm Excitation. Fluorescence intensity vs Emission of crude oil WAF equilibration.

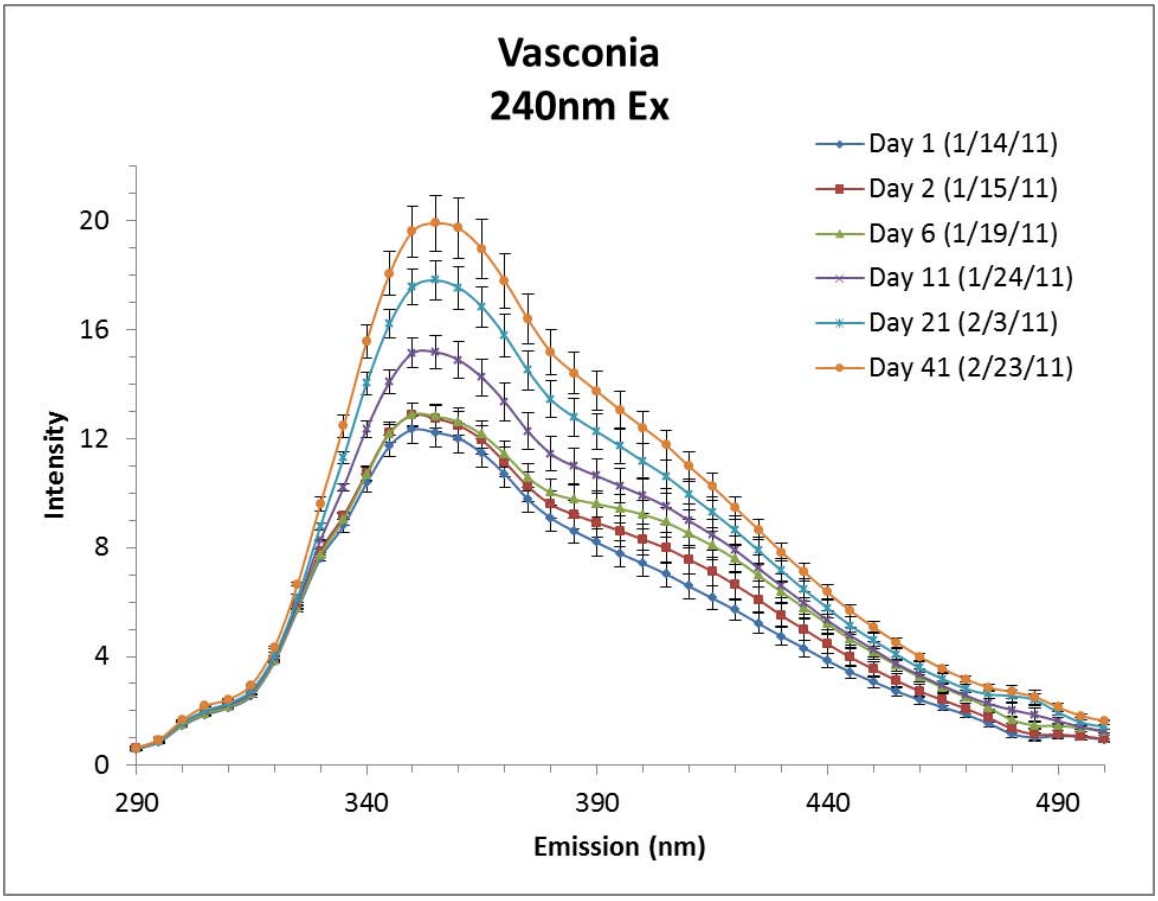

Figure 3.13. Vasconia EEM Cross-section at 240 nm Excitation. Fluorescence intensity vs Emission of crude oil WAF equilibration.

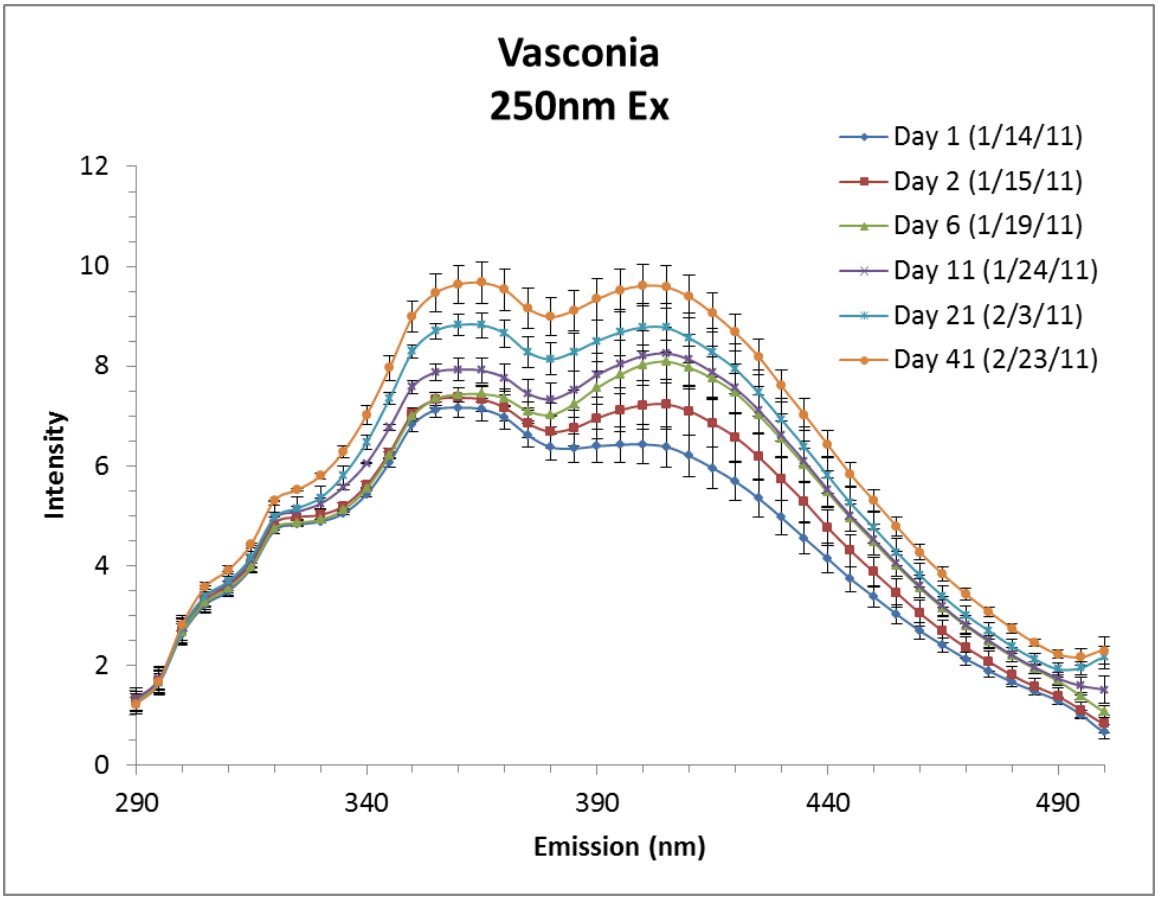

Figure 3.14. Vasconia EEM Cross-section at 250 nm Excitation. Fluorescence intensity vs Emission of crude oil WAF equilibration.

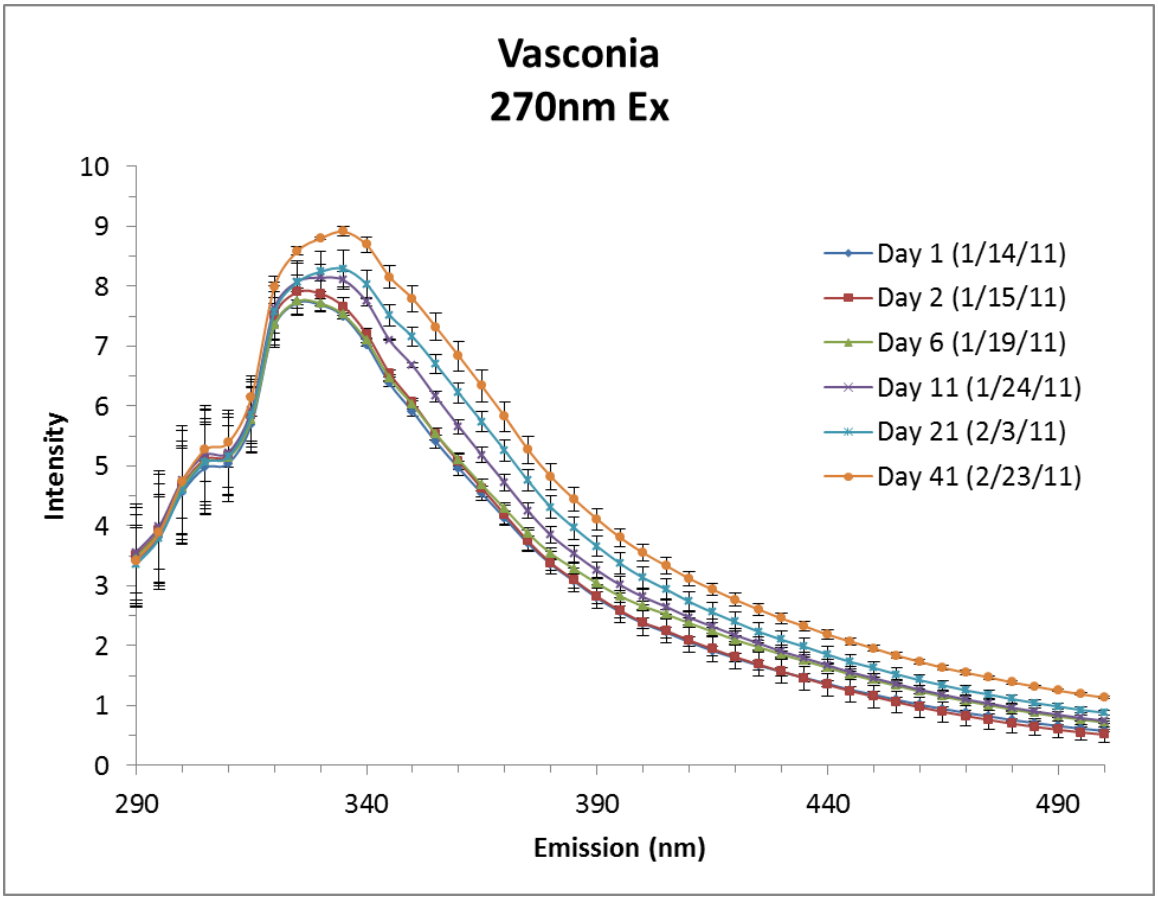

Figure 3.15. Vasconia EEM Cross-section at 270 nm Excitation. Fluorescence intensity vs Emission of crude oil WAF equilibration.

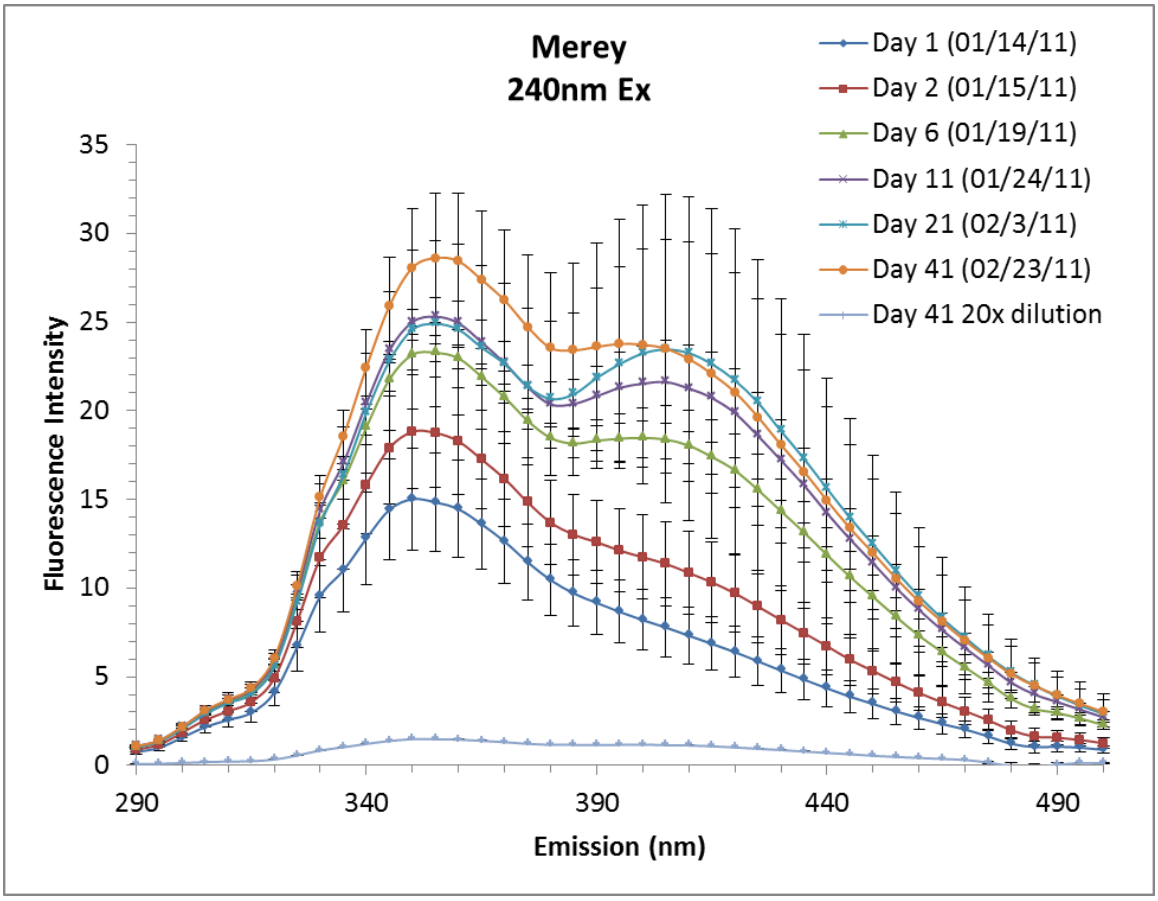

Figure 3.16. Merey EEM Cross-section at 240 nm Excitation. Fluorescence intensity vs Emission of crude oil WAF equilibration.

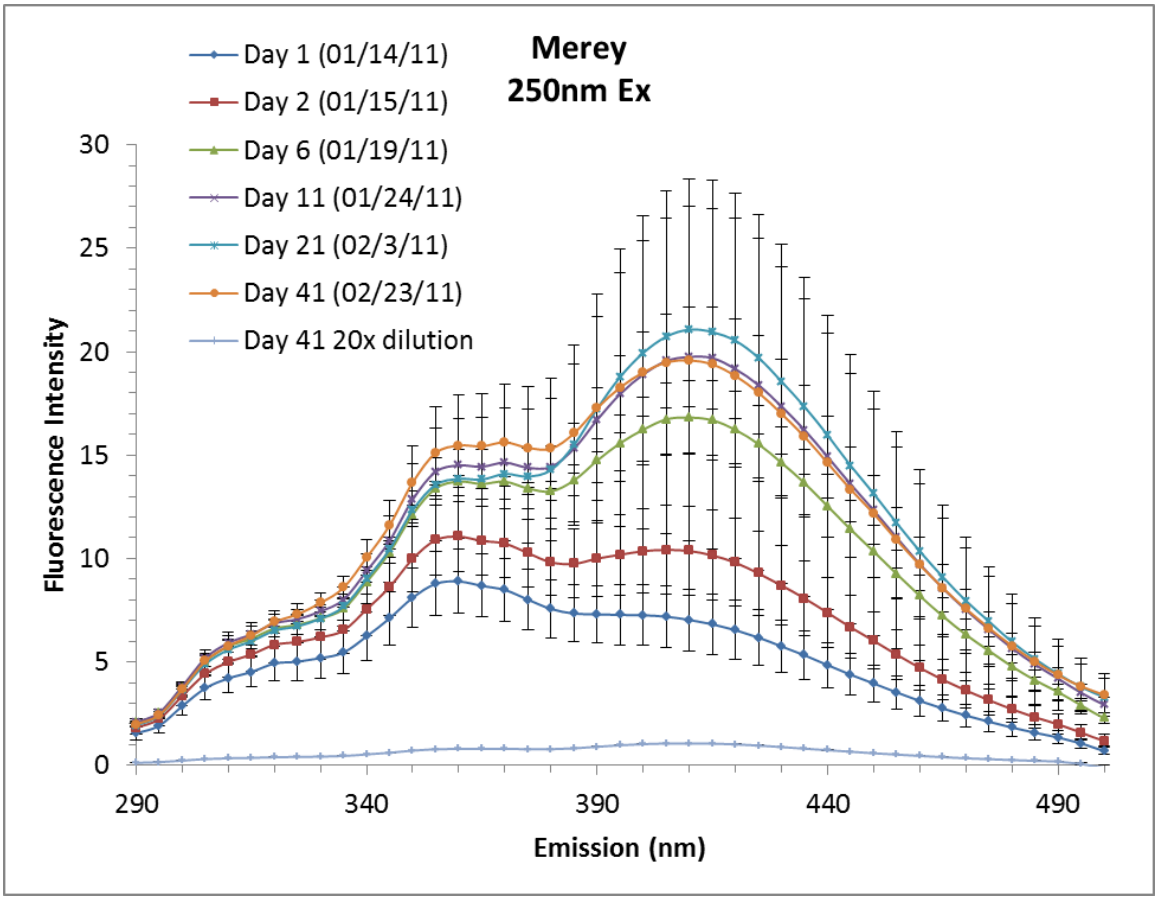

Figure 3.17. Merey EEM Cross-section at 250 nm Excitation. Fluorescence intensity vs Emission of crude oil WAF equilibration.

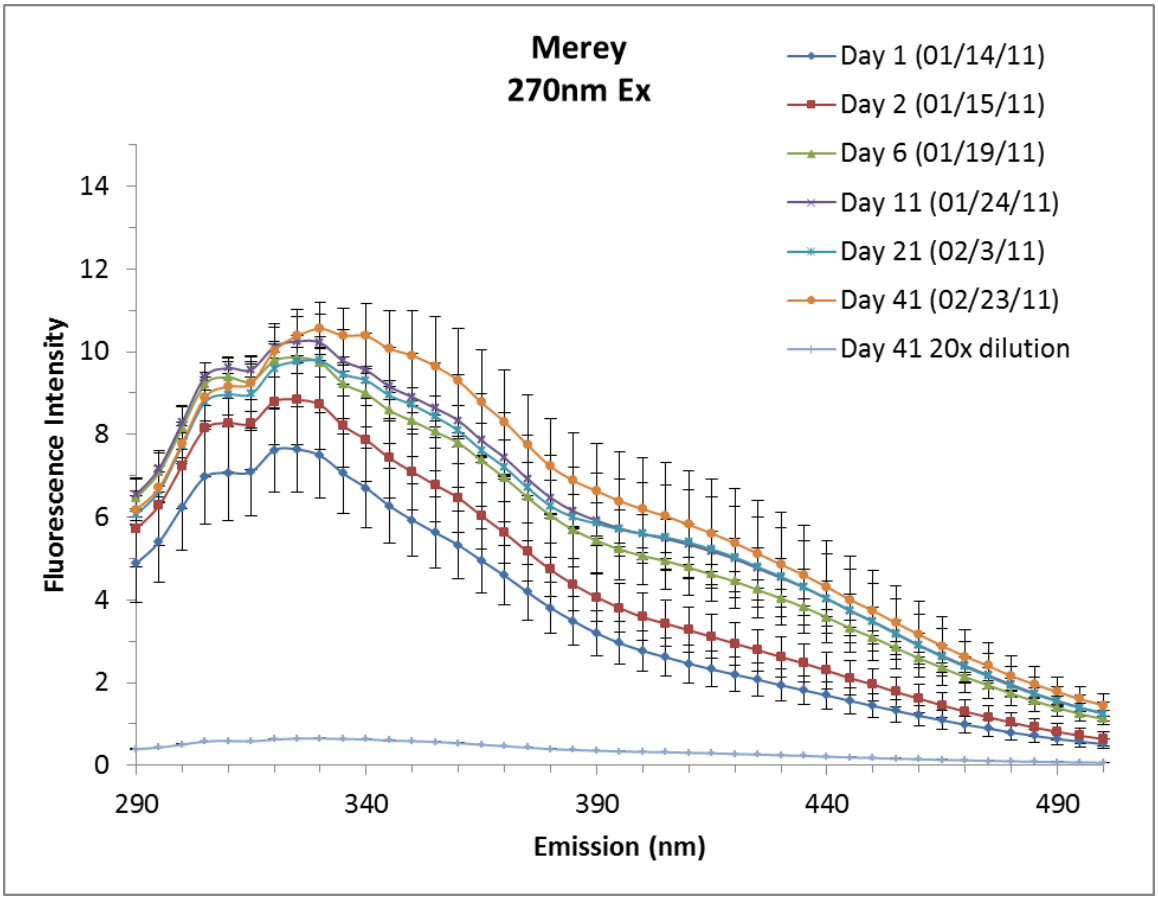

Figure 3.18. Merey EEM Cross-section at 270 nm Excitation. Fluorescence intensity vs Emission of crude oil WAF equilibration.

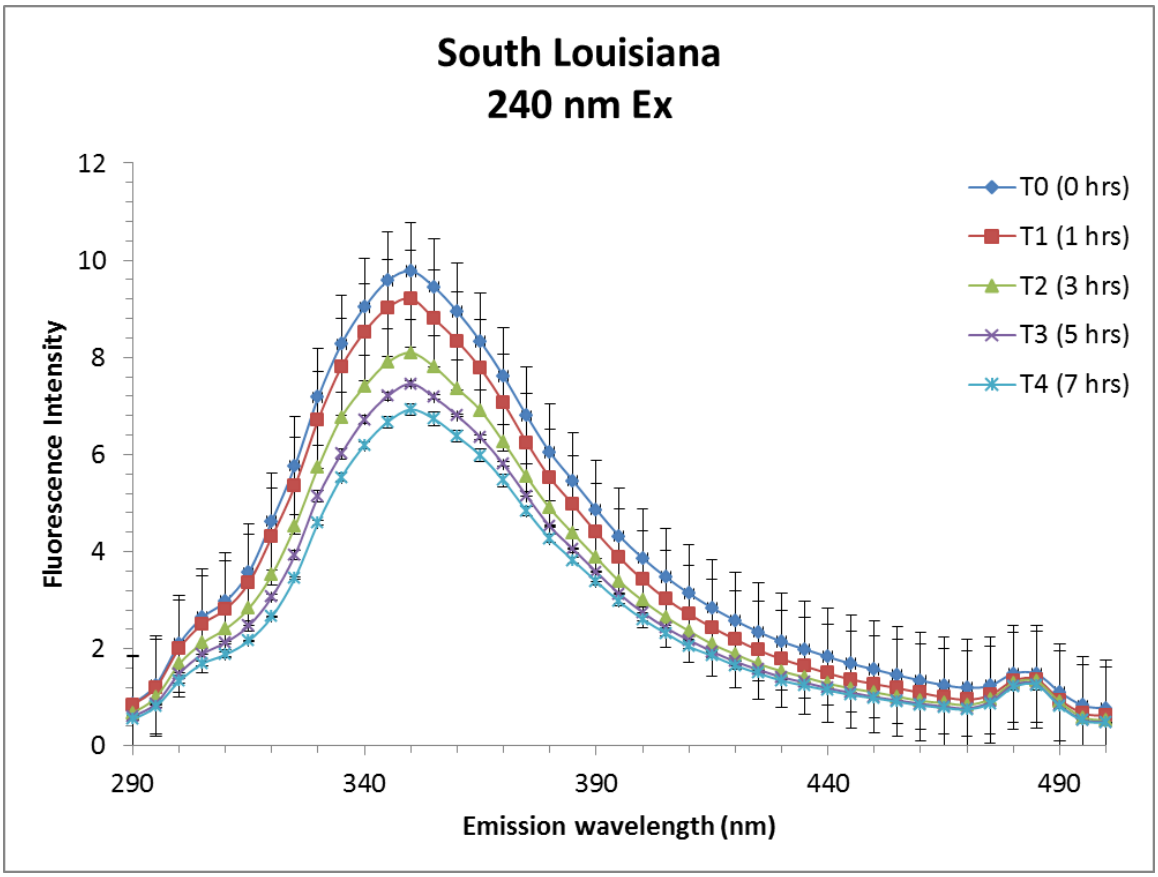

Figure 3.19. South Louisiana EEM Cross-section at 240 nm Excitation. Fluorescence intensity vs Emission for crude oil WAF Photooxidation experiment.

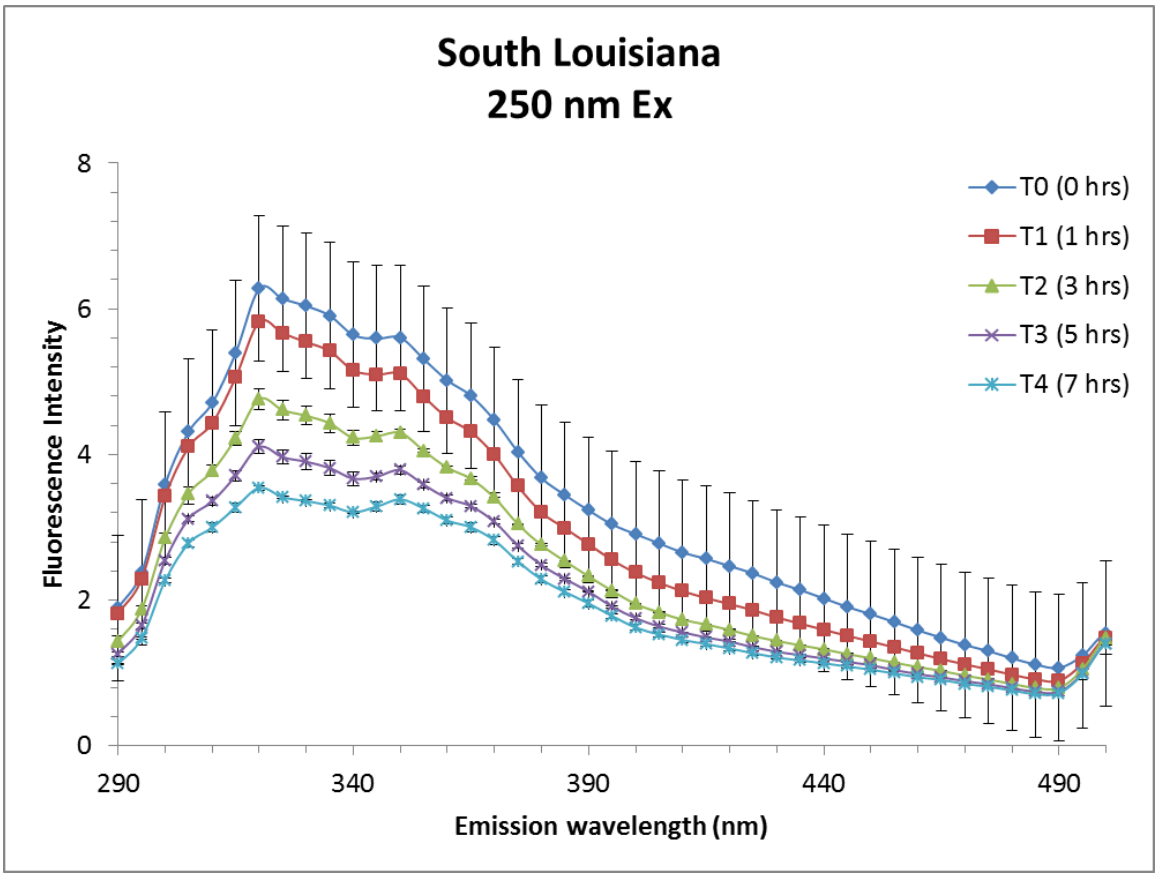

Figure 3.20. South Louisiana EEM Cross-section at 250 nm Excitation. Fluorescence intensity vs Emission for crude oil WAF Photooxidation experiment.

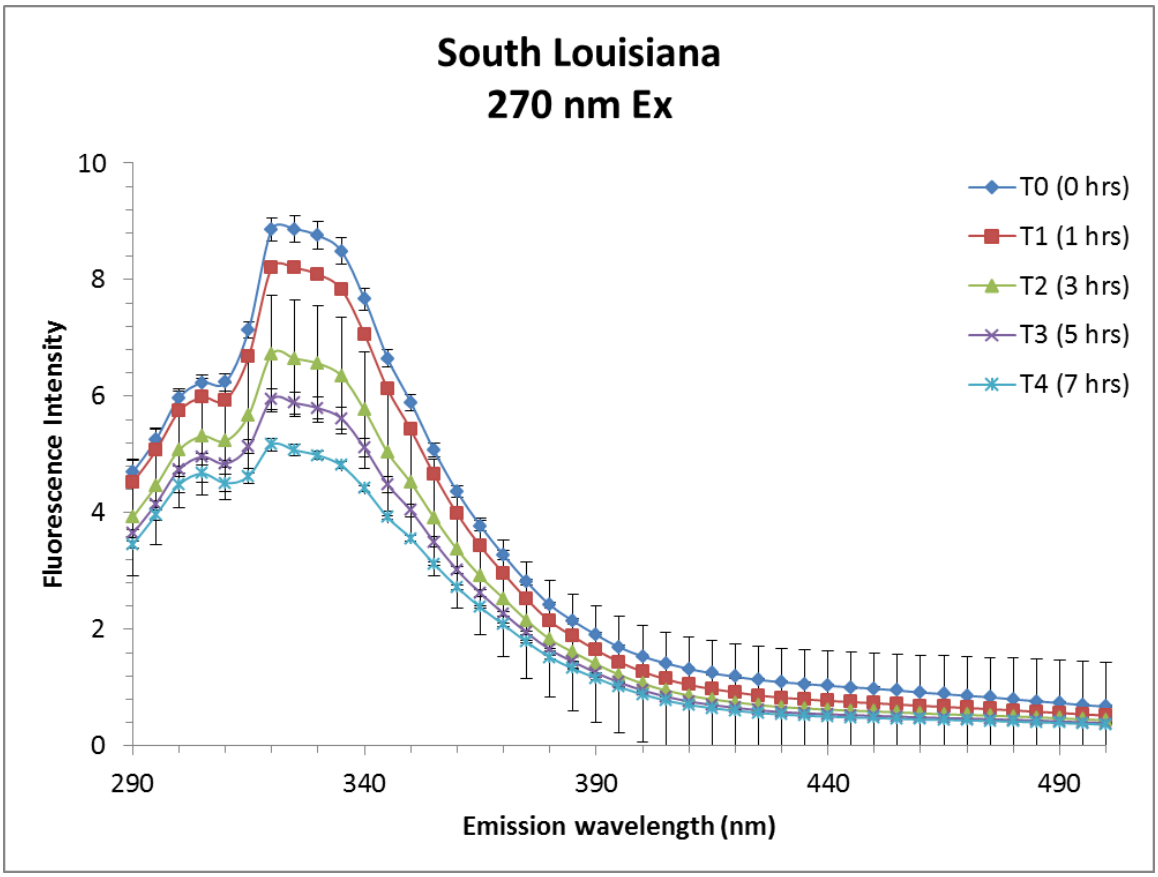

Figure 3.21. South Louisiana EEM Cross-section at 270 nm Excitation. Fluorescence intensity vs Emission for crude oil WAF Photooxidation experiment.

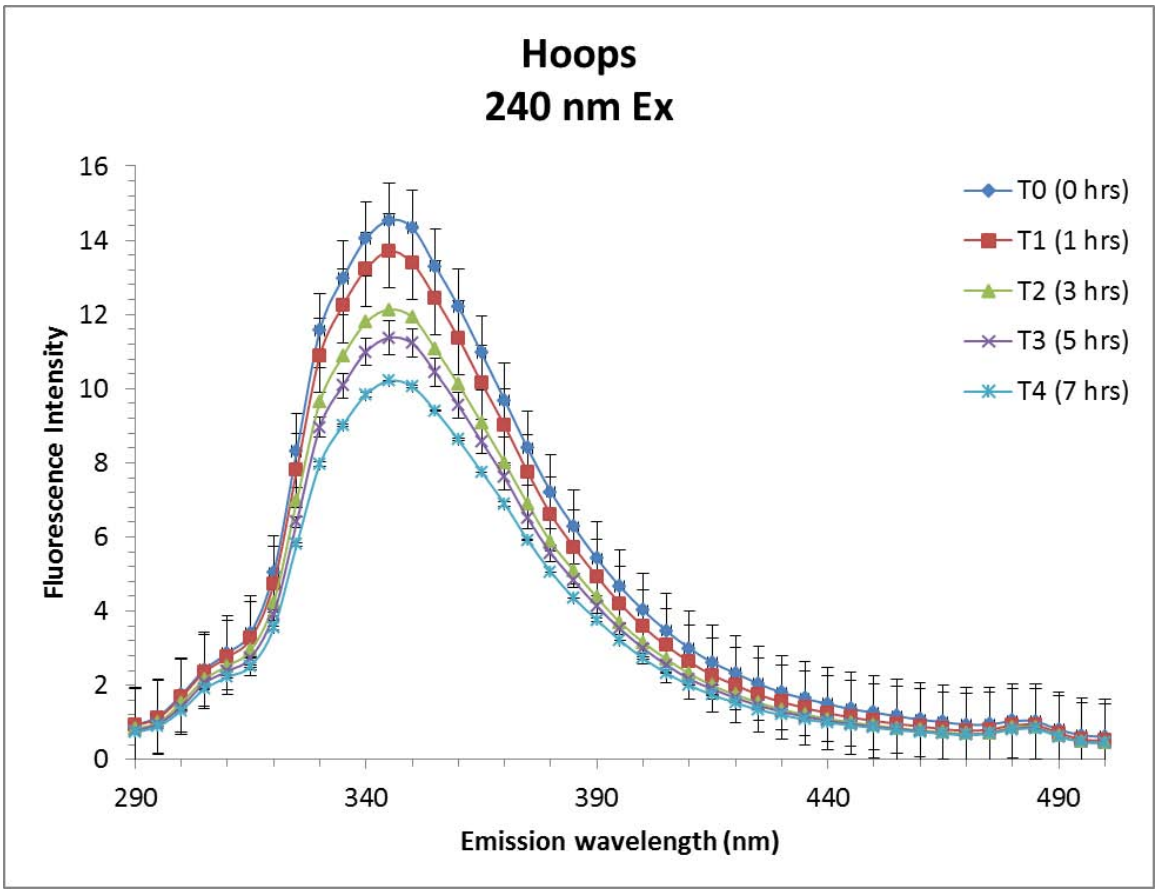

Figure 3.22. Hoops EEM Cross-section at 240 nm Excitation. Fluorescence intensity vs Emission for crude oil WAF Photooxidation experiment.

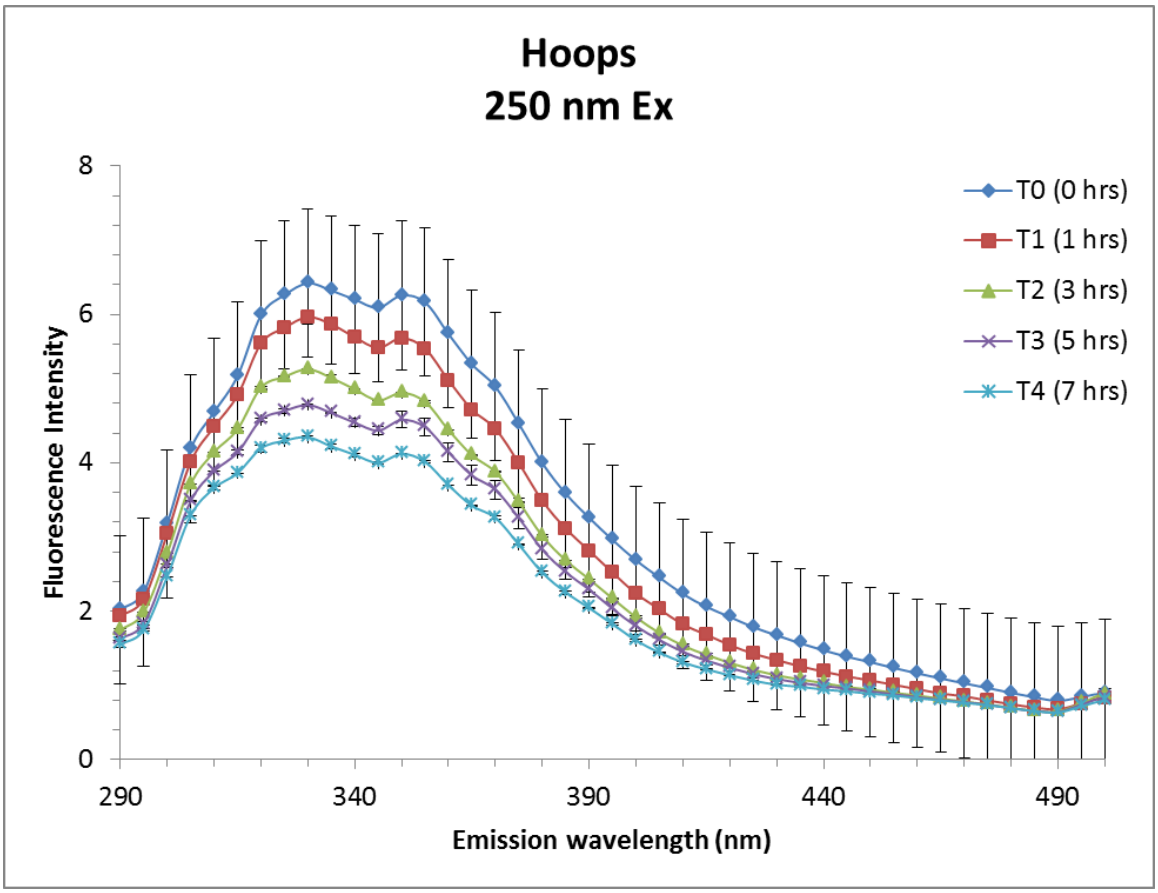

Figure 3.23. Hoops EEM Cross-section at 250 nm Excitation. Fluorescence intensity vs Emission for crude oil WAF Photooxidation experiment.

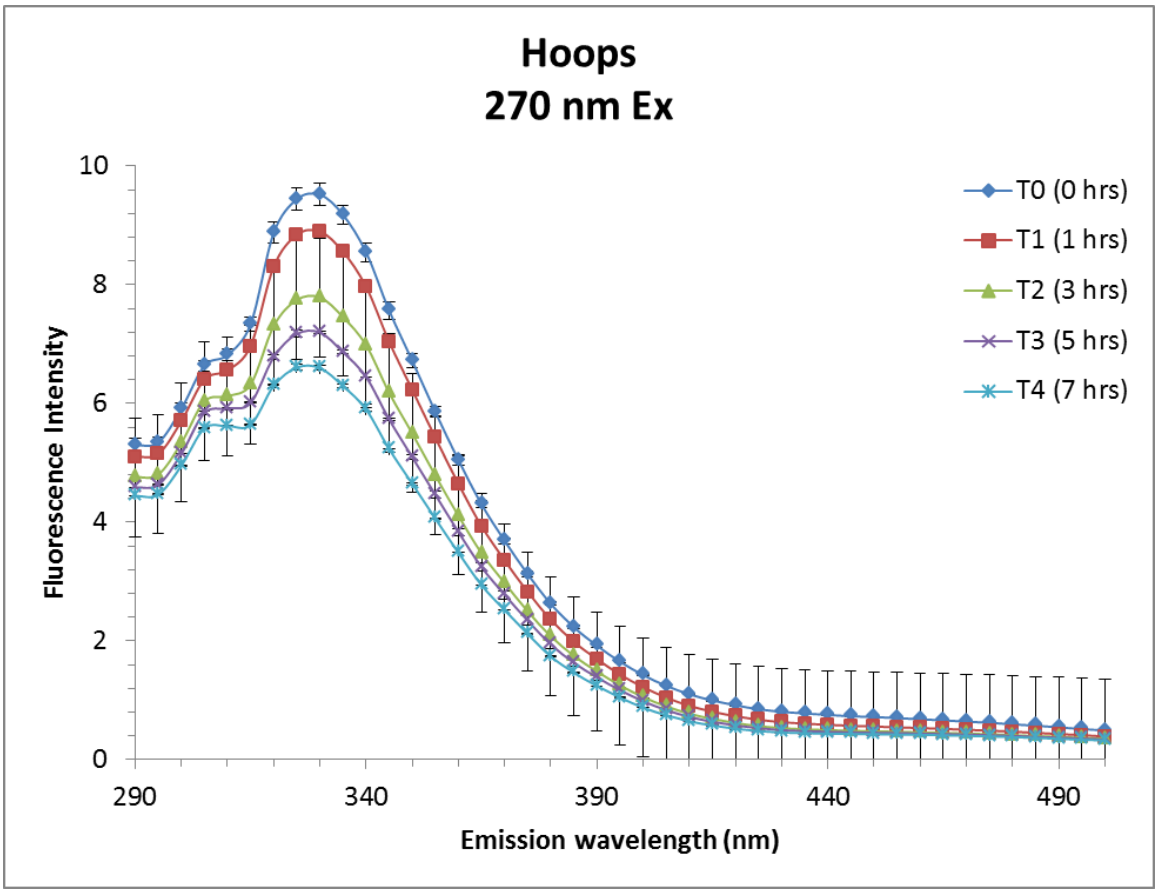

Figure 3.24. Hoops EEM Cross-section at 270 nm Excitation. Fluorescence intensity vs Emission for crude oil WAF Photooxidation experiment.

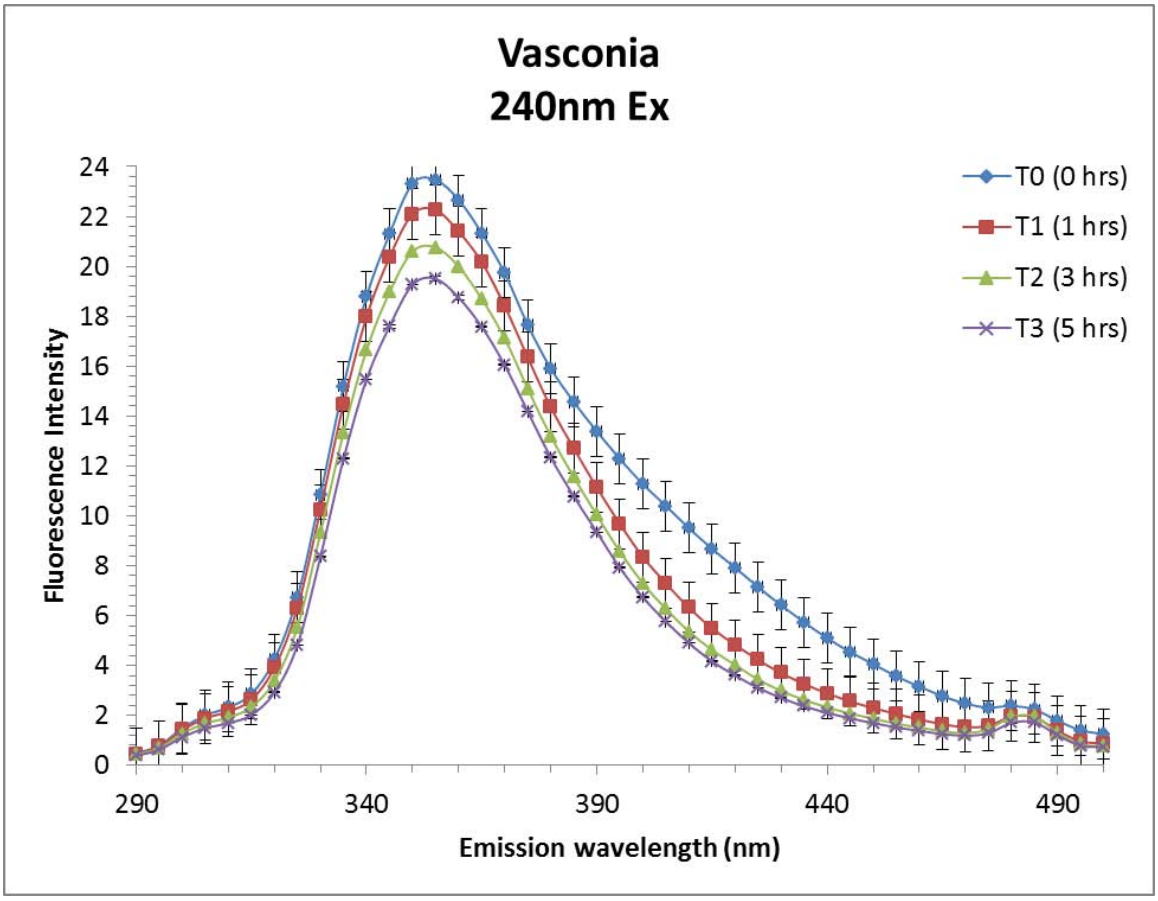

Figure 3.25. Vasconia EEM Cross-section at 240 nm Excitation. Fluorescence intensity vs Emission for crude oil WAF Photooxidation experiment.

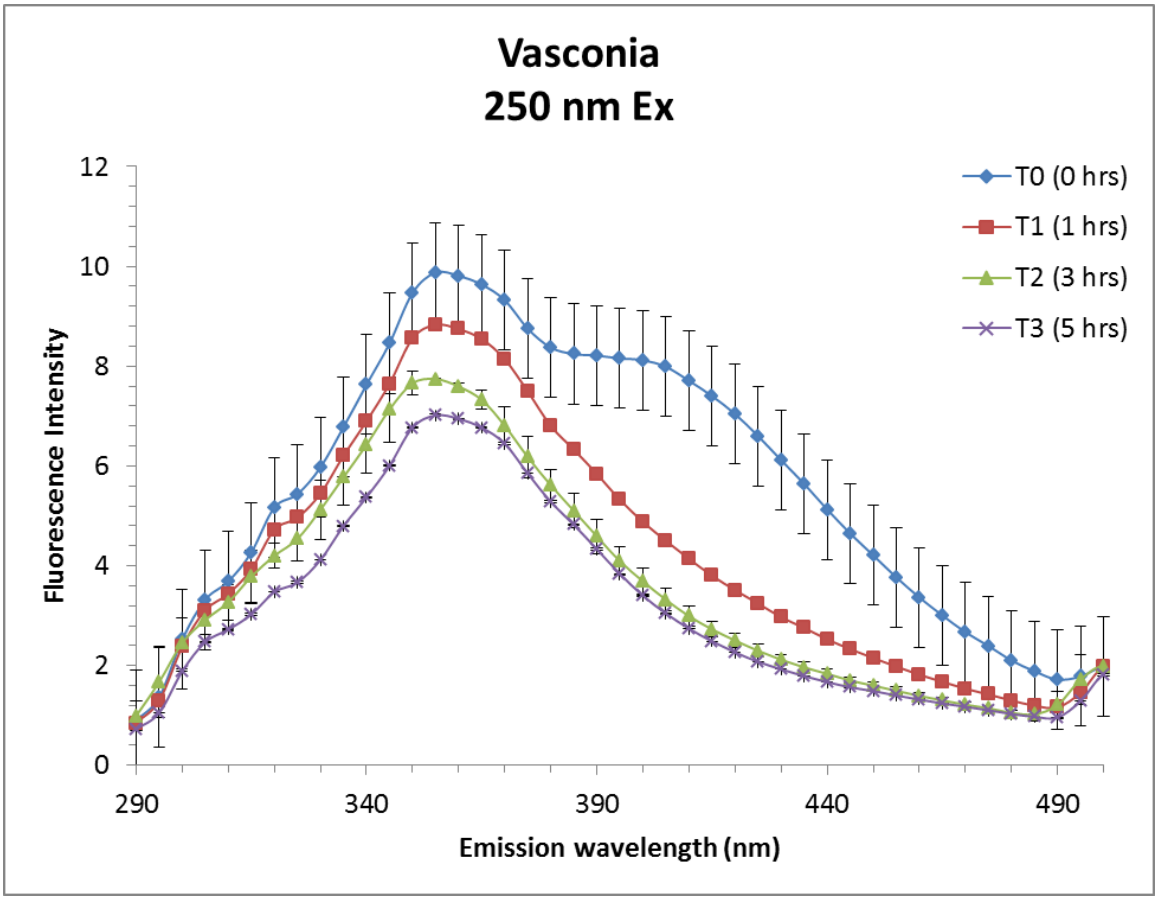

Figure 3.26. Vasconia EEM Cross-section at 250 nm Excitation. Fluorescence intensity vs Emission for crude oil WAF Photooxidation experiment.

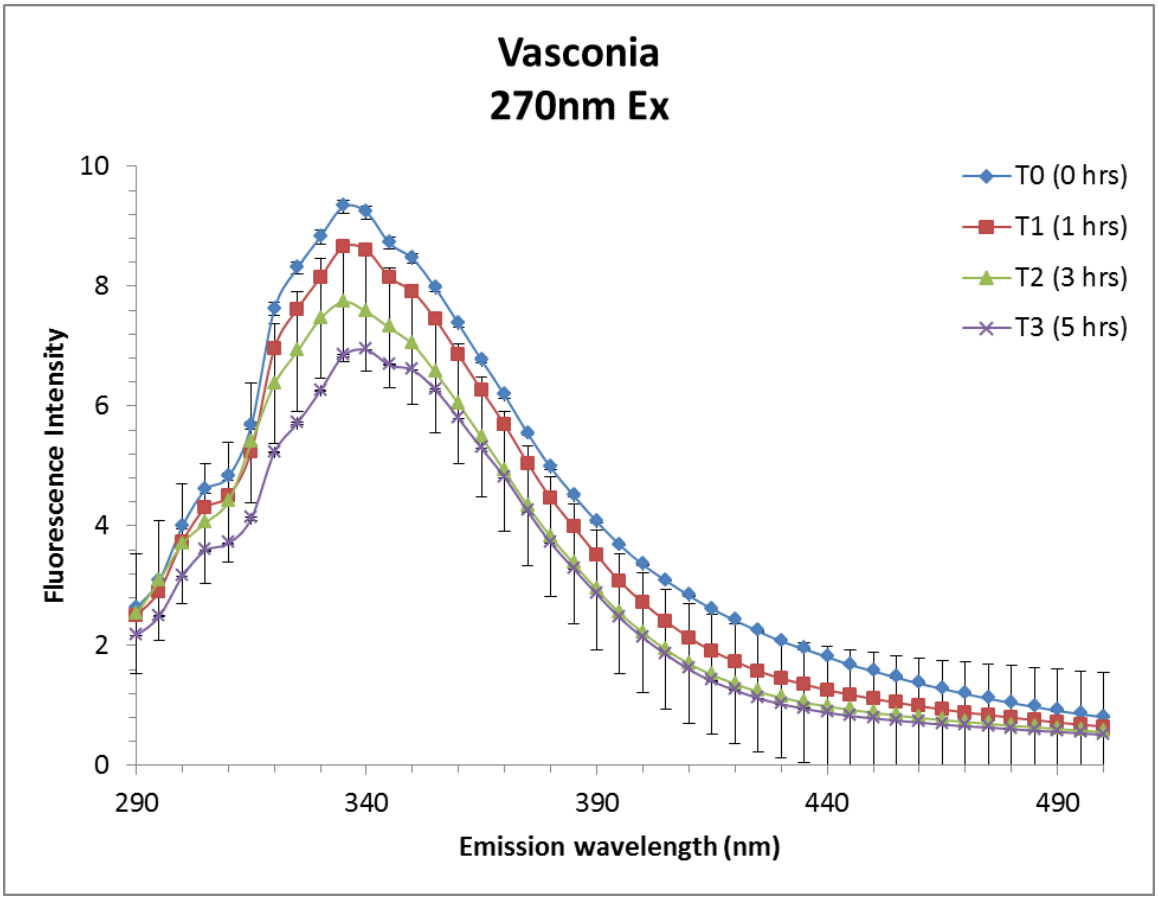

Figure 3.27. Vasconia EEM Cross-section at 270 nm Excitation. Fluorescence intensity vs Emission for crude oil WAF Photooxidation experiment.

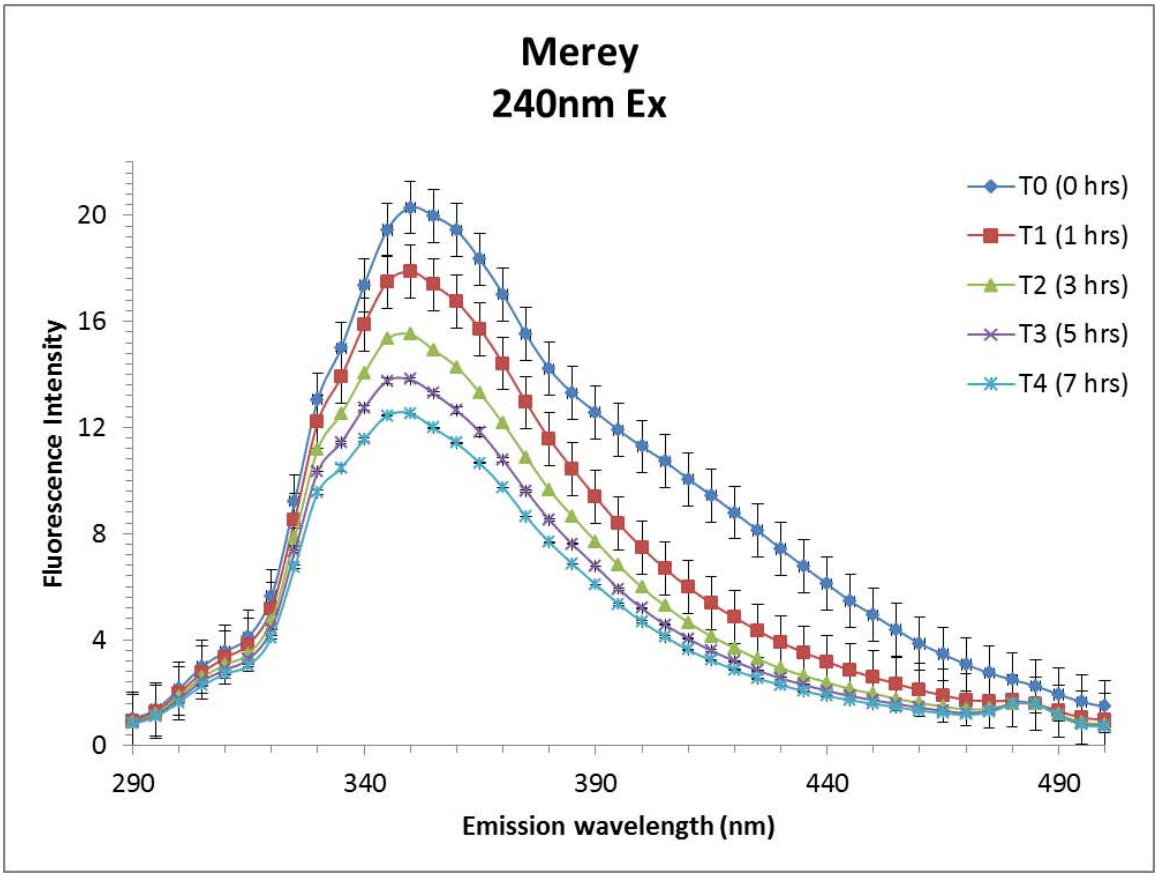

Figure 3.28. Merey EEM Cross-section at 240 nm Excitation. Fluorescence intensity vs Emission for crude oil WAF Photooxidation experiment.

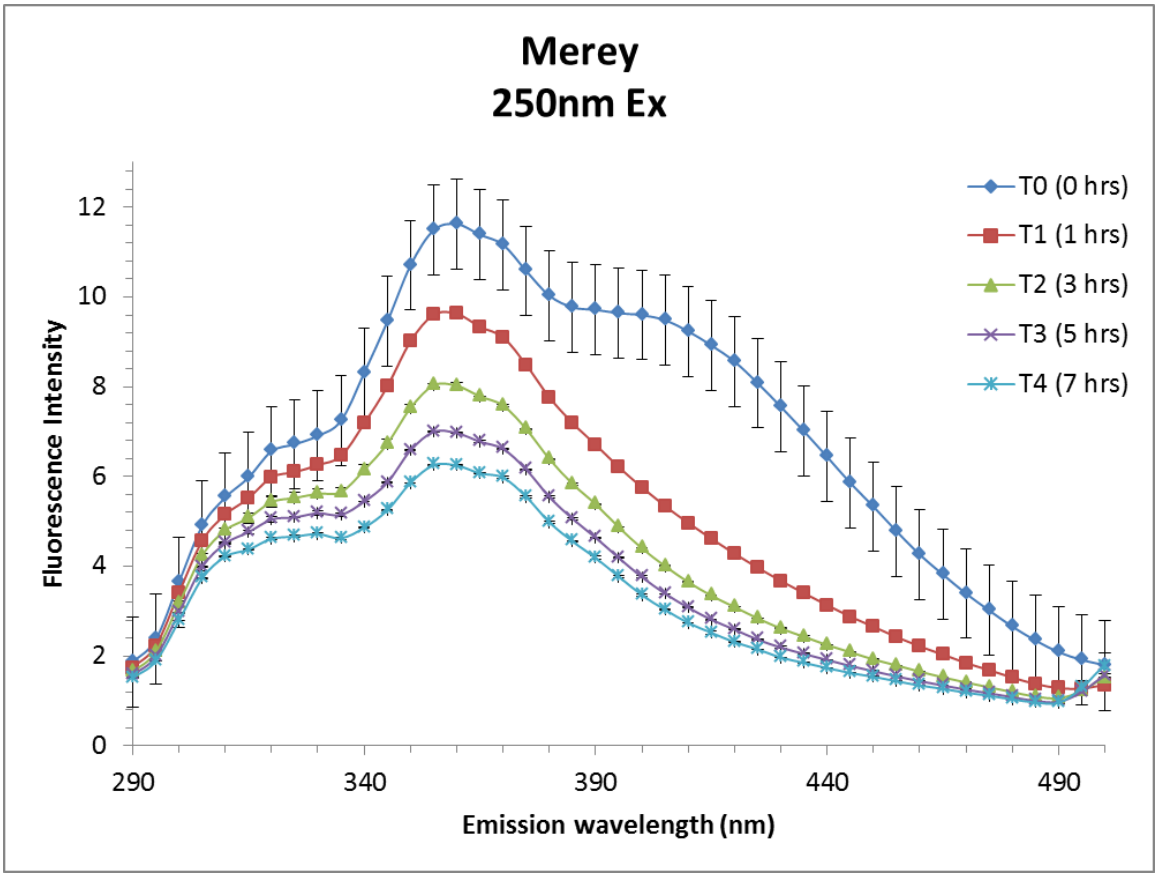

Figure 3.29. Merey EEM Cross-section at 250 nm Excitation. Fluorescence intensity vs Emission for crude oil WAF Photooxidation experiment.

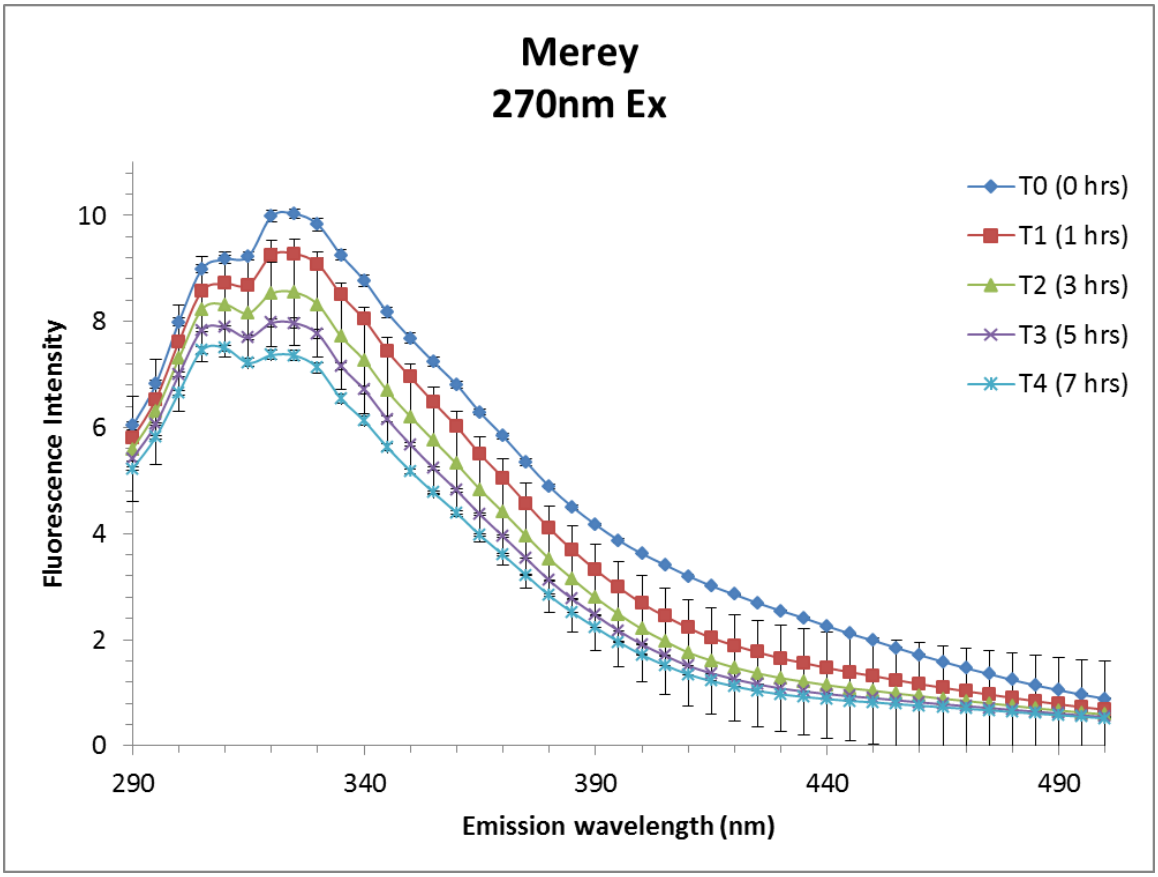

Figure 3.30. Merey EEM Cross-section at 270 nm Excitation. Fluorescence intensity vs Emission for crude oil WAF Photooxidation experiment.

Table 3.3. Key Fluorescence Excitation and Emission Pairs for all Crude Oil. These include Qua Iboe and Vasconia WAF equilibration and photooxidation experiments. Fluorescence emissions shifted slightly for some peaks (¤ blue shift, § red shift). The predominant emission maximum is listed in the table.

WAF Equilibration					
Crude oil (ID)	South Louisiana (SL)	Qua Iboe (QI)	HOOPS (H)	Vasconia (V)	Merey (M)
Excitation (nm)	Emission (nm)				
240	345¤	350	345	355§	350§
240	-	-	-	-	405
250	320	320§	330§	360§	360
250	350	350	350	400	405
270	300	305§	305	305	310
270	320	320	325	335§	325§
Photodegradation					
Crude oil (ID)	South Louisiana (SL)	Qua Iboe (QI)	HOOPS (H)	Vasconia (V)	Merey (M)
Excitation (nm)	Emission (nm)				
240	350	-	345	355	350
240	-	-	-	-	-
250	320	-	330	355	360¤
250	350	-	350	400	405
270	305	-	305§	305	310
270	320	-	325	335§	320¤

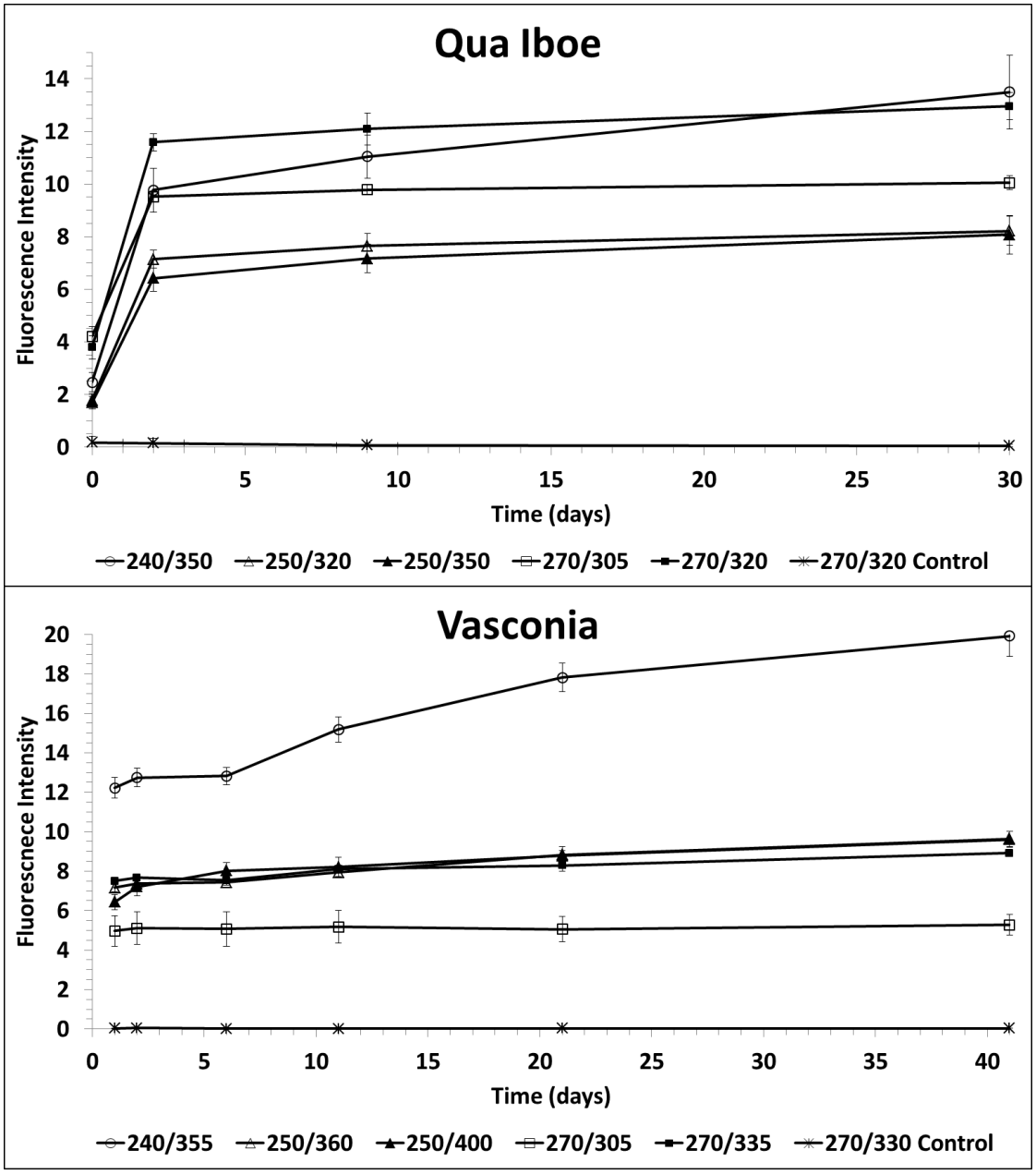

Figure 3.31. WAF Equilibration for Qua Iboe and Vasconia Crude Oil. Fluorescence over Time (days) for key ex/em peaks of Qua Iboe and Vasconia crude oil shows fluorescence stability of the WAF solution over time.

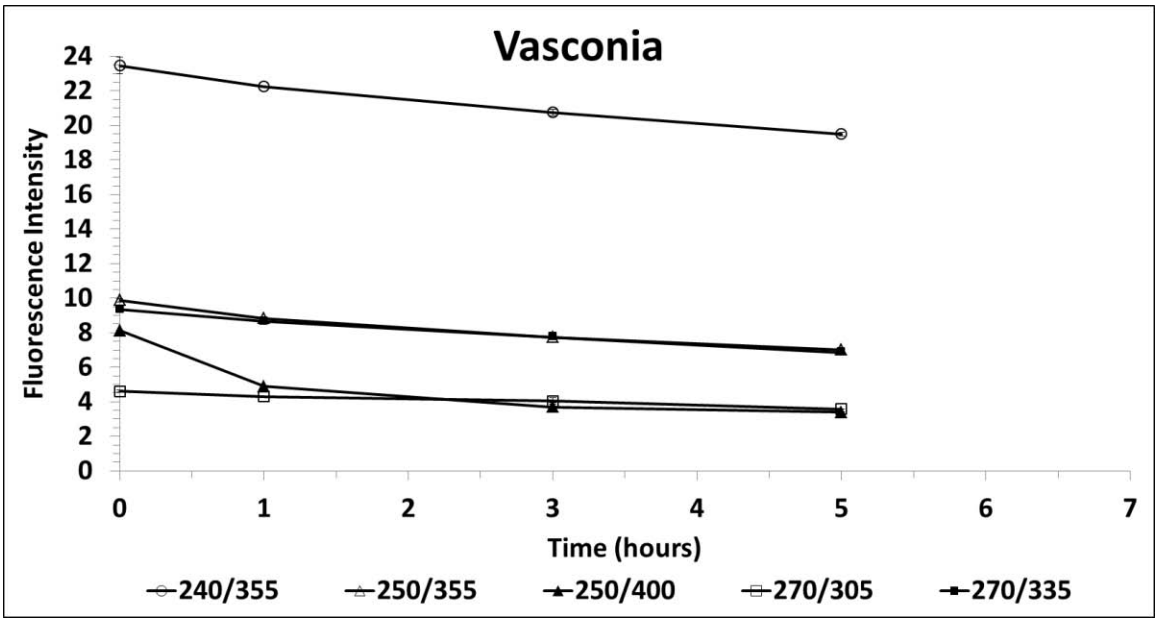

Figure 3.32. Photooxidation for Vasconia Crude Oil. Fluorescence Intensity vs Time for Vasconia Crude Oil.

Table 3.4. Percent Loss Calculations for all Crude Oil. % Light Loss represents apparent loss due to photodegradation of fluorescence intensity after 7 hrs of full spectrum UV exposure of crude oil WAF (5 hrs of exposure for Vasconia WAF). % Dark Loss represents the decrease in fluorescence intensity after 7 hrs of the dark control (5 hrs of exposure for Vasconia WAF).

South Louisiana			
Ex/Em	**% Light Loss**	**% Dark Loss**	**% Photodegradation Loss**
240/350	29	5	24
250/320	44	14	30
250/350	40	8	32
270/305	25	9	16
270/320	42	14	28
Hoops			
Ex/Em	**% Light Loss**	**% Dark Loss**	**% Photodegradation Loss**
240/345	30	2	28
250/330	32	6	26
250/350	34	3	31
270/305	16	3	13
270/325	30	6	24
Vasconia			
Ex/Em	**% Light Loss**	**% Dark Loss**	**% Photodegradation Loss**
240/355	17	1	16
250/355	29	2	27
250/400	58	2	56
270/305	22	3	19
270/335	27	3	23
Merey			
Ex/Em	**% Light Loss**	**% Dark Loss**	**% Photodegradation Loss**
240/350	38	10	28
250/360	46	10	36
250/405	68	10	58
270/310	18	10	8
270/325	27	11	16

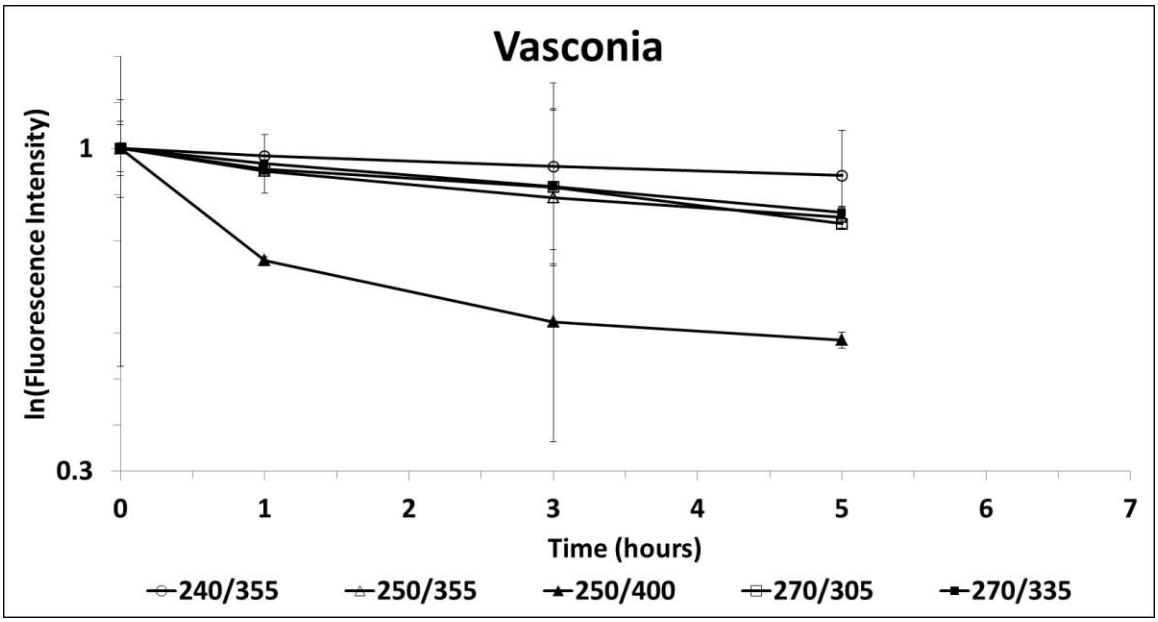

Figure 3.33. First-order Kinetic Model of Photooxidation for Vasconia Crude Oil. ln(Fluorescence Intensity) normalized to T0 vs Time (hrs) of photooxidation for key ex/em pairs for Vasconia crude oil.

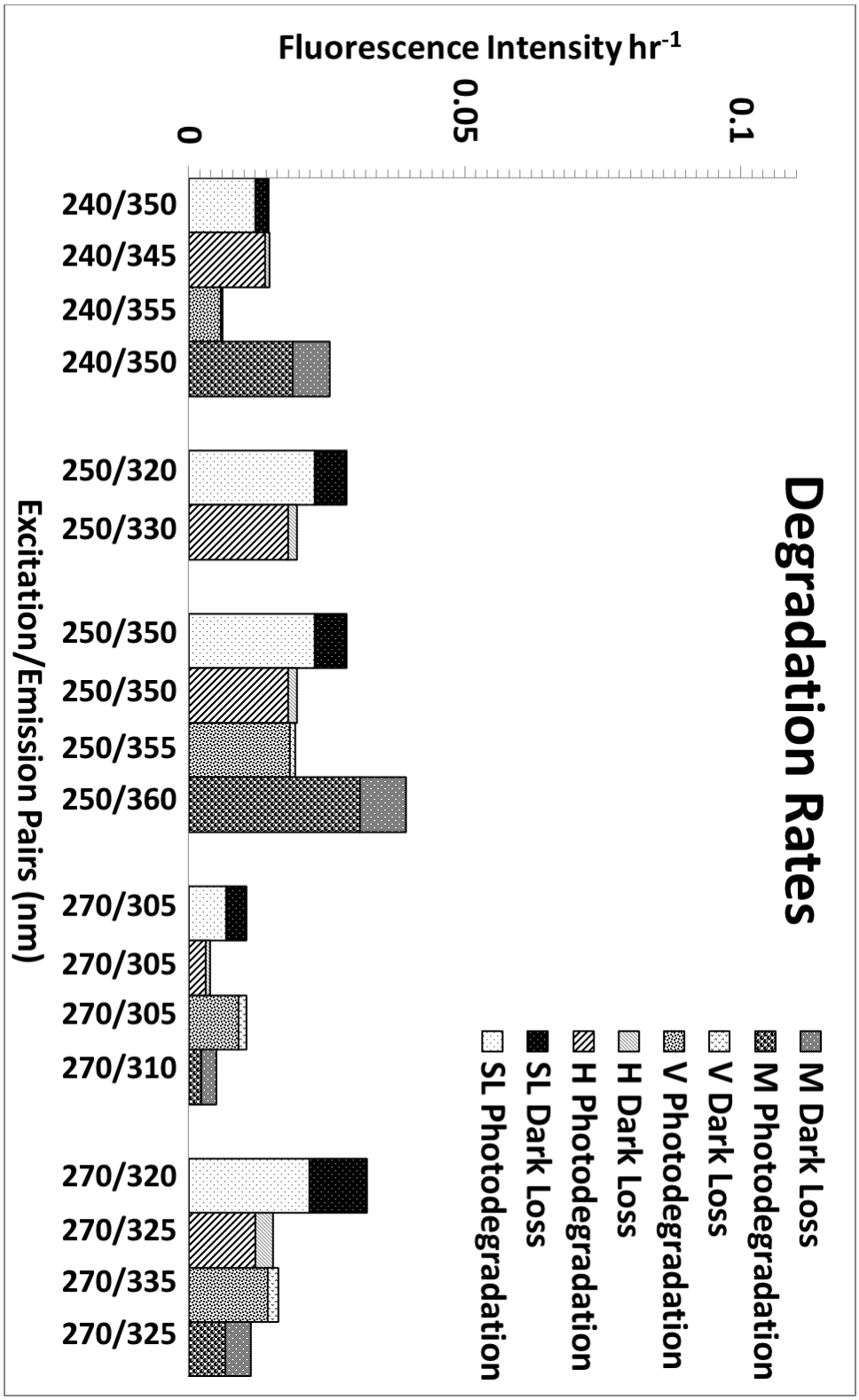

Figure 3.34. Photooxidation Rate Constants for all Crude Oil. South Louisiana, Hoops, Vasconia, and Merey crude oil rate constants. The k values (Fluorescence Intensity hr^{-1}) were calculated using first-order kinetic model.

CHAPTER 4

Summary and Conclusions

4.1 WAF Equilibration

Throughout the range of oils tested, the fluorescence spectra of crude oil water accommodated fractions (WAFs) revealed key excitation wavelength similarities. After a length of time (2-10 days, depending on the oil) most crude oil WAF fluorescence signals equilibrate to a maximum intensity. However, Qua Iboe, Vasconia, and Merey oil fluorescence emission signals from 240 nm excitation continued to increase. All three of these oils have more dense waxy (Qua Iboe and Vasconia) or tar-like (Merey) residues than South Louisiana and Hoops. The waxy residues found in Qua Iboe and Vasconia, called resin, are more polar, higher molecular weight compounds with lower solubility, which may cause longer equilibration time, and can contribute to Stokes shifts (red or blue shifting), energy transfer, and collisional quenching, all of which contribute to changes in fluorescence signals. Asphaltenes are the insoluble tarry residues found in Merey, and were not found in solution. How much these components are contributing to, or interfering with, the fluorescence intensity of the 240 nm excitation signals of Qua Iboe, Vasconia, and Merey is unclear at this time.

Despite their compositional differences, crude oil WAF displayed similar fluorescence emissions between 300 nm and 405 nm, and excitation between 240 nm and 270 nm.

4.2 Photooxidation

Calculated percent loss and first-order degradation rate constants indicate persistence of some fluorescent components in solution. Fluorescence measurements were taken at intervals over a period of five and seven hours demonstrating the effects of sunlight on a range of crude oil WAF. For Merey and Vasconia, their key emission peaks at 250nm excitation and emission at 400nm and 405nm, respectively, seem to be extremely susceptible to photooxidation. These signals resemble the high molecular weight PAHs anthracene and derivatives (Berlman 1971) that correspond with a high susceptibility to photooxidation.

The most persistent peaks were seen at 270 nm excitation for all crude oil WAFs. These signals had the lowest percent loss and the lowest calculated rate constants of all the peak pairs. They correspond to fluorene and naphthalene signals seen in literature, lighter weight PAHs that are less susceptible to photooxidation (Berlman 1971; Beltran et al., 1998; Christensen et al., 2005).

4.3 GCxGC-TOFMS

Merey and South Louisiana crude oils were chosen as representatives for our GCXGC-TOFMS analysis because of their distinct differences in fluorescence spectra and physical properties. PAHs in solution were identified, and concentrations were calculated for the two oils. Based on these identified PAHs and using ex/em pair references, key ex/em fluorescence peaks can be matched to their source, including

naphthalene, fluorene, and their derivatives. Soluble compounds, like naphthalene, were found in relatively high concentrations, where less soluble or insoluble compounds like acenaphthene, phenanthrene and fluorene were found in relatively low concentrations. The PAH concentrations found in Merey and South Louisiana WAF solutions were expected to correspond to their fluorescence intensity (Merey fluorescence intensity being greater than that of South Louisiana). However, this was not the case. This unexpected result could be due to energy transfer and collisional quenching of South Louisiana's relatively high concentration of naphthalene components in solution. The partitioning of similar non-fluorescing and polar compounds will differ between oils due to their complex chemical composition; concentration of these components in WAF solution should be considered. However, the difference in fluorescence intensity could also be due to highly fluorescent components like fluorene, anthracene, phenanthrene and their derivatives. These compounds have higher fluorescence quantum efficiency than naphthalene and its derivatives in other solvents (Berlman 1971), and may have a higher quantum efficiency in WAF solution, and therefore a greater influence on the fluorescence signal intensity.

4.4 Conclusions

The overall goal of this research was to investigate the spectral fluorescence properties of the water-accommodated fraction of crude oil in seawater. Studying how fluorescence signatures change when crude oil WAF is exposed to weathering conditions helped us determine that there were pervasive fluorescence signatures found throughout a variety of crude oil WAF, how photooxidation affected fluorescence over time, that some

fluorescence signatures were resistant to degradation, and that they could be used to differentiate oil spill properties and discriminate from background signals.

Obvious trends in fluorescence excitation and emission suggest similar composition of the fluorescent components in the crude oil WAFs found in this study. Both WAF equilibration and photooxidation experiments resulted in a consistent range of excitation and emission wavelengths for all crude oil WAF fluorescence signatures (240-270 nm ex and 305-360 nm emission). Of the fluorometers used during the DWH, only one would be able to detect our WAF signatures: the Chelsea Instruments Aromatic Hydrocarbon Fluorometer, which detects fluorescence signals at 239/360 nm ex/em (Ch 2 Table 2.1).

Loss calculations and kinetic modeling of key peak pairs showed that photodegradation had a greater affect than volatilization on WAF fluorescence, and there were persistent peaks for all crude oils (270 nm excitation, 300-310 nm and 320-335 nm emission). It is important to note that the persistent signals at 270 nm excitation would not be detected by Chelsea Instruments fluorometer.

GCxGC-TOFMS analysis of two crude oils with very different physical properties (South Louisiana and Merey) revealed similar WAF compositions, though different polycyclic aromatic hydrocarbon (PAH) concentrations. Results indicate several PAH groups responsible for their unique fluorescence signals including naphthalene, fluorene, anthracene, phenanthrene and their derivatives. Fluorene, found in both South Louisiana and Merey, fluoresces within the key excitation/emission range of crude oil WAF determined by these experiments, and is likely a contributing factor causing the persistent fluorescence signals at 270 nm excitation.

High concentrations of PAHs and non-fluorescing compounds in South Louisiana WAF could be causing quenching of its fluorescence signal. Non-fluorescing and polar components were not evaluated in in this study. Complex interactions, like quenching, energy transfer and peak shifting, could lead to some difficulty with in situ tracking of dissolved crude oil. These could also be considered unique to the fluorescence signature of crude oil WAFs. Key excitation/emission wavelength pairs determined in these studies show minimal peak shifting occurring and persistent peaks from all crude oil WAFs were found over a specific range. Until these crude oils are fully characterized, many questions will remain regarding the cause of these results.

Naturally fluorescent compounds in solution, like colored dissolved organic matter (CDOM), could potentially interfere with WAF fluorescence signals. However, our findings show that emission peaks at each key excitation wavelength can be differentiated from most other fluorophores commonly found in seawater, with the potential exception of Tyrosine-like compounds at 275nm ex, 310nm em (P.G Coble 1996). GCxGC-TOFMS data revealed no Tyrosine-like compounds in South Louisiana and Merey WAF and it has been shown that crude oil fluorescence can be distinguished from CDOM fluorescence (Patsayeva 1995; JAG 2010).

With this work, we now have a greater understanding of the effects of weathering on crude oil. We now recognize that the fluorescence signature of crude oil will be dynamic as its WAF equilibrates, evidenced by Stokes shifting. This study has identified fluorescence peaks that can be used to track a variety of oils, and more conservative peaks for tracking oil as it degrades. Current in situ instruments could be modified to

detect fluorescence over those key wavelength ranges with the goal of tracking PAHs in seawater.

4.5 Future Research

Further investigation is needed for a more complete understanding of the effects of weathering on crude oil WAF fluorescence in seawater. WAF equilibration and photooxidation studies revealed specific excitation and emission ranges for targeting PAHs in crude oil WAF. An exploration of the effects of microbial degradation and dispersants on crude oil WAF in addition to our study will offer a more comprehensive grasp of crude oil weathering that can be applied toward improving in situ fluorescence technology.

The characteristics of data collected in this study lent itself to "peak picking" techniques. The high information volume of current and future data can also be processed using methods like principal component analysis (PCA) or parallel factor analysis (PARAFAC). These multivariate analysis methods can provide a broader and relatively fast data analysis compared to other techniques (Stedmon et al., 2003).

Studies focused on determining the cause of Stokes shifts, and whether energy transfer or quenching is indeed strongly influencing fluorescence signals as crude oil WAF degrades, is needed. A more detailed investigation of the polar and non-fluorescent components of crude oil WAF, partitioning studies, and quantum efficiency studies of the fluorescent components might shed light on the differences in fluorescence intensity versus concentration we saw in South Louisiana and Merey oil.

4.6 Application and Outlook

The complexity of crude oil composition is evident, but over the range of crude oils studied a distinct pattern has emerged in the fluorescence signals of corresponding WAFs. This study has brought a better understanding of the effect of weathering on crude oil fluorescence. Our results show that a variety of crude oil can be tracked via fluorescence spectroscopy over the key wavelength range between 240-270 nm excitation and 305-360 nm emission. This study has identified persistent fluorescence peaks found throughout all crude oil WAFs that would not be detected by current instrumentation (270 nm excitation and 305-310 nm and 320-350 nm emission). Modified in situ instruments could track signals over this range, specifically targeting dissolved PAHs in seawater.

Continued increase in oil exploration, exploitation, and the potential for negative environmental consequences demands better spill response and recovery. The 2010 DWH spill brought to light new questions and concerns about crude oil dispersed throughout the water column. Research investigating fluorescence properties of the water-accommodated fraction of crude oil was undertaken due to concerns over sensitivity and specificity toward dispersed oil of in situ fluorometers used during the DWH spill. This data has a significant part to play in the continued drive toward understanding the impacts of crude oil in the environment.

Tragedies like the DWH spill have a far reaching effect. Concern remains over the short and long term impact of PAH contamination on the environment, including food sources such as fish and mollusks (Mendelssohn et al., 2012). Modified in situ fluorometers based on research found here, and future studies, can be used to improve

first response of oil spills to track PAHs in solution, or in long term monitoring of spill sites for low level PAHs.

REFERENCES

Allan, S.E., Smith, B.W., and Anderson, K.A. (2012) Impact of the Deepwater Horizon Oil Spill on Bioavailable Polycyclic Aromatic Hydrocarbons in Gulf of Mexico Coastal Waters. Environ. Sci. Technol., 46, 2033-2039.

Backhus, D. A., and Gschwend, P.M. (1990) Fluorescent Polycyclic Aromatic Hydrocarbons as Probes for Studying the Impact of Colloids on Pollutant Transport in Groundwater. Environ. Sci. Technol., 24, 1214-1223

Beltran, J.L., Ferrer, R., and Guiteras, J. (1998) Multivariate Calibration of Polycyclic Aromatic Hydrocarbon Mixtures from Excitation-emission Fluorescence Spectra. Analytica Chimica Acta, 373, 311-319.

Berlman, I.B. (1971) Handbook of Fluorescence Spectra of Aromatic Molecules. New York: Academic Press, 1971.

Boehm, P.D., and Page, D.S. (2007) Exposure Elements in Oil Spill Risk and Natural Resource Damage Assessments: A review. Human and Ecological Risk Assessment, 13, 419-448.

Booksh, K.S., Muroski, A.R., and Myrick, M.L. (1996) Single-Measurement Excitation/Emission Matrix Spectrofluorometer for Determination of Hydrocarbons in Ocean water. 2. Calibration and Quantitation of Naphthalene and Styrene. Anal. Chem., 68, 3539-3544.

Booth, A.M., Sutton, P.A., Lewis, C.A., Lewis, C.A., Scarlett, A., Chau, W., Widdows, J., and Rowland, S.J. (2007) Unresolved Complex Mixtures of Aromatic Hydrocarbons: Thousands of Overlooked Persistent Bioaccumulative, and Toxic Contaminants in Mussels. Environ. Sci. Technol., 41, 457-464.

Bridie, A.L., Wanders, T.H., Zegveld, W., and Van Der Heijde, H.B. (1980) Formation, Prevention and Breaking of Sea Water in Crude Oil Emulsions 'Chocolate Mousses'. Marine Pollution Bulletin, 11, 343-348.

Buenrostro-Gonzalez, E., Lira-Galeana, C., Gil-Villegas, A., and Wu, J. (2004) Asphaltene Precipitation in Crude Oils: Theory and experiments. AIChE Journal, 50, 2552-2570.

Bugden, J.B.C., Yeung, C.W., Kepkay, P.E., and Lee, K. (2008) Application of Ultraviolet Fluorometery and Excitation-emission Matrix Spectroscopy (EEMS)

of Fingerprint Oil and Chemically Dispersed Oil in Seawater. Marine Pollution Bulletin, 56, 677-685.

Camilli, R. Reddy, C.M., Yoerger, D.R., Van Mooy, B.A., Jakuba, M.V., Kinsey, J.C., McIntyre, C.P., Sylva, S.P., and Maloney, J.V. (2010) Tracking Hydrocarbon Plume Transport and Biodegradation at Deepwater Horizon. Science, 330, 201-204.

Carrales Jr., M., Martin, R.W. (1975) Sulfur Content of Crude oils. US Bureau of Mines Information Circular, 8676.

Chandrasekar, S., Sorial, G.A., and Weaver, J.W. (2006) Dispersant Effectiveness on Oil Spills - Impact of Salinity. Journal of Marine Science, 63, 1418-1430.

Christensen, J.H. and Tomasi, G. (2007) Practical Aspects of Chemometrics for Oil Spill Fingerprinting. J. Chromatogr. A, 1169, 1-22.

Christensen, J.H., Hansen, A.B., Tomasi, G., Mortensen, J., and Andersen, O. (2004) Integrated Methodology for Forensic Oil Spill Identification. Environ. Sci. Technol, 38, 2912-2918.

Coble, P.G. (2007) Marine Optical Biogeochemistry: The Chemistry of Ocean Color. Chemical Reviews, 107, 402-418.

Cormack, D. (1999) Response to Marine Oil Pollution: Review and Assessment, Volume 2 of Environmental Pollution, Kluwer Academic Publishers.

Couillard, C.M., Lee, K., Legare, B., King, T.L. (2005) Effect of Dispersant on the Composition of the Water-accommodated Fraction of Crude Oil and its Toxicity to Larval Marine Fish. Environmental Toxicology and Chemistry, 24, 1496-1504.

Dabestani, R. and Ivanov, I.N. (1999) A Compilation of Physical, Spectroscopic and Photophysical Properties of Polycyclic Aromatic Hydrocarbons. Photochemistry and Photobiology, 70, 10-34.

DeHaan, C.J., and Sturges, W. (2005) Deep Cyclonic Circulation in the Gulf of Mexico. Journal of Physical Oceanography, 35, 1801-1812.

Diercks, A., Highsmith, R.C., Asper, V.L., Joung, D., Zhou, Z., Guo, L., et al. (2010) Characterization of subsurface polycyclic aromatic hydrocarbons at the Deepwater Horizon site. Geophysical Research Letters, 37, art. no. L20602.

Dutta, T.K., and Harayama, S. (2000) Fate of Crude Oil by the Combination of Photooxidation and Biodegradation. Environ. Sci. Technol., 34, 1500-1505.

Ehrhardt, M.G., Burns, K.A., and Bicego, M.C. (1992) Sunlight-induced Compositional Alterations in the Seawater-soluble Fraction of a Crude Oil. Marine Chemistry, 37, 53-64.

Environmental Protection Agency, United States (2012) Priority Pollutants, Code of Federal Regulations, 40 CFR 423, Appendix A. (http://water.epa.gov/scitech/methods/cwa/pollutants.cfm)

Fingas, M. (2008) A Review of Knowledge on Water-In-Oil Emulsions. International Oil Spill Conference, Proceedings , 1269-1273.

Gonzalez, J.J., Vinas, L., Franco, M.A., Fumega, J., Soriano, J.A., Grueiro, G., et al. (2006) Spatial and Temporal Distribution of Dissolved/Dispersed Aromatic Hydrocarbons in Sea Water in the Area Affected by the Prestige Oil Spill. Marine Pollution Bulletin, 53, 250-259.

Gorden Jr., D.C., Keizer, P.D., Hardstaff, W.R., and Aldous, D.G. (1976) Fate of Crude Oil Spilled on Seawater Contained in Outdoor Tanks. Environ. Sci. Tech., 10, 580-585.

Groenzin, H. and Mullins, O.C. (1999) Asphaltene Molecular Size and Structure. J. Phys. Chem. A, 103, 11237-11245.

Hamdan, L.J., and Fulmer, P.A. (2011) Effects of COREXIT® EC9500A on Bacteria From a Beach Oiled by the Deepwater Horizon Spill. Aquatic Microbial Ecology, 63, 101-109.

Hazen, T.C., Dubinsky, E.A., DeSantis, T.Z., Anderson, G.L., Piceno, Y.M., Singh, N., Jansson, J.K., Probst, A., Borglin, S.E., Fortney, J.L., Stringfellow, W.T., Bill, M., Conrad, M.E., Tom, L.M., Chavarria, K.L., Alusi, T.R., Lamendella, R., Joyner, D.C., Spier, C., Baelum, J., Auer, M., Zemla, M.L., Chakraborty, R., Sonnenthal, E.L., D'haeseleer, P., Holman, H.N., Osman, S., Lu, Z., Van Nostrand, J.D., Deng, Y., Zhou, J., and Mason, O.U. (2010) Deep-Sea Oil Plume Enriches Indigenous Oil-Degrading Bacteria. Science, 330, 204-208.

Hegazi, E., Hamdan, A., and Mastromarino, J. (2001) New Approach for Spectral Characterization of Crude Oil Using Time-Resolved Fluorescence Spectra. Applied Spectroscopy, 55, 202-207.

Hemmer, M.J., Barron, M.G., and Greene, R.M. (2010) Comparative Toxicity of Louisiana Sweet Crude oil (LSC) and Chemically Dispersed LSC to Two Gulf of Mexico Aquatic Test Species. July 31, 2010, USEPA Dispersed Oil Toxicity Testing, 1-13.

Hornafius, J.S., Quigley, D., and Luyendyk, B.P. (1999) The World's Most Spectacular marine Hydrocarbon Seeps (Coal Oil Point, Santa Barbara Channel, California): Quantification of Emissions. Journal of Geophysical Research, 104, 20703-20711.

Huggett, R. J., Stegeman, J.J., Page, D.S., Parker, K.R., Woodin, B., and Brown, J.S. (2003) Biomarkers in Fish from Prince William Sound and the Gulf of Alaska: 1999-2000. Environ. Sci. Technol. 37, 4043-4051.

Hyne, N.J. (2001) Nontechnical Guide to Petroleum Geology, Exploration, Drilling and Production, 2nd Edition, Penn Well Corporation.

Johansen, O., Rye, H. (2003) DeepSpill-Field Study of a Simulated Oil and Gas Blowout in Deep Water. Spill Science & Technology Bulletin, 8, 433-443.

Joint Analysis Group. (2010) Review of Preliminary Data to Examine Subsurface Oil in the Vicinity of MC252#1. May 19 to June 19, 2010.

Kepkay, P.E., Yeung, C.W., Bugden, J.C., Li, Z. and Lee, K. (2008) Ultraviolet Fluorescence Spectroscopy (UVFS): A New Means of Determining the Effect of Chemical Dispersants on Oil Spills. International Oil Spill Conference, 639-644.

Kirby, J.H. (2012) Findings of Persistency of Polycyclic Aromatic Hydrocarbons in Residual Tar Product Sourced from Crude Oil Released during the Deepwater Horizon MC252 Spill of National Significance. Findings of Persistency of Polycyclic Aromatic Hydrocarbons, Saturday, April 14, 2012.

Lakowicz, J. (2006) Principles of Fluorescence Spectroscopy, 3rd edition, Springer.

Laws, E.A. (2000) Aquatic pollution: An Introductory Text, 3rd edition, John Wiley & Sons, Inc.

Leahy, J.G. and Colwell (1990) Microbial Degradation of hydrocarbons in the Environment. Microbiological Reviews, 54, 305-315.

Lyons, W.C. and Plisga, G.J. (2005) Standard Handbook of Petroleum and Natural Gas Engineering (2nd Edition). Elsevier.

Maher, W.A. (1982) Preparation and Characterization of Water-soluble Fractions of Crude and Refined Oils for Use in Toxicity Studies. Environmental Contamination and Toxicology, 29, 268-272.

Maher, W.A. (1986) Preparation of Water Soluble Fractions of Crude Oils for Toxicity Studies. Environmental Contamination and Toxicology, 36, 226-229.

Maltrud, M., Peacock, S., and Visbeck, M. (2010) On the Possible Long-term Fate of Oil Released in the Deepwater Horizon Incident, Estimated Using Ensembles of Dye Release Simulations. Environmental Research Letters, 5, 1-7.

Marr, L.C., Kirchstetter, T.W., and Harley, R.A., Miguel, A.H., Hering, S.V., and Hammond, S.K. (1999) Characterization of Polycyclic Aromatic Hydrocarbons in Motor Vehicle Fuels and Exhaust Emissions. Environ. Sci. Technol., 33, 3091-3099.

Mendelssohn, I.P., Anderson, G.L., Baltz, D.M, Caffey, R.H., Carman, K.R., Fleeger, J.W., Joye, S.B., Lin, Q., Maltby, E., Overton, E.B., and Rozas, L.P. (2012) Oil Impacts on Coastal Wetlands: Implications for the Mississippi River Delta Ecosystem After the Deepwater Horizon Oil Spill. Bioscience, 62(6), 562-574.

Monterey Bay Aquarium Research Institute. (2010) NOAA Ship Gordon Gunter Cruise GU-10-02, Gulf of Mexico June 2 - 3, 2010 Operations of the MBARI AUV Dorado Data Report. June 2010.

Montgomery, M.T., Osbourn, C.L., Furukawa, Y., and Gieskes, J.M. (2011) Increased Capacity for Polycyclic Aromatic Hydrocarbon Mineralization in Bioirrigated Coastal Marine Sediments. Bioremediation Journal, 12, 98-110.

Murphy, K.R., Butler, K.D., Spencer, R.G.M., Stedmon, C.A., Boehme, J.R., and Aiken, G.R. (2010) Measurement of Dissolved Organic Matter Fluorescence in Aquatic Environments: An Interlaboratory Comparison. Environ. Sci. Technol. 44, 9405-9412.

National Research Council, Committee on Oil in the Sea: Inputs, Fates, and Effects. (2003) Oil in the Sea III: Inputs, Fates, and Effects, The National Academies Press.

Neff, J.M., Ostazeski, S., Gardiner, W., and Stejskal, I. (2000) Effects of Weathering on the Toxicity of Three Offshore Australian Crude Oils and a Diesel Fuel to Marine Animals. Environmental Toxicology and Chemistry, 19, 1809-1821.

Nicodem, D.E., Fernandes, M.Z., Guedes, C.B., and Correa, R.J. (1997) Photochemical Processes and the Environmental Impact of Petroleum Spills. Biogeochemistry, 39, 121-138.

Nicodem, D.E., Guedes, C.B., and Correa, R.J. (1998) Photochemistry of Petroleum I. Systematic Study of a Brazilian Intermediate Crude Oil. Marine Chemistry, 63, 93-104.

NOAA / HAZARDOUS Materials Response and Assessment Division. (1992) Oil Spill Case Histories 1967-1991 Summaries of Significant U.S. and International Spills. September 1992. Report No. HMRAD 92-11.

Oil Spill Research Institute. (2000) Post Mortem of In-Situ and Remote Sensing, Detection and Tracking of the Exxon Valdez Crude Oil in Prince William Sound via Excitation-Emission Matrix Fluorometery. Prince William Sound Science Center 2000 Annual Report.

Orain, M., Baranger, P., Rossow, B., and Grisch, F. (2011) Fluorescence Spectroscopy of Naphthalene at High Temperatures and Pressures: Implications for Fuel-concentration Measurements. Applied Physics B, 102, 163-172.

Ostgaard, K. and Jensen, A. (1983) Preparation of Aqueous Petroleum Solutions for Toxicity Testing. Environ. Sci. Technol., 17, 548-553.

Patra, D. and Mishra, A.K. (2001) Excitation Dependent Fluorescence Quantum Yield in Hydrocarbon Fuels Containing Polycyclic Aromatic Compounds. Polycyclic Aromatic Compounds, 18, 381-396.

Patsayeva, S. V. (1995) Fluorescent Remote Diagnostics of Oil Pollutions: Oil in Films and Oil Dispersed in the Water Body. EARSeL Advances in Remote Sensing, 3, 170-178.

Peterson, D.G., Rice, S.D., Short, J.W., Esler, D., Bodkin, J.L., Ballachey, B.E., and Irons, D.B., (2003) Long-Term Ecosystem Response to the Exxon Valdez Oil Spill. Science, 302, 2082-2086.

Prince, R.C., Garrett, R.M., Bare, R.E., Grossman, M.J., Townsend, T., Suflita, J.M., Lee, K., Owens, E.H., Sergy, G.A., Braddock, J.F., et al. (2003) The Roles of Photooxidation and Biodegradation in Long-term Weathering of Crude and Heavy Fuel Oils. Spill Science and Technology Bulletin, 8, 145-156.

Ralston, C.Y., Mitra-Kirtley, S., and Mullins, O.C. (1996) Small Population of One to Three Fused-Aromatic Ring Moieties in Asphaltenes. Energy and Fuels, 10, 623-630.

Reddy, C.M., Arey, J.S., Seewald, J.S., Sylva, S.P., Lemkau, K.L., Nelson, R.K., Carmichael, C.A., McIntyre, C.P., Fenwick, J., Ventura, G.T., Van Mooy, B.S., and Camilli, R. (2011) Composition and Fate of Gas and Oil Released to the Water Column During the Deepwater Horizon Oil Spill. PNAS. published ahead of print July 18, 2011, doi:10.1073/pnas.1101242108

Reed, W.E. and Kaplan, I.R. (1977) The Chemistry of Marine Petroleum Seeps. Journal of Geochemical Exploration, 7, 255-293.

Reisfeld, A., Rosenberg, E., and Gutnick, D. (1972) Microbial Degradation of Crude Oil: Factors Affecting the Dispersion in Sea Water by Mixed and Pure Cultures. Applied Microbiology, 24, 363-368.

Rodgers, R.P. and McKenna, A.M. (2011) Petroleum Analysis. Analytical Chemistry, 83, 4665-4687.

Rudzinski, W.E., Aminabhavi, T.M. (2000) A Review on Extraction and Identification of Crude Oil and Related Products Using Supercritical Fluid Technology. Energy and Fuels, 14, 464-475.

Ryder, A.G. (2005) Analysis of Crude Petroleum Oils Using Fluorescence Spectroscopy. Reviews in Fluorescence, 2, 169-198.

Schwarz, F.P., and Stanley, P.W. (1976) Fluorescence Measurements of Benzene, Naphthalene, Anthracene, Pyrene, Fluoranthene, and Benzo[e]pyrene in Water. Analytical Chemistry, 48, 524-528.

Sharma, K., Sharma, S.P., and Lahiri, S.C. (2009) Characterization and Identification of Petroleum Hydrocarbons and Biomarkers by GC-FTIR and GC-MS. Petroleum Science and Technology, 27, 1209-1226.

Stasiuk, L.D., and Snowdon, L.R. (1997) Fluorescence Micro-spectrometry of Synthetic and Natural Hydrocarbon Fluid Inclusions: Crude Oil Chemistry, Density and Application to Petroleum Migration. Applied Geochemistry, 12, 229-241.

Stedmon, C.A., and Bro, R. (2008) Characterizing Dissolved Organic Matter Fluorescence with Parallel Factor Analysis: A Tutorial. Limnology and Oceanography: Methods, 6, 572-579.

Stedmon, C.A., Markager, S., and Bro, R. (2003) Tracing Dissolved Organic Matter in Aquatic Environments Using a New Approach to Fluorescence Spectroscopy. Marine Chemistry, 82, 239-254.

Steffens, J., Landulfo, E., Courrol, L.C., and Guardani, R. (2010) Application of Fluorescence to the Study of Crude Petroleum. Journal of Fluorescence, 21, 859-864.

Strausz, O.P., Safarik, I., Lown, E.M. (2009) Cause of Asphaltene Fluorescence Intensity of Variation with Molecular Weight and its Ramifications for Laser Ionization Mass Spectrometry. Energy and Fuels, 23, 155-1562.

Turro, N.J., (1991) Modern Molecular Photochemistry, University Science Books.

U.S. Energy Information Administration. (2011) International Energy Outlook, Department of Energy Organization.

Van Holde, K.E., Johnson, W.C., Ho, P.S. (2006) Principles of Physical Biochemistry, Second edition, Pearson/Prentice Hall.

Wang, Z., Stout, S.A., and Fingas, M. (2006) Forensic Fingerprinting of Biomarkers for Oil Spill Characterization and Source Identification. Environmental Forensics, 7, 105-146.

Watson, M.D., Fechtenkotter, A., and Mullen, K. (2001) Big is Beautiful-"Aromaticity" Revisited from the Viewpoint of Macromolecular and Supramolecular Benzene Chemistry. Chem. Rev., 101, 1267-1300.

Welsh, S.E. (2000) Loop Current Rings and the Deep Circulation in the Gulf of Mexico. Journal of Geophysical Research, 105, 16,951-16,959.

Yamada et al. (2003) Study on the Fate of Petroleum-derived Polycyclic Aromatic Hydrocarbons (PAHs) and the Effect of Chemical Dispersant Using an Enclosed Ecosystem, Mesocosm. Marine Pollution Bulletin, 47, 105-113.

Zhu, Y., Mullins, O.C. (1992) Temperature Dependence of Fluorescence of Crude Oils and Related Compounds. Energy & Fuels, 6, pp. 545-552.

Ziolli, R.L. and Jardim, W.F. (2002) Operational Problems Related to the Preparation of the Seawater Soluble Fraction of Crude Oil. J. Environ. Monit., 4, 138-141.